Inter-cell interference coordination in wireless networks

Mohamad Yassin

▶ **To cite this version:**

Mohamad Yassin. Inter-cell interference coordination in wireless networks. Networking and Internet Architecture [cs.NI]. Université de Rennes; Université Saint-Joseph (Beyrouth), 2015. English. NNT : 2015REN1S106 . tel-01247157v2

HAL Id: tel-01247157

https://theses.hal.science/tel-01247157v2

Submitted on 17 May 2016

HAL is a multi-disciplinary open access archive for the deposit and dissemination of scientific research documents, whether they are published or not. The documents may come from teaching and research institutions in France or abroad, or from public or private research centers.

L'archive ouverte pluridisciplinaire **HAL**, est destinée au dépôt et à la diffusion de documents scientifiques de niveau recherche, publiés ou non, émanant des établissements d'enseignement et de recherche français ou étrangers, des laboratoires publics ou privés.

ANNÉE 2015

THÈSE / UNIVERSITÉ DE RENNES 1

sous le sceau de l'Université Européenne de Bretagne

En Cotutelle Internationale avec

l'Université Saint Joseph de Beyrouth, Liban

pour le grade de

DOCTEUR DE L'UNIVERSITÉ DE RENNES 1

Mention : Informatique

Ecole doctorale MATISSE

présentée par

Mohamad YASSIN

préparée à l'IRISA (UMR 6074)

et à l'Ecole Supérieure d'Ingénieurs de Beyrouth (ESIB, USJ)

Inter-Cell Interference Coordination in Wireless Networks

Thèse soutenue à Rennes
le 13 Novembre 2015

devant le jury composé de :

André-Luc BEYLOT
Professeur à l'ENSEEIHT / rapporteur

Véronique VÈQUE
Professeur à l'Université Paris-Sud / rapporteur

Jalel BEN OTHMAN
Professeur à l'Université Paris 13 / examinateur

Bernard COUSIN
Professeur à l'Université de Rennes 1 / directeur de thèse

Dany MEZHER
Professeur à l'USJ, Liban / directeur de thèse

Samer LAHOUD
Maître de Conférences à l'Université de Rennes 1 / co-directeur de thèse

A mes chers parents.
A Hammy, Nadine, Farah et Ahmad.

”وَاخْفِض لَهُمَا جَنَاحَ الذُّلِّ مِنَ الرَّحْمَةِ وَقُل رَّبِّ ارْحَمْهُمَا كَمَا رَبَّيَانِي صَغِيرًا “
الإسراء ٢٤

“et par miséricorde, abaisse pour eux l’aile de l’humilité, et dis: “O mon Seigneur, fais-leur, à tous deux, miséricorde comme ils m’ont élevé tout petit”.”

Saint Coran, Sourate 17, Verset 24.

Remerciements

Avant tout détail technique, j'aimerai rendre louange à *Dieu*, le Tout Miséricordieux, le Très Miséricordieux. Je rends grâce à *Allah*, Seigneur de l'univers, Détenteur d'une grâce immense, pour tous ses bienfaits. Je remercie mes très chers parents, *Ali* et *Imane*, qui ont sacrifié tout pour nous et auxquels je serai toujours redevable. Je remercie très spécialement *Hammy*, *Nadine*, *Farah* et *Ahmad* qui ont toujours été là pour moi. Je remercie mon cousin *Jad* et sa femme *Camille* qui se sont déplacés depuis Paris pour ma soutenance, ainsi que mon ami *Mahmoud* qui s'est déplacé depuis Grenoble. Je remercie également mes compagnons de travail et amis *Farah*, *Hassan*, *Hady*, *Melhem*, *M. Kanj*, *Chiheb*, *M. Aboulhassan*, *Rida*, *Lama*, *A. Mheich*, *M. Shamas*, *Jean*, *Siwar*, *Mahdi*, *Cédric*, *Gabriel*, ainsi que tous les membres de l'équipe ADOPNET de l'IRISA.

J'exprime ma profonde gratitude envers mes directeurs de thèse *Bernard* et *Dany* pour leur soutien, leur confiance et leurs conseils. Je remercie également *Fadi Geara*, le doyen de la faculté d'ingénierie de l'Université Saint Joseph de Beyrouth pour m'avoir accueilli au sein de l'ESIB durant ma thèse. Je remercie très profondément mes encadrants, *Samer* et *Marc*, pour leur aide, leur disponibilité, leur soutien et leur confiance. J'apprécie fortement leurs capacités d'analyse, leur enthousiasme et l'intérêt qu'ils m'ont accordé tout au long de ma thèse. Je tiens à exprimer ma sincère reconnaissance envers *Kinda* qui était toujours disponible pour apporter son aide sur le plan scientifique et humain. Je remercie chaleureusement *André-Luc Beylot* et *Véronique Vèque* d'avoir accepté de rapporter ma thèse, et je remercie très sincèrement *Jalel Ben Othman* d'avoir accepté de présider mon jury de thèse. Ce fut un honneur et un plaisir de les avoir dans mon jury de thèse.

Pour leur financement tout au long de ma thèse, je remercie le Conseil National de la Recherche Scientifique (CNRS Liban), Rennes Métropole et le Conseil de la Recherche de l'Université Saint Joseph de Beyrouth.

Finalement, j'adresse un grand merci à toutes les personnes que j'ai croisées durant ma thèse, et qui m'ont apporté soutien et encouragement.

Résumé

Introduction

Grâce aux avancées technologiques dans le domaine des réseaux cellulaires et des équipements mobiles, le nombre d'applications multimédia à haut débit dans les réseaux mobiles ne cesse d'augmenter. La quantité de trafic dans ces réseaux a augmenté de 70 pourcent en 2012 [Cis13] et de 81 pourcent en 2013 [Cis14]. Conformément à ce taux de croissance, on prévoit que le trafic de données dans les réseaux mobiles en 2017 sera 13 fois plus important que celui en 2012. Pour satisfaire aux besoins des équipements mobiles, les réseaux LTE/LTE-A ont été introduits afin d'améliorer l'efficacité spectrale et d'augmenter les débits des utilisateurs.

Vu l'augmentation sans cesse des demandes de trafic dans les réseaux mobiles, l'amélioration de la capacité du réseau s'avère un avantage, voire une nécessité. Ceci peut être achevé en déployant plusieurs petites cellules (*ex :* femto-cellules, micro-cellules, pico-cellules), utilisant le même spectre de fréquences, au sein de la zone de couverture des macro-cellules. Le déploiement dense améliore l'efficacité spectrale, mais aggrave le problème d'interférences intercellulaires. Elles sont dues à l'utilisation simultanée des ressources radio dans deux ou plusieurs cellules adjacentes, et elles ont des conséquences néfastes sur la performance du réseau et sur les débits des utilisateurs. D'où l'intérêt de l'utilisation des techniques de coordination des interférences intercellulaires, dont l'objectif est atteint en modifiant l'allocation des ressources et des puissances de transmission entre les différentes cellules. Ces modifications peuvent avoir lieu à l'echelle du réseau, en ajustant la distribution des ressources radio et des puissances de transmission entre les différentes cellules, mais aussi à l'intérieur de chaque cellule, en effectuant l'ordonnancement des utilisateurs pour améliorer le débit du système, son Efficacité Spectrale (ES), ou son Efficacité Energétique (EE).

Le projet *Mobile and wireless communications Enablers for the Twenty-twenty Information Society* (METIS) a défini un ensemble d'objectifs techniques pour les futurs réseaux

mobiles, ce qui nécessite l'amélioration des réseaux actuels afin de répondre à ces besoins. En comparaison avec les réseaux mobiles de la Quatrième Génération (4G), les principaux objectifs visés pour les réseaux futurs sont :

- Un volume de données par surface 1000 fois plus grand,
- Des débits de 10 à 100 fois plus importants que les débits actuels,
- Un nombre d'équipements connectés de 10 à 100 fois plus grand,
- Une durée de vie des batteries 10 fois plus grande,
- Un délai de bout-en-bout 5 fois plus petit que le délai actuel.

Ainsi, les réseaux mobiles de la Cinquième génération (5G) doivent répondre à ces besoins, tout en améliorant l'ES, l'EE et la capacité du système [MET15]. Par conséquent, l'efficacité des techniques actuelles de coordination des interférences intercellulaires sera mise en question. De nouvelles approches pour la gestion des ressources radio et des puissances de transmission sont alors requises afin d'atteindre les objectifs prédéfinis des futurs réseaux mobiles.

Contributions et plan de la thèse

Dans le cadre de cette thèse, on s'intéresse à proposer des solutions pour remédier aux problèmes des interférences intercellulaires dans les réseaux mobiles de dernière génération. La gestion efficace des ressources disponibles devient de plus en plus importante, surtout avec la prolifération des équipements mobiles et l'augmentation exponentielle des trafics de données dans les réseaux cellulaires. Les principaux intérêts des opérateurs mobiles résident dans l'augmentation de l'ES, l'EE et la capacité du réseau. L'amélioration des performances des utilisateurs frontaliers est également un objectif important pour les opérateurs, étant donné que ces utilisateurs sont les plus sensibles aux interférences intercellulaires.

Cette dissertation comporte six chapitres décrivant les contributions de la thèse, les différentes comparaisons effectuées et les résultats obtenus. Dans un premier lieu, un aperçu général du problème de gestion des ressources radio dans les réseaux mobiles de dernière génération est présenté dans le chapitre 1. On souligne également la nécessité de l'élimination des interférences intercellulaires, puis on résume les principales contributions de la thèse et on fournit le plan détaillé du document.

Avant d'exposer notre propre vision sur l'allocation des ressources radio et des puissances de transmission dans les réseaux cellulaires, nous enquêtons d'une manière exhaustive les différentes techniques de coordination des interférences intercellulaires existantes. Ces techniques sont qualitativement comparées, puis classées selon le taux de coopération requis entre les différentes stations de base. Une autre classification basée sur les principes de fonctionnement de ces techniques est également effectuée. Cette analyse qualitative, rapportée dans le chapitre 2, est ensuite suivie d'une investigation quantitative de plusieurs modèles de gestion d'interférences, où les scenarios simulés sont caractérisés par des distributions uniformes et non-uniformes des utilisateurs et par différentes conditions radio. Les résultats obtenus permettent de sélectionner la technique qui convient le mieux à chacun des scenarios simulés.

Dans le chapitre 3, nous abordons le problème multicellulaire d'allocation des ressources et des puissances de transmission d'une manière centralisée. Nous formulons ce problème d'optimisation centralisé, puis nous le décomposons en deux sous-problèmes indépendants : l'allocation de ressources qui sera prise en charge localement par chaque cellule, et l'allocation des puissances de transmission qui sera gérée d'une manière centralisée pour toutes les cellules. De plus, une approche distribuée basée sur la théorie des jeux est proposée pour l'allocation des puissances de transmission. Les joueurs étant les stations de base qui prennent leurs décisions indépendamment les unes des autres. Les techniques centralisées de minimisation des interférences intercellulaires offrent la solution optimale au prix d'une grande charge de signalisation. Par contre, les solutions décentralisées réduisent le trafic de signalisation sans garantir l'optimalité de la solution obtenue.

Une heuristique de contrôle de puissance est ensuite introduite dans le chapitre 4. Elle est basée sur les retours d'information sur la qualité des canaux radio, envoyés par les utilisateurs à la station de base. L'allocation des puissances de transmission est modifiée localement par chaque cellule de manière à éviter le gaspillage d'énergie, surtout pour les utilisateurs qui sont proches de la station de base, et pour réduire les interférences ressenties par les utilisateurs des stations de base voisines. Nous proposons également une technique autonome qui gère la distribution des ressources radio entre les différentes zones de chaque cellule. Cette technique répond aux besoins des utilisateurs dans chaque zone en adaptant la distribution des ressources d'une manière dynamique, sans modifier l'allocation des puissances de transmission entre les différentes cellules. De cette manière, on améliore l'équité dans la distribution des débits entre les utilisateurs de chaque cellule, sans générer des interférences additionnelles dans les cellules voisines.

Dans le chapitre 5, nous abordons le compromis entre les techniques de gestion d'interférences intercellulaires centralisées et décentralisées. Nous proposons une approche hybride où l'allocation des ressources radio et des puissances de transmission est faite d'une manière coopérative entre les différentes cellules. Notre algorithme se déroule en deux étapes : dans un premier lieu, les cellules voisines collaborent afin d'ajuster les puissances de transmission allouées aux ressources radio. Pendant cette étape, des informations concernant la satisfaction des utilisateurs et l'allocation des puissances sont échangées entre ces cellules. Ensuite, la distribution des ressources entre les différentes zones de chaque cellule est modifiée localement, selon les besoins des utilisateurs dans chaque zone.

Enfin, les contributions de cette thèse ainsi que les thématiques de recherche futures sont présentées dans le chapitre 6.

Conclusion et perspectives

Dans cette thèse, nous avons abordé le problème d'allocation des ressources radio et des puissances de transmission dans les réseaux mobiles de dernière génération. En effet, l'énorme croissance du nombre d'équipements mobiles, la prolifération des applications multimédia à haut débit et l'évolution rapide vers l'Internet des objets ont mené à un déploiement dense des stations de base utilisant la totalité du spectre disponible afin de répondre à ces besoins croissants. La réutilisation dense des fréquences augmente la capacité du réseau, par contre, des interférences intercellulaires ayant un impact négatif sur la performance du réseau sont générées. D'où la nécessité de l'utilisation des techniques de gestion du spectre et d'allocation des puissances de transmission.

D'abord, nous avons commencé cette dissertation en effectuant une enquête exhaustive des travaux figurant dans l'état de l'art. Une comparaison qualitative suivie d'une analyse quantitative sont effectuées afin de sélectionner la technique la plus adéquate à chaque scenario simulé. Nous avons ensuite formulé un problème multicellulaire centralisé d'allocation des ressources radio et des puissances de transmission, qui prend en compte l'impact des interférences sur les performances des différents utilisateurs. Une autre approche décentralisée est également proposée pour gérer l'allocation des puissances, en se basant sur la théorie des jeux. Les joueurs sont les stations de base qui prennent leurs propres décisions indépendamment les unes des autres. De plus, nous avons proposé une heuristique de contrôle de puissance où l'allocation des puissances de transmission se fait en se référant aux retours d'informations sur la qualité des canaux radio, dans le but d'éviter le gaspillage d'énergie et de réduire les interférences intercellulaires. Un autre algorithme autonome de gestion des ressources radio est introduit. Il modifie l'allocation des ressources entre les différentes zones de chaque cellule de telle manière à répondre aux

besoins des utilisateurs dans chaque zone. Les puissances attribuées aux ressources ne sont pas modifiées pour ne pas génèer des interférences additionnelles. Enfin, nous avons abordé le compromis entre les méthodes centralisées et décentralisées en introduisant une approche hybride pour la gestion des ressources radio et l'allocation des puissances de transmission. Des informations concernant l'utilisation des ressources et les demandes des utilisateurs sont échangées entre les stations de base voisines afin de modifier l'allocation des puissances d'une manière coopérative. Puis, la distribution du spectre entre les différentes zones de chaque cellule s'effectue localement, au niveau de chaque station de base.

Les contributions réalisées dans le cadre de cette thèse constituent des solutions intéressantes pour la gestion des ressources radio et des puissances de transmission dans les réseaux mobiles actuels et futurs. Néanmoins, nous avons réussi à identifier plusieurs pistes pour nos futurs travaux de recherche.

Les réseaux hétérogènes se présentent comme une alternative efficace pour répondre aux besoins croissants en débits et pour augmenter la capacité du réseau. Ils sont composés de plusieurs Technologies d'Accès Radio (TAR) qui coexistent dans la même zone géographique. La sélection du réseau d'accès radio s'ajoute au problème de minimisation des interférences inter-TAR et intra-TAR. Les techniques proposées dans cette thèse peuvent être utilisées pour réduire les interférences intercellulaires dans les réseaux hétérogènes, une fois le problème de sélection du réseau d'accès est résolu. De plus, on pourra formuler un problème d'optimisation qui considère à la fois la sélection du réseau d'accès radio, la gestion des ressources et l'allocation des puissances de transmission. Les objectifs étant la maximisation du débit total du système, l'augmentation de la capacité du réseau, ou l'amélioration de l'ES et de l'EE.

L'étude du compromis entre la maximisation de l'ES et la maximisation de l'EE s'avère également un sujet de grande importance. En effet, la réduction de la consommation d'énergie est devenue un intérêt de plus en plus important pour les opérateurs des réseaux mobiles. L'ES est améliorée quand la puissance de transmission augmente. Par contre, l'EE est réduite, puisque la quantité d'énergie consommée augmente. Le contrôle du compromis ES-EE est faisable en modifiant l'allocation des ressources radio et des puissances de transmission. Dans ce contexte, on pourra définir un problème d'optimisation multi-objectifs qui vise la maximisation de l'ES sans dégrader l'EE du système. Les contraintes d'un tel problème d'optimisation sont relatives au débit minimal par utilisateur et vont garantir un niveau raisonnable de qualité de service.

Abstract

The exponentially increasing demand for mobile broadband communications have led to the dense deployment of cellular networks with aggressive frequency reuse patterns. The future Fifth Generation (5G) networks are expected to overcome capacity and throughput challenges by adopting a multi-tier architecture where several low-power Base Stations (BSs) are deployed within the coverage area of the macro cell. However, Inter-Cell Interference (ICI) caused by the simultaneous usage of the same spectrum in different cells, creates severe problems. ICI reduces system throughput and network capacity, and has a negative impact on cell-edge User Equipment (UE) performance. The ecological concern is also an important issue, since the carbon dioxide emissions continue to raise due to the dense deployment of BSs.

Inter-Cell Interference Coordination (ICIC) techniques are required to mitigate the impact of ICI on system performance. ICIC schemes are classified into centralized, decentralized, and hybrid approaches. In the centralized approach, a central control entity manages resource and power allocation based on the information received from the different cells. It provides the optimal resource allocation at the expense of a high signaling overhead. In decentralized ICIC schemes, each cell makes its own resource allocation decisions, and the central control entity is not required. However, decentralized ICIC schemes do not guarantee the optimal resource and power allocation. The hybrid approaches are proposed as a tradeoff between the centralized and the decentralized approaches. Resource allocation between the different cells is performed by a central control entity, while UE scheduling is decentralized to the base stations.

In this thesis, we address the resource and power allocation problem in multiuser Orthogonal Frequency Division Multiple Access (OFDMA) networks such as LTE/LTE-A networks and dense small cell networks. We start by overviewing the state-of-the-art schemes, and provide an exhaustive classification of the existing ICIC approaches. This qualitative classification is followed by a quantitative investigation of several interference mitigation techniques under uniform and non-uniform UE distributions, and for various

network loads and radio conditions. The obtained results allow us to select the most adequate technique for each network scenario.

Then, we formulate a centralized multi-cell joint resource and power allocation problem, and prove that this problem is separable into two independent convex optimization problems. The objective function of the formulated problem consists in maximizing system throughput while guaranteeing throughput fairness between UEs. ICI is taken into account, and resource and power allocation is managed accordingly in a centralized manner. Furthermore, we introduce a decentralized game-theoretical method to solve the power allocation problem without the need to exchange signaling messages between the different cells. A multi-player game is defined, where the cells are the players, and they make their own decisions independently of each other. The solution to the proposed decentralized optimization problem corresponds to a Nash Equilibrium.

We also propose a decentralized heuristic power control algorithm based on the received Channel Quality Indication (CQI) feedbacks. The intuition behind this algorithm is to avoid power wastage for UEs that are close to the serving cell, and reducing ICI for UEs in the neighboring cells. An autonomous ICIC scheme that aims at satisfying throughput demands in each cell zone is also introduced. The obtained results show that this technique improves UE throughput fairness, and it reduces the percentage of unsatisfied UEs without generating additional signaling messages.

Lastly, we provide a hybrid ICIC scheme as a compromise between the centralized and the decentralized approaches. For a cluster of adjacent cells, resource and power allocation decisions are made in a collaborative manner. First, the transmission power is adjusted after receiving the necessary information from the neighboring cells. Second, resource allocation between cell zones is locally modified, according to throughput demands in each zone.

Keywords Inter-cell interference coordination; OFDMA; 3GPP LTE; 5G; dense small cell networks; spectral efficiency; energy efficiency; resource allocation; power allocation; throughput fairness.

Contents

List of Figures

List of Tables

Abbreviations

3G	Third Generation
3GPP	Third Generation Partnership Project
4G	Fourth Generation
5G	Fifth Generation
AMC	Adaptive Modulation and Coding
BR	Bad Radio conditions
BS	Base Station
CDF	Cumulative Distribution Function
CDMA	Code Division Multiple Access
CoMP	Coordinated Multi-Point
CQI	Channel Quality Indication
C-RAN	Cloud Radio Access Network
DL	Downlink
eNodeB	Evolved Node B
EPC	Evolved Packet Core
E-UTRAN	Evolved Universal Terrestrial Radio Access Network
FFR	Fractional Frequency Reuse
GR	Good Radio conditions
GSM	Global System for Mobile communications
ICI	Inter-Cell Interference
ICIC	Inter-Cell Interference Coordination
IoT	Internet of Things
IP	Internet Protocol
LTE	Long Term Evolution
LTE-A	Long Term Evolution Advanced

MCS	Modulation and Coding Scheme
METIS	Mobile and wireless communications Enablers for the 2020 Information Society
MME	Mobility Management Entity
NE	Nash Equilibrium
NGMN	Next Generation Mobile Networks
OFDM	Orthogonal Frequency Division Multiplexing
OFDMA	Orthogonal Frequency Division Multiple Access
PC	Power Control
P-GW	Packet data network Gateway
QoS	Quality of Service
RAN	Radio Access Network
RAT	Radio Access Technology
RB	Resource Block
RRM	Radio Resource Management
RS	Reference Signal
SAE	System Architecture Evolution
SC-FDMA	Single Carrier Frequency Division Multiple Access
SFR	Soft Frequency Reuse
SGW	Serving Gateway
SINR	Signal to Interference and Noise Ratio
TTI	Transmit Time Interval
UE	User Equipment
UMTS	Universal Mobile Terrestrial radio access System

Chapter 1

Introduction

The significant advances in cellular networks and mobile devices have led to a rapidly growing demand for high speed multimedia applications. To support this increasing data traffic, the capacity of cellular networks can be improved via the dense deployment of small cells with aggressive frequency reuse. Thus, resource allocation and interference management is a key research challenge in present and future cellular networks. In this chapter, we provide a global description of the inter-cell interference problems in cellular networks as well as the motivation behind our research work on interference mitigation techniques. The main contributions of the thesis, and the thesis organization are also presented hereafter.

1.1 Background

During the last few decades, the traffic demands in mobile networks have tremendously increased. The global mobile data traffic grew by 70 percent in 2012 [Cis13], and it grew by 81 percent in 2013 [Cis14]. Consequently, mobile data traffic in 2017 will be 13 times that of 2012. This rapidly growing demand drove the 3GPP to introduce the Long Term Evolution (LTE) of the Universal Mobile Terrestrial radio access System (UMTS). LTE-Advanced (LTE-A) [3GP08] was also proposed to improve cell-edge spectral efficiency, and to increase the peak transmission rates. However, network capacity and spectral efficiency should be further improved in order to address the exponentially-increasing demands for mobile broadband communications.

Network capacity improvement can be achieved through the dense deployment of base stations with small coverage areas, within the coverage zones of macro cells and using the same frequency spectrum. Although it improves the overall spectral efficiency, the aggressive frequency reuse scheme increases the interference caused by UEs using the same radio resources. Given the negative impact of ICI on system performance, on cell-edge UEs throughput, and on network capacity, the utilization of adequate interference mitigation techniques becomes a necessity for the next generation cellular networks. ICIC techniques are designed to alleviate the impact of ICI, and to improve system performance. These target objectives are achieved by modifying various system resources allocation such as frequency resources and transmission power. For instance, several RRM schemes perform resource allocation between the different cells, and packet scheduling among the active UEs in each cell, in order to improve system performance and to increase its spectral efficiency.

The METIS project has stated a set of technical objectives [MET13] that require extending today's wireless communication systems to support new usage scenarios. These objectives can be summarized as follows:

- 1000 times higher mobile data volume per area,
- 10 to 100 times higher typical user data rate,
- 10 to 100 times higher number of connected devices,
- 10 times longer battery life for low power devices,
- 5 times reduced end-to-end latency.

The resulting 5G system should be able to meet these goals while guaranteeing a more efficient energy and resource utilization, in order to allow a constant growth in capacity at acceptable overall cost and energy dissipation [MET15]. Therefore, the traditional techniques for radio resource management and power allocation may not be efficient in future mobile networks.

1.2 Inter-Cell Interference

1.2.1 LTE/LTE-A Architecture

The LTE/LTE-A system architecture consists of a radio access network, called Evolved-Universal Terrestrial Radio Access Network (E-UTRAN) and a core network known as Evolved Packet Core (EPC). The network architecture is shown in Fig. 1.1, and it is labeled System Architecture Evolution (SAE).

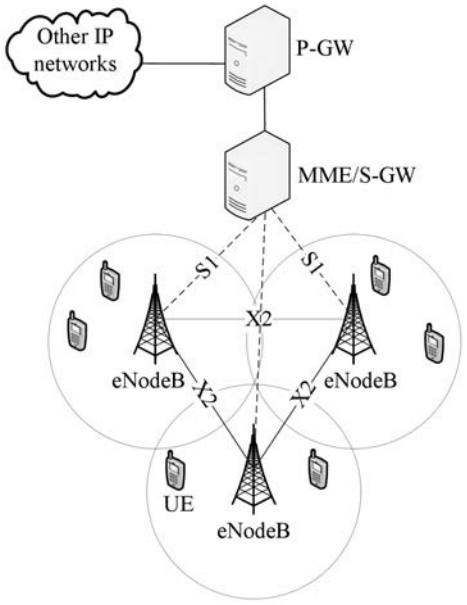

Figure 1.1: LTE/LTE-A system architecture

The Mobility Management Entity (MME) and the Serving Gateway (S-GW) are located at the core network, and they are connected to the LTE/LTE-A base stations, called evolved-NodeBs (eNodeBs) via the S1 interface. The MME entity handles several functions related to network access control, radio resource management, and mobility management, while the S-GW acts as a local mobility anchor point for inter-eNodeB handovers and for the handling of data packet transfer between the core network and the UEs. The Packet data network Gateway (P-GW) provides connectivity between the core network and other Internet Protocol (IP) networks. It also serves as an anchor for mobility between 3GPP and non-3GPP technologies. The radio access network is comprised of eNodeBs and UEs. Each eNodeB is connected to its neighboring cells through

the X2 interface that allows the exchange of signaling messages and information related to resource usage and power allocation.

In LTE/LTE-A systems, Orthogonal Frequency Division Multiple Access (OFDMA) technique is selected as the multiple access technique on the downlink of the radio interface. The available bandwidth is divided into several orthogonal subcarriers [3GP12b], which eliminates intra-cell interference. The smallest scheduling unit is called Resource Block (RB), and it consists of 12 subcarriers in the frequency domain, and six OFDM symbols in the time domain in the case of normal cyclic prefix, or seven OFDM symbols in the time domain in the case of short cyclic prefix. RB duration is 0.5 ms, and it occupies a spectrum of 180 kHz. The scheduling period is called Transmit Time Interval (TTI), and it equals 1 ms. During one TTI, each RB is exclusively assigned to one UE in a given cell, and it could be simultaneously used in the neighboring cells for different UEs. Consequently ICI problems occur due to the dense usage of the available frequency resources.

1.2.2 Dense Small Cell Networks

Due to the increasing demand for mobile broadband communications, the dense deployment of low power base stations within the coverage area of existing macro cells improves network capacity, and increases the available bandwidth per UE. Figure 1.2 shows an LTE/LTE-A cell served by a macro base station, with several small cells coexisting in the same geographical area. Small cells include microcells, picocells, femtocells, and relay nodes.

The Next Generation Mobile Networks (NGMN) alliance expects the emergence of new use cases and business models driven by the customers' and operators' needs [NGM15]. Beyond 2020, mobile broadband access should be guaranteed in densely populated areas, such as dense urban city centers, or events where thousands of people are located within a small geographical area. Interference management challenges will arise due to the following reasons [HRTA14]:

- Dense deployment of wireless devices.
- Coverage imbalance due to varying transmit powers of the different base stations coexisting in the same geographical area.

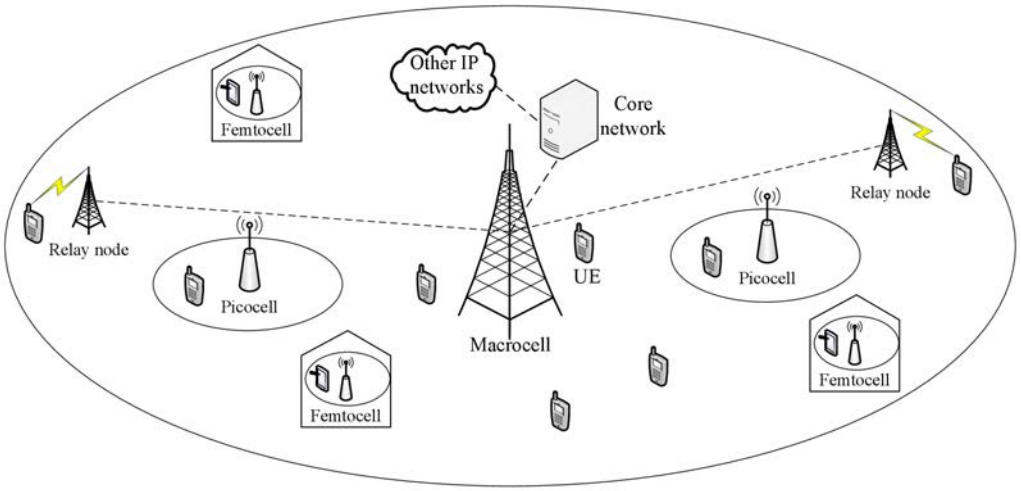

Figure 1.2: LTE/LTE-A macro cell with dense small cell deployment

- Public or private access restrictions in the different tiers.
- Cooperation among base stations, and direct communications between the UEs.

1.2.3 Radio Resource Management

In cellular networks, RRM functionalities include the partitioning of the available spectrum between base stations (macro cells and small cells), resource allocation among the different UEs within each cell, link adaptation, handover management, and admission control. Link adaptation function is achieved through Adaptive Modulation and Coding (AMC) and transmission power control. Among these functionalities, resource partitioning between the different cells, UE scheduling, and transmission power control are the ones used to alleviate the negative impact of ICI on system performance.

Bandwidth allocation between the different cells may need to be performed in dense small cell networks. For instance, resource allocation between the backhaul links and the radio access links should be performed in relay-based networks. Otherwise, inter-cell interference increases, which causes additional degradation to the system performance. Moreover, UE scheduling aims at maximizing the spectral efficiency and the achievable

throughput. This functionality is located at the medium access layer of the cellular system. It occurs periodically, and it is usually based on the QoS requirements, or on the received channel quality feedbacks. For example, the scheduling period in LTE/LTE-A networks equals one TTI, and the scheduler may take into account the received CQI feedbacks. To further improve cell throughput, transmission power control operates along with AMC. ICI could also be reduced by adjusting the transmission power allocation among the adjacent cells. Note that resource and power allocation could take place either locally at the base station, or in a centralized control entity.

1.3 Thesis Scope and Contributions

The objective of this thesis is to contribute to the domain of interference mitigation techniques for present and future mobile networks. We particularly focus on multiuser OFDMA networks, including heterogeneous LTE/LTE-A networks and dense small cell networks. It is of crucial importance for mobile network operators to increase network capacity, spectral efficiency, and energy efficiency, given the exponentially growing demand for mobile broadband communications. Other concerns include increasing system throughput and improving the performance of cell-edge UEs that are mainly affected by ICI. Numerous ICIC schemes have been surveyed in [HKHE13, LCLV14] where the different trends in the literature are described. We identify three classes of interference mitigation approaches: centralized, decentralized, and hybrid approaches.

The centralized approach requires the existence of a centralized controller that manages resource and power allocation across the entire network. Although it finds the optimal solution, the centralized approach is characterized by an important processing load, and it generates a large amount of signaling messages that are exchanged periodically between the cells and the controller. When the decentralized approach is adopted, each cell performs resource and power allocation locally, regardless of the decisions made by the other cells. No additional signaling traffic is generated, but the optimal resource allocation is not guaranteed. The hybrid approach achieves a compromise between the centralized and the decentralized approaches. A central controller adjusts resource allocation between the different cells, then each cell allocates the available resources to the active UEs independently of the other cells.

In this dissertation, we discuss, classify, and investigate the existing ICIC approaches for multi-user OFDMA networks. Contrarily to the existing surveys that provide qualitative descriptions of the different ICIC schemes, we perform quantitative comparisons of state-of-the-art ICIC schemes under uniform and non-uniform UE distributions, and for different network loads. This analysis allows us to draw conclusions about the most adequate technique for each network scenario. An exhaustive classification of ICIC schemes is also provided.

After overviewing the literature trends, we address the multi-cell resource and power allocation problem in a centralized manner. In [QLS09, VZRB15] the multi-cell optimization problem is also considered. However, the impact of ICI between the adjacent cells is neglected, which mitigates the accuracy of the proposed solutions. Our objective function consists in maximizing system throughput while guaranteeing throughput fairness between the active UEs. ICI caused by the aggressive frequency reuse strategy is taken into account, and resource and power allocation is managed accordingly. In the same context, the decentralized ICIC is investigated by introducing a resource allocation scheme based on game theory. The players are the base stations, and they make their own resource allocation decisions independently of the other base stations in the network. Although decentralized ICIC schemes do not guarantee the optimal solution, their main advantage consists in reducing the signaling overhead and the computational complexity in comparison with the centralized schemes.

We also investigate autonomous and cooperative heuristic ICIC schemes. Our goal is to improve cell-edge UEs performance without reducing system throughput, and using low complexity algorithms. Resource and power allocation are adjusted according to the received CQI feedbacks, or based on the satisfaction level of each cell. The performance of these techniques are compared to that of the centralized solution, and to other state-of-the-art techniques. The decentralized ICIC schemes do not generate additional signaling traffic, while the cooperative schemes are proposed as a compromise between the centralized and the decentralized approaches.

1.4 Thesis Outline

This thesis document consists of six chapters organized as follows: an extensive survey of the existing ICIC techniques is performed in Chapter 2. These techniques are classified according to the amount of cooperation required between the different base stations. They are also categorized based on their underlying working principles. Moreover, we investigate the performance of each technique under uniform and non-uniform UE distributions, and for different network loads and radio conditions. The obtained results allow us to define the most adequate technique for each network scenario. In Chapter 3 of this dissertation, the multi-cell resource and power allocation problem is formulated as a centralized optimization problem. Our formulation is valid not only for LTE/LTE-A networks, but also for dense small cell deployments that will be most likely adopted by the 5G systems in order to address the exponentially increasing data traffic demands. It is proven that the joint resource and power allocation problem is separable into two independent problems: a resource allocation problem performed locally at each cell, and a centralized power allocation problem. Moreover, we propose a distributed game-theoretical ICIC scheme, where the players are the base stations (macro cells and small cells). A multi-player game is defined, where the BSs are assumed to make their own decisions without knowing the decisions of each other. Therefore, comparisons are made between the centralized and the distributed multi-cell resource and power allocation problems. Although centralized ICIC schemes provide the optimal resource and power allocation, they generate an additional signaling overhead due to the information sent from the base stations to the centralized control entity.

In Chapter 4, we introduce a heuristic downlink power allocation algorithm that adjusts the transmission power allocated to the different frequency resources in a distributed manner. Power allocation decisions are based on the received channel quality feedbacks. The objective is to avoid power wastage, especially for the UEs that are close to their serving base stations, and to reduce ICI for the UEs in the neighboring cells. Within the same context, we propose an autonomous dynamic ICIC technique that adjusts resource allocation between cell zones according to UE distribution and throughput demands in each zone. This technique aims at improving throughput fairness between the active UEs, and reducing the percentage of unsatisfied UEs. Moreover, no additional signaling messages are required.

For Chapter 5, the tradeoff between centralized and autonomous ICIC schemes is addressed by introducing a cooperative interference mitigation scheme. Resource and power allocation decisions are jointly made by each cell in collaboration with its neighbors. The objectives sought are increasing UE satisfaction, improving throughput fairness, and increasing both spectral efficiency and energy efficiency. The algorithm consists of two phases: in the first phase, signaling messages are exchanged to get the necessary information about UE satisfaction and power allocation in the neighboring cells. Transmission power adjustments are made during this phase. In the second phase, resource allocation between cell zones is modified according to UE demands in each zone.

Finally, Chapter 6 summarizes the thesis main contributions, presents the perspectives, and describes the future research topics.

Chapter 2

Inter-Cell Interference Coordination Techniques for Multi-User OFDMA Networks

The main challenge for present and future mobile networks is to efficiently use the available spectrum, and to provide satisfying quality of service for users. They are designed in a manner that allows providing high throughput and high capacity. A frequency reuse factor of one is required to improve spectral efficiency, while other important concerns for mobile network operators include energy efficiency, throughput fairness, and user satisfaction. Due to the scarcity of the available spectrum, all the cells are allocated the same frequency resources, leading to significant inter-cell interference problems. Given the negative impact of interference on system performance, several interference mitigation techniques have been proposed, where restrictions are made on resource blocks usage, power allocation, or both. In this chapter, we conduct a comprehensive survey on the existing ICIC techniques. We classify these techniques, and we study their performance while taking into consideration various design parameters. The techniques are compared throughout intensive system level simulations under several parameters such as different network loads, radio conditions, and user distributions. Simulation results show the advantages and the limitations of each technique compared to the frequency reuse-1 model. Thus, we are able to identify the most suitable ICIC technique for each network

scenario.

2.1 Introduction

With the rapidly growing demand for mobile broadband communications and with the proliferation of mobile applications, Third Generation (3G) Universal Mobile Terrestrial Radio Access System (UMTS) is no longer able to satisfy UE throughput demands. 3GPP introduced LTE [3GP06a] and LTE-A standards [3GP12a, 3GP13] to increase system capacity, to support the high-speed multimedia applications, and to allow UEs to achieve higher transmission rates. In LTE/LTE-A networks, OFDMA is chosen as the multiple access technique for the downlink of the radio interface. The advent of smartphones and tablets, the increasing number of personal connected devices including wearables and sensors, and the fast evolution towards Internet of Things (IoT) are motivating the Telecom enterprises and wireless communications enablers to define the architecture, specifications, and requirements of the 5G networks. 5G wireless networks are expected to be a mixture of network tiers of different transmission powers, backhaul connections, and different radio access technologies [HRTA14]. Thus, radio resource allocation and interference management will be an important challenge in these networks.

OFDMA scheme [SSB09] is based on OFDM technology that subdivides the available bandwidth into a multitude of narrower mutually orthogonal subcarriers, which can carry independent information streams. A physical RB is defined as 12 subcarriers in the frequency domain (180 kHz) and seven OFDM symbols in the time domain as shown in Fig. 2.1, which is equivalent to one time slot (0.5 ms). RB and power allocation are performed periodically by the schedulers every TTI that equals one millisecond. In multi-user OFDMA networks [SL05], intra-cell interference is eliminated, since data is transmitted over independent orthogonal subcarriers. Similarly, Single Carrier Frequency Division Multiple Access (SC-FDMA) technique, characterized by a lower peak-to-average power ratio, is usually used on the uplink to transmit data from UEs to the base station [WYMC09]. However, the frequency reuse-1 model leads to ICI strongly affecting SINR of active UEs, especially cell-edge UEs, which leads to a significant degradation in the total throughput. Moreover the existence of network elements with different maximum transmission power, *e.g.*, macrocells, picocells, and femtocells, makes ICI problem more complicated.

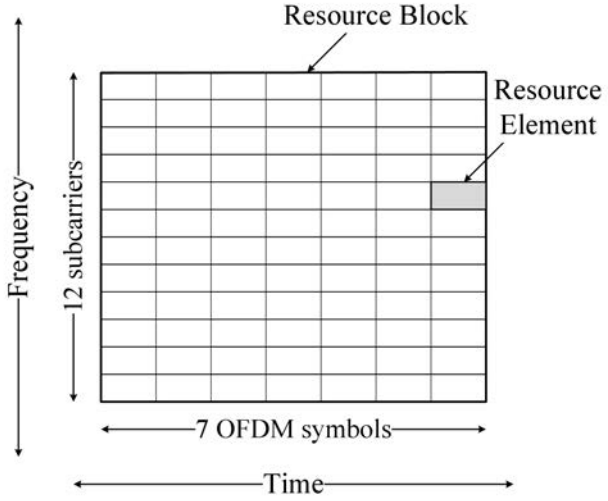

Figure 2.1: Physical resource block structure

ICI arises as a prohibitive problem due to simultaneous transmissions over the same frequency resources in adjacent network cells. It decreases SINR especially for cell-edge UEs [XYY12], that are relatively far from the serving base station. Thus, it has a negative impact on UE throughput, it decreases the spectral efficiency, and it reduces the quality of provided services.

Hard frequency reuse schemes (*e.g.*, reuse factor m) become inefficient due to utilization of $\frac{1}{m}$ of the available bandwidth. Thus, the peak data rate is reduced. For instance, adjacent base stations of a GSM network are allocated different frequencies [DK88, Don79] in order to avoid interference between neighboring transmitters. A number of adjacent GSM cells are grouped into a cluster where the same frequency resources are used only once. A cluster size of one is not used due to high co-channel interference problems that occur. Although ICI within each cluster is eliminated, spectral efficiency is largely reduced. In 3G networks, the interference experienced by a UE is due to cross-correlation between spreading codes, and it can be considered as noise [JPJS05]. Therefore, ICI problems do not exist in CDMA-based 3G networks.

Although frequency reuse-m models eliminate ICI, they are not adequate for present and future mobile networks. In fact, one major objective of 3GPP LTE standard is to increase network capacity in order to accommodate additional UEs. According to reuse-m schemes, each base station is allowed to allocate a portion of the available spectrum. This restriction is not tolerated in LTE nor in 5G, since it greatly reduces

the spectral efficiency. Thus, other frequency and power allocation schemes are used to reduce ICI; they are commonly known as ICIC [DSZ12] techniques.

FFR [HA09] and SFR [Hua05] are static ICIC techniques used to improve spectral efficiency of the fourth generation wireless standards. While FFR sets restrictions on RB allocation between the different UEs in each cell, SFR performs both radio resource management and power allocation for the used RBs. These techniques are independently used in each cell without any cooperation between adjacent base stations. Other ICIC techniques exploit the communications between adjacent base stations to reduce ICI. In LTE, signaling messages about RB and power allocation are exchanged between adjacent eNodeBs over X2 interface, that interconnects neighboring cells. For instance, a recently proposed technique divides ICIC problem into a multi-cell scheduling and a multi-user scheduling problem [KHQT13b]. The former uses an On/Off approach to determine the restricted RBs for each eNodeB, while the latter attributes RBs to UEs according to their radio conditions. ICIC can also be seen as a cooperative problem where LTE base stations collaborate in order to find the power allocation mask that minimizes inter-cell interference [DA10]. It is an adaptive SFR scheme that reduces transmission power on RBs allocated to UEs that experience good radio quality (close to the base station). However, the time scale of the proposed algorithm is in order of tens of seconds, which is disadvantageous when the system state is quickly varying with time.

With the introduction of CoMP transmissions [LSC+12] in LTE-A networks, ICIC techniques rely more on dynamic coordination between base stations. Scheduling decisions are improved when they are made jointly for a cluster of cells [DVR03] thereby enhancing performance through interference avoidance. Small cells (including picocells, femtocells and home eNodeBs) deployment along with existing macro base stations brings out the challenge of ICIC in heterogeneous networks. Indeed, serious interference [XHC12] problems occur due to co-channel deployments with the macro cells. e-ICIC techniques are used to allow for time-sharing of spectrum resources between macro base stations and small cells.

Given the diversity of existing ICIC techniques, mobile network operators have the opportunity to implement the most convenient one for their intended objectives. In fact, the performance of some techniques largely depends on network parameters such as UE distribution between cell zones, existing ICI problems, and the number of UEs in each

cell. Some techniques aim at improving cell-edge UEs throughput, without taking into account the overall spectral efficiency. Consequently, the knowledge of ICIC techniques performance is a critical factor when selecting the one that best fits operator's goals. In the remainder of this chapter, we conduct an exhaustive review and classification of existing interference mitigation and radio resource management techniques. We also provide a comprehensive survey of the performance of ICIC techniques in LTE Networks. Various network loads, radio conditions, and user distributions are considered, in order to study the impact of design parameters on ICIC techniques performance. We investigate the performance of frequency reuse-m model and other ICIC techniques, and we inspect the advantages and limitations of each of the examined techniques compared to the frequency reuse-1 model under different network loads and UE distributions. A MATLAB-based LTE downlink system level simulator [VUT14, IWR10] is used to compare the performance of the frequency reuse-1 model with that of reuse-3 model, FFR, and SFR techniques. The objective of ICIC is to reduce interference problems in order to avoid their harmful impact on user throughput and system performance. An efficient ICIC technique improves both spectral efficiency and energy efficiency of the mobile network, which is a substantial goal for mobile network operators.

2.2 Classification of ICIC Techniques

Rather than promoting standardized techniques, 3GPP provides support for proactive and reactive schemes, and it allows constructors and operators to configure a wide range of non-standardized ICIC techniques [FKR+09]. We classify these techniques into centralized, decentralized, and hybrid schemes.

Centralized ICIC techniques require the existence of a central management entity that controls the entire network. It collects information related to channel quality and UE throughput demands. Then, it finds the optimal resource allocation between the existing base stations, and it also performs resource allocation among UEs (scheduling). The centralized approach offers the optimal resource allocation solution. However, a large amount of signaling messages is generated. Thus, it is only recommended for small-sized cellular networks.

The decentralized non-cooperative approach allows each cell to determine its own resource allocation, without the need to cooperate with other cells. The existence of a centralized control entity is not required. This approach does not generate any additional signaling overhead, and it is characterized by a low implementation complexity. However, it does not guarantee the optimal resource allocation. Hence, decentralized ICIC techniques are adequate for large-sized cellular networks.

Hybrid ICIC techniques are also qualified as *semi-centralized*. They are proposed as a compromise between the centralized and the decentralized techniques. In these schemes, a centralized control entity collects channel quality information and UE throughput demands in order to adjust resource allocation between the network cells, while RB allocation to the active UEs is locally performed by each base station. The hybrid approach achieves a tradeoff between the previously mentioned approaches, and it is suitable for medium-sized cellular networks. ICIC techniques classification based on the cooperation required between the cells is illustrated in Fig. 2.2.

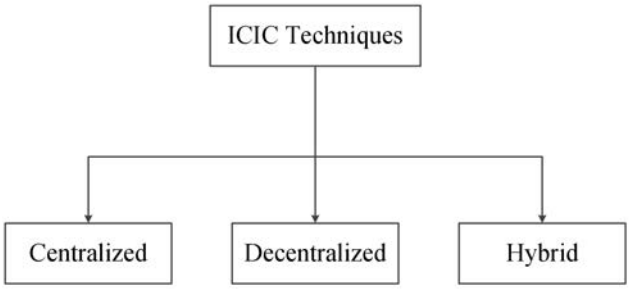

Figure 2.2: Cooperation-based classification of ICIC techniques

Besides the amount of cooperation required between the different cells to achieve ICI mitigation, we perform another classification of the existing ICIC techniques based on their working principles. The following categories are identified: frequency reuse, cooperative approaches, frequency scheduling, femtocell-aware, graph theory, game theory, convex optimization, and power minimization. They are illustrated in Fig. 2.3. In the

remainder of this section, we describe the different classification principles, and we survey the existing ICIC techniques under each category. Our qualitative comparisons are summarized in Table 2.1.

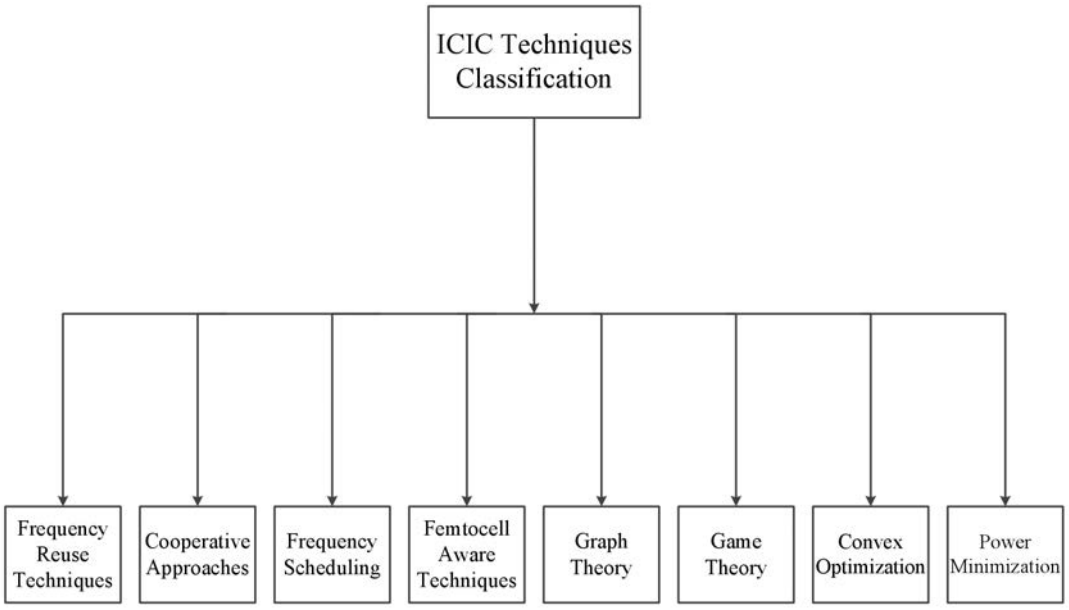

Figure 2.3: Classification of ICIC techniques

2.2.1 Frequency Reuse Techniques

Frequency reuse-based ICIC techniques, such as fractional frequency reuse and soft frequency reuse, have been widely suggested to minimize interference between adjacent cells, and to increase bandwidth efficiency. However, FFR and SFR are not able to dynamically adapt to situations where the throughput demands or the UE positions are not homogeneously distributed between the different cells.

Within this category, several techniques are proposed to improve the performance of the traditional FFR and SFR schemes. For instance, resource allocation and interference coordination problems are jointly considered in [Ass08]. The proposed scheme is based on FFR, and it searches for the optimal dimensions of cell-center and cell-edge zones as well as the optimal frequency reuse factor. In [GGLBL13], a multi-objective algorithm

for improving SFR performance is proposed. It addresses the tradeoff between enhancing network capacity and improving cell-edge performance. From an operator perspective, SFR optimization is a problem in which the interest is placed not only in maximizing the overall network spectral efficiency, but also in guaranteeing to UEs a certain levels of QoS, at the lowest possible cost. It enhances the performance of SFR in realistic irregular cellular networks by simultaneously improving the system spectral efficiency and reducing ICI in the cell-edge zone.

2.2.2 Cooperative Approaches

Cooperative ICIC techniques make use of the communications between the neighboring cells in order to mitigate ICI. Resource allocation becomes more efficient when additional information about resource usage, power allocation, and UE throughput demands are exchanged between adjacent cells.

An interference avoidance scheme is presented in [RY10] where the objective is to mitigate interference for cell-edge UEs without reducing network throughput. The proposed scheme is comprised of a two-level algorithm: one at the base station level and the other at a central controller to which a group of base stations are connected. First, each cell calculates its own restrictions on resource allocation locally, after receiving channel quality information from its active UEs. These decisions are forwarded to a centralized entity that processes requests from several adjacent sectors, and the final restrictions on resource allocation are sent by the control entity to each of the concerned sectors.

In [LJC11], a cooperative ICIC scheme for the downlink of LTE femtocells is introduced. A dedicated signaling channel is established over the X2 interface in order to exchange information related to inter-cell interference and traffic load of each cell. An optimization problem that maximizes the sum of the logarithmic rate of all UEs is formulated. Resource and power allocation procedure is divided into two steps. In the first step, resources are allocated to the active UEs using a proportional fair scheduling technique, while in the second step, power allocation is performed on the scheduled resources by solving the Lagrangian of the maximization problem using the Karush-Kuhn-Tucker conditions.

2.2.3 Frequency Scheduling Techniques

A simple manner to achieve interference mitigation is by performing frequency scheduling that takes into account information concerning channel quality and interference. A centralized downlink proportional fair scheduling is proposed in [YC11], where interference mitigation in heterogeneous networks of macro and femto cells is addressed. It allows each cell to be aware of its neighboring dominant interfering base stations. Dominant interferers are identified based on their received signal power, with respect to a predefined interference threshold. A proportional fair scheduler running at the central control entity allocates the available resources to the active UEs based on the received interference and CQI information. Hence, resources allocated to a UE will not be simultaneously scheduled to its dominant interferers, and ICI is reduced.

2.2.4 Femtocell-Aware Techniques

Small cells, including picocells and femtocells, are deployed to enhance the coverage of the existing macrocells, and to improve the spectral efficiency. Nevertheless, this deployment leads to significant interference in such heterogeneous networks. Femotcell-aware ICIC techniques modify resource allocation between the macro LTE/LTE-A cells and the small cells deployed within their coverage area.

In [WZJW09], the available spectrum is divided into a macro-dedicated portion and a femto-sharing portion. A list of macro UEs that are potential interferes to nearby femtocells is identified. The idea is to allocate resources from the macro-dedicated spectrum to these UEs, while other UEs can be allocated resources from the macro-dedicated and from the femto-sharing portions. Within the same context, two resource allocation approaches are proposed in [PCVC14]. The first one is autonomous, and it does not imply communication among femtocells. Thus, each femtocell independently takes its own scheduling decisions. An optimization problem that aims at minimizing the downlink transmission power is formulated, and it is solved by each femtocell using local information only. The second approach is cooperative, where the neighboring cells coordinate their resource allocation to cell-edge UEs through a message passing approach over the femtocell gateway. It is recommended when the femtocells have sufficiently high bandwidth and low latency at the backhaul. The coordination is realized by adding an additional constraint to the

optimization problem of the autonomous approach. It guarantees that power constraints imposed by the neighboring cells are fulfilled at the local femtocell.

2.2.5 Graph Theory

When a multitude of small cells are randomly deployed within the coverage area of an LTE/LTE-A network, managing interference problems between these cells becomes very complicated. In this case, the resource allocation problem can be solved using graph theory, where a graph is used to represent the interference relationships.

In [Nec09], the scheduling process is divided into two parts. First, a graph is created based on the interference relations among all UEs. Its edges represent critical interference relations in-between UEs *i.e.*, those who are connected must not be served by the same set of resources. Second, a graph coloring algorithm is used to assign resources to the active UEs, while taking into account constraints related to the interference graph. Similarly, a two-steps approach based on graph theory is presented in [CTZK09]. In the first step, an interference graph is constructed by connecting the interfering UEs. Moreover, each edge is given an integer cost or weight that characterizes the potential interference between two UEs. It is inferred from the geographical locations of the UEs. In the second step, resource allocation is performed by finding among the possible resource assignments, the one that best leverages the instantaneous channel quality. In [LCN+12], each node of the interference graph represents a base station, and each link indicates that the two connected nodes are interfering with each other. The proposed graph coloring approach maximizes the number of colors assigned for resource allocation. An optimization problem that aims at maximizing the usage of the available resources is formulated, with constraints related to interference and QoS requirements. For instance, two linked nodes are not assigned the same color. Although this approach improves the spectral efficiency, a centralized system implementation is required. A large amount of signaling overhead is generated, and the overall complexity is prohibitively high.

2.2.6 Game Theory

Game theory is a mathematical modeling tool that helps to achieve equilibrium among multiple decision-makers. It assigns a strategy so that each decision-maker cannot increase the payoff by changing its strategy while others maintain theirs. In resource allocation scenarios, decision-makers are the base stations, and the strategies correspond to resource management.

In [ZCA15], a stochastic game theory-based approach is formulated to investigate the optimal channel selection in dynamic network environment. Each cell is modeled as a game player, that independently selects its best channel for transmission. A state-based utility function is defined for each cell, where the target is minimizing the received interference. Each player autonomously tunes its channel strategy to maximize its expected utility. It is proven that the proposed game has at least one pure strategy Nash equilibrium point that minimizes the expected network interference, either globally or locally. Within the same context, authors of [IWAYB13] propose a resource allocation algorithm based on cooperative game theory. The cooperative game is a competition between coalitions of players rather than between individual players. At the first level, a fair resource distribution among flow classes is performed. A cooperative game is used to form coalitions between the flow classes (the players) to distribute the available bandwidth among them. At the second level, each flow class distributes its corresponding portion of resources to all the flows belonging to it.

2.2.7 Convex Optimization

Resource and power allocation problem can be formulated as a constrained maximization of an objective function. Convex optimization problems [Ber99, BV09] consist in minimizing a convex function (or maximizing a concave function) over a convex constraint set. Moreover, we can make use of Lagrange duality properties to link the original problem into a dual problem. This leads to iterative algorithms that converge to the global optimum [PC06].

Energy-efficient resource and power allocation for a cluster of coordinated cells is considered in [VZRB15]. A global energy efficiency for the noise-limited regime is defined, and ICI is neglected. The concave objective function is maximized under constraints

related to the downlink transmission power allocation. The proposed algorithms run in a centralized controller that collects channel measurements from the different eNodeBs. Similarly, a convex optimization problem is formulated in [XLZ+12], where a single cell OFDMA network is considered. The energy efficiency objective function is studied and a low-complexity suboptimal algorithm is proposed to reduce the computational burden of the optimal solution.

Table 2.1: Surveyed ICIC Techniques

ICIC Class	**Example**	**Description**
Frequency Reuse	[Hua05]	• SFR as proposed by Huawei for LTE UTRAN.
	[Ass08]	• FFR-based ICIC technique. • Optimal dimension of the cell-center and cell-edge zones. • Optimal frequency reuse factor for the cell-edge zone.
	[GGLBL13]	• SFR-based ICIC technique. • Multi-objective optimization of SFR parameters. • Improving spectral efficiency and reducing ICI.
Cooperative	[RY10]	• Local decisions made by each base station. • Control entity forwards restrictions on resource allocation to each cell.
	[LJC11]	• Exchanging interference and load information over X2 interface. • Proportional fair scheduling and power allocation based on a Lagrangian method.
Frequency Scheduling	[YC11]	• Centralized resource allocation using CQI and interference information.

Femtocell-Aware	[WZJW09]	• The available spectrum is divided into macro-dedicated portion and femto-sharing portion. • Interfering macro UEs are assigned resources from the macro-dedicated spectrum, while other UEs are assigned resources from the two portions.
	[PCVC14]	• Power minimization through autonomous and coordinated ICIC approaches. • The coordinated approach outperforms the autonomous approach at the expense of inter-cell communication.
Graph Theory	[Nec09]	• Creating a graph based on the interference relations between UEs. • Allocating the resources to the active UEs using a graph coloring algorithm.
	[CTZK09]	• Constructing the weighted interference graph between the interfering UEs. • Finding the resource allocation that best leverages the instantaneous channel quality.
	[LCN+12]	• Interference graph coloring approach that maximizes the spectral efficiency. • Centralized system implementation to solve the proposed optimization problem.
Game Theory	[ZCA15]	• Each cell autonomously adjusts its resource allocation strategy to maximize its own utility. • The Nash equilibrium minimizes the expected network interference either globally or locally.

Game Theory	[IWAYB13]	• Resource allocation based on a cooperative game, where the players are the flow classes. • Competition between coalitions of players. • Small number of players and reduced complexity.
Convex Optimization	[VZRB15]	• Energy efficiency maximization for a cluster of coordinated cells. • Noise-limited energy efficiency function is defined, and ICI is neglected.
	[XLZ+12]	• A single cell OFDMA network is considered. • Energy efficiency is maximized. • Low-complexity suboptimal algorithm is proposed to reduce the computational burden.
Power Minimization	[PCVC14]	• Joint resource and power allocation problem independently solved at each base station. • Minimize the total transmission power subject to throughput demands constraints.
	[YLIK14]	• Downlink power control algorithm using CQI feedbacks. • Improving energy efficiency and reducing ICI.

2.2.8 Power Minimization Approaches

We also identify another category of ICIC techniques that avoid ICI by reducing the transmission power of the base stations. Transmission power adjustment will potentially reduce the interference caused to the neighboring cells.

An optimization problem is defined in [PCVC14], where the objective is to minimize the required transmission power for the base station. Resources and transmission powers

are jointly allocated, and constraints on the minimum throughput per UE and on the transmission power of each base station are defined. The proposed scheme runs independently at each base station, but some signaling overhead is required in order to exchange information related to the maximum transmission power estimated at each cell. These information are taken into account by the neighboring cells when locally solving their joint resource and power allocation problem. In [YLIK14], a heuristic downlink power allocation strategy is introduced. Power is allocated to each resource according to the received CQI feedbacks. It is a distributed algorithm that operates independently of the chosen scheduler, and it aims at avoiding the power wastage. Results show that the energy efficiency is improved, and ICI is reduced.

2.3 Comparative Analysis of ICIC Techniques in LTE Networks

Several works surveyed the existing ICIC techniques and classified them according to cell cooperation and frequency reuse such as [FKR+09, HKHE13]. However, some of them only report qualitative comparisons of the existing ICIC techniques; while others perform simulations under uniform UE distributions and ordinary network scenarios. In the following, we investigate several interference mitigation techniques under various UE distributions, and we show the impact of each technique on throughput distribution and throughput fairness among all the active UEs. This analysis highlights the efficiency of each technique for each of the simulated scenarios.

2.3.1 Frequency Planning Techniques for GSM Networks

In GSM, frequency allocation is planned taking into account the following issues: radio coverage, interference estimation and traffic distribution [DPMZ98]. Traditionally, adjacent GSM cells are grouped into clusters where only a portion of the available spectrum is used in each cell. Therefore, we reduce ICI since frequency resources are not simultaneously used by adjacent base stations. If m is the number of cells within a cluster (also called: cluster size), then $\frac{1}{m}$ of the available subcarriers are used in each cell according to frequency reuse-m model. Figure 2.4 illustrates a GSM network where frequency reuse-3 model is used to manage frequency resources distribution between the different cells.

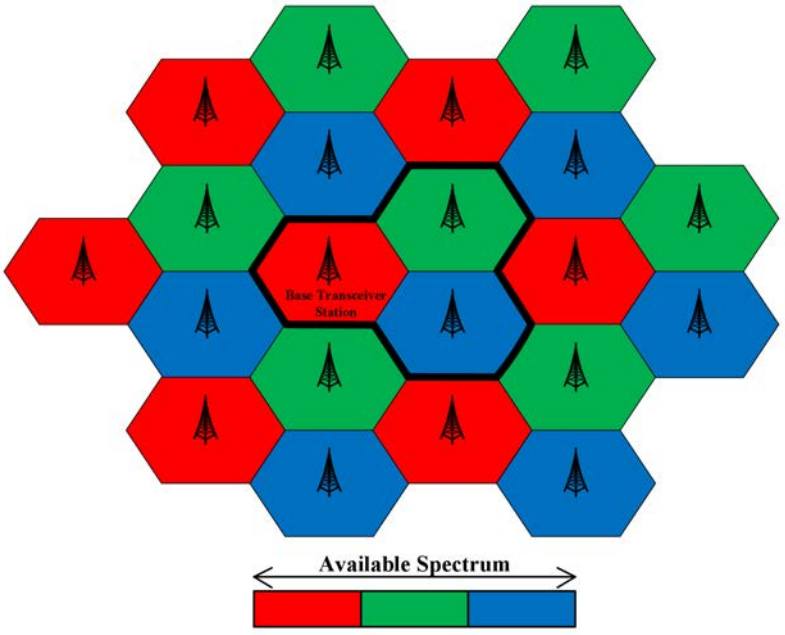

Figure 2.4: The frequency reuse-3 model in GSM

Although frequency reuse-m model mitigates ICI, the main disadvantage of such technique is that it reduces network capacity. With less resources available in each cell, the operator is not able to accommodate all the existing UEs. Thus the quality of the provided services is degraded, and user satisfaction is reduced, especially when the number of UEs per cell increases. A possible alternative is to reduce cluster size when the number of UEs or their generated traffic increases. Thus, frequency planning in GSM can be seen as a compromise between network capacity and interference mitigation.

A dynamic channel allocation strategy is introduced in [DPMPS97] where authors use the information exchanged between base stations in order to avoid conflicting carrier acquisitions. Frequency allocation between the different cells is tuned in real time, based on the average traffic and UE speed in the cells. Multiple reuse patterns is another method to achieve high capacity using tight frequency reuse in combination with frequency hopping [EJK$^+$98]. The idea is to apply an advanced frequency planning method, based on the usage of different separate reuse patterns, along with frequency hopping in order to combine these reuse patterns into an average reuse. This allows to maximize interference diversity, and to support high traffic levels in the different cells.

2.3.2 ICIC in LTE Networks

Operators of the LTE/LTE-A networks have great interest in implementing ICIC techniques to increase spectrum profitability and to improve UE experience. In this subsection, we provide more details about FFR and SFR techniques that will be compared with the frequency reuse-1 and reuse-3 models via system level simulations.

2.3.2.1 Fractional Frequency Reuse

FFR [HA09] is a traditional static ICIC technique. It does not require any cooperation between network eNodeBs. Each cell is statically divided into cell-center and cell-edge zones. The former contains UEs close to the base station, while the latter contains UEs close to the border of the cell. Since they are closer to the neighboring cells and relatively far from their serving eNodeBs, cell-edge UEs will experience more ICI. Therefore, the main objective of FFR is to protect RBs attributed for these UEs from interference problems.

FFR modifies RBs distribution between the different zones of the cell in order to create a *protected* set of RBs for cell-edge UEs. Figure 2.5 illustrates a cluster of three LTE cells where spectrum allocation between cell-center and cell-edge zones is done according to FFR technique. Cell-center UEs are also called full reuse UEs since their allocated spectrum is used according to frequency reuse-1 model in the neighboring cells. RBs allocated for the protected UEs are called partial reuse RBs since their usage in the adjacent cells is based on frequency reuse-3 model.

Although FFR reduces ICI for cell-edge UEs, the main drawback of this static ICIC technique is that it does not dynamically adapt RB distribution between cell zones according to users demands in each zone. In addition, UE geographical classification requires the knowledge of the exact position of all the active UEs in the network. Thus, an additional positioning information is required to determine cell-center and cell-edge UEs.

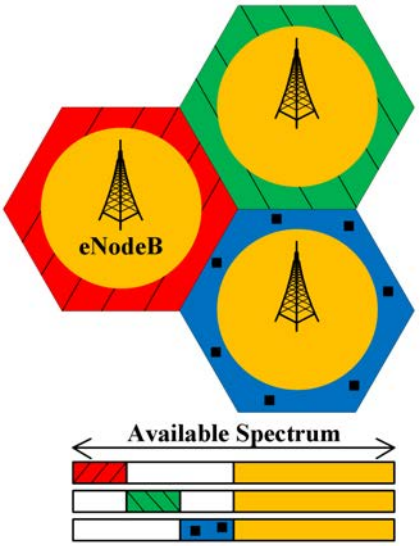

Figure 2.5: Fractional frequency reuse technique

2.3.2.2 Soft Frequency Reuse

SFR is another static ICIC technique where both RB distribution and downlink power allocation are performed to reduce ICI [QZXB12]. On the downlink of a multiuser OFDMA system, such as LTE, Signal to Interference and Noise Ratio (SINR) for a UE k on the RB n in the cell i is given by:

$$\mathrm{SINR}^{i}_{k,n} = \frac{P^{i}_{n} \cdot G^{i}_{k,n}}{\sum\limits_{j \neq i} P^{j}_{n} \cdot G^{j}_{k,n} + P_{TN}}, \tag{2.1}$$

where P^{i}_{n} is the downlink transmission power allocated by the base station i for the RB n, $G^{i}_{k,n}$ is channel gain for UE k served by eNodeB i on RB n, and P_{TN} is the thermal noise power on the considered RB. The achievable rate on RB n for UE k in the cell i is therefore given by:

$$R^{i}_{k,n} = f(\mathrm{SINR}^{i}_{k,n}), \tag{2.2}$$

where $f(.)$ is the adaptive modulation and coding function that maps SINR to rate. In each cell, a portion of the available spectrum is reserved for cell-edge UEs, and it

is permanently allocated the maximum downlink transmission power. The remaining RBs are allocated for cell-center UEs, but with a lower transmission power [JPJ13]. In addition, there is no common spectrum allocated for cell-edge UEs of the adjacent cells. Figure 2.6 shows the basic principles of SFR technique.

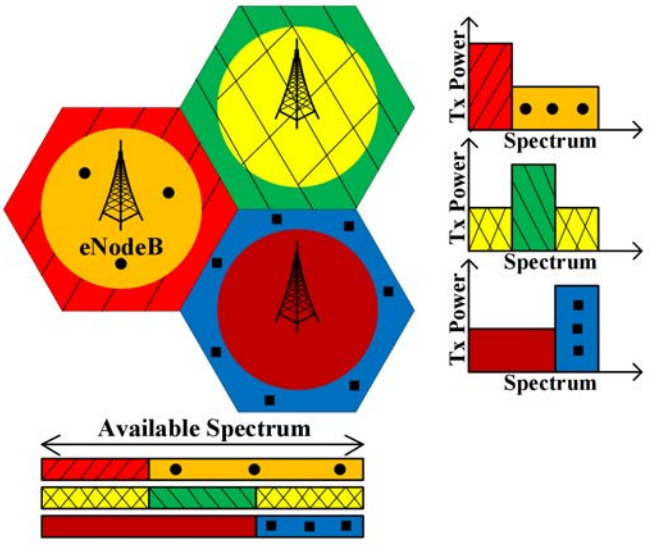

Figure 2.6: Soft frequency reuse technique

For both FFR and SFR techniques, we define $\overline{\text{SINR}}_k^i$ as the mean wideband SINR for UE k served by eNodeB i. It is the mean value of $\text{SINR}_{k,n}^i$ for the considered UE over all the available RBs. This variable gives us information about the average channel quality, radio conditions, and ICI for UE k, since SINR is a function of the useful received power and the interfering received power. Instead of using geographical positions, mean wideband SINR values are used to classify UEs. If mean SINR of a UE is lower than a predefined SINR value called $\text{SINR}_{threshold}$, it is considered as a Bad Radio (BR) conditions UE; otherwise, it is classified as Good Radio (GR) conditions UE. BR UEs are commonly known as cell-edge UEs, while the remaining UEs are called cell-center UEs.

2.4 System Model

2.4.1 Deployment Model

Our system model consists of seven adjacent macro base stations serving active UEs within their coverage area. Base station coverage is modeled as a sectorized hexagonal layout, as shown in Fig. 2.7, and CI denotes the cell identifier. Each site consists of three adjacent hexagonal sectors, where each sector is served by an eNodeB having its own scheduler, bandwidth, and power allocation policy.

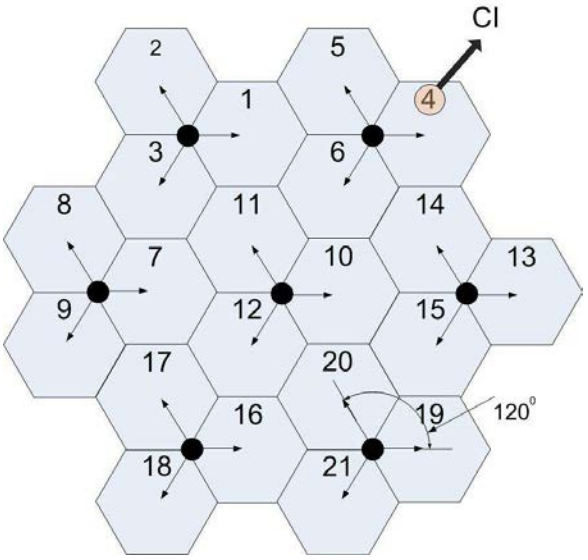

Figure 2.7: Cell layout

2.4.2 Propagation Model

The system developed is based on the home eNodeB to UE path loss models. The considered models are mentioned in [3GP06b] and [3GP06c]. Path loss calculation for signals traveling from the serving eNodeB to the UE is given by:

$$PL = 15.3 + 37.6 \log_{10}(D), \tag{2.3}$$

where PL is the path loss from eNodeB to UE, and D (in meters) is the distance between the active UE and its serving eNodeB.

Table 2.2: SINR-Data Rate Mapping Table

Minimum SINR [dB]	**Modulation and Coding Scheme**	**Data Rate [kbit/s]**
1.7	QPSK(1/2)	168
3.7	QPSK(2/3)	224
4.5	QPSK(3/4)	252
7.2	16QAM(1/2)	336
9.5	16QAM(2/3)	448
10.7	16QAM(3/4)	504
14.8	64QAM(2/3)	672
16.1	64QAM(3/4)	756

2.4.3 Antenna Gain Model

Antenna pattern can be expressed as following:

$$A(\theta) = -\min(12(\frac{\theta}{\theta_{3dB}})^2, 20) \text{ [in dB]}, \tag{2.4}$$

$$-180^\circ < \theta < 180^\circ, \tag{2.5}$$

where $A(\theta)$ is antenna gain, and θ_{3dB} is the beamwidth, which is equal to 70°.

2.4.4 SINR-Data Rate Mapping

As stated in (2.2), the value of achievable data rate that can be attained by a UE is a function of the SINR value. Table 2.2 shows the mapping of SINR values to the data rates per RB [RBSP09]. In our simulations, the single antenna transmission scheme is used. It is the transmission mode 1 as specified by 3GPP [3GP13].

2.4.5 UE Distribution

Given the impact of UE distribution between cell zones on ICIC techniques performance, we consider the percentage of GR or BR UEs as an essential parameter to evaluate the compared techniques. In fact, UEs geographical positions, as well as UE distribution between cell zones have a great impact on ICI, and on the achievable throughput in each

zone. Various UE distributions are considered in our simulations. We simulate scenarios where UEs are uniformly distributed between GR and BR zones, and other scenarios characterized by non-homogeneous UE distributions. For instance, the majority of active UEs are either in GR zone or in BR zone.

2.5 Simulation Scenarios

2.5.1 Simulation Environment

We use a MATLAB-based LTE downlink system level simulator [VUT14, IWR10], developed by Vienna University of Technology as the simulation platform. Frequency reuse-1 model and FFR technique are included in the original version of the simulator. However, homogeneous power allocation is only considered. We adjusted the power allocation scheme in order to allow allocating different power levels to the available RBs. We have also integrated SFR technique and reuse-3 model along with the existing FFR and reuse-1 schemes. Simulation parameters for the simulated LTE system [3GP06a, 3GP10] and the ICIC techniques are summarized in Table 2.3.

Cell geometry for our simulated LTE system is hexagonal, and each LTE site consists of three adjacent hexagonal sectors, where each sector is served by an eNodeB. Sectors are equipped with 120° directional transmit antennas with an azimuth offset of 30°. eNodeBs cover a specific area in which many UEs are located. At the UE side, SINR is calculated in the link measurement model. It is determined by the useful signal, interference and noise power; thus, it depends on network layout, path loss, shadow fading and time-variant small-scale fading [ZM05]. The macroscopic path loss between eNodeB and UE includes both the propagation path loss due to the distance and the antenna gain. CQI feedbacks are generated using an SINR-to-CQI mapping and made available to the eNodeB via a feedback channel with adjustable delay. CQI is used to select the appropriate modulation and coding scheme to achieve the target block error rate.

Inter-eNodeB distance equals 500 m, which corresponds to an LTE network deployed in an urban area. In each cell, 25 RBs are available, since the operating bandwidth equals 5 MHz [EDB07]. However, traffic model is full buffer *i.e.*, all the available RBs are

permanently allocated for the active UEs in the network. UE scheduling is performed every one millisecond. Path loss model is the one defined by 3GPP in [3GP06c, 3GP06b], and feedback reception at eNodeBs is delayed by three milliseconds. When homogeneous power allocation is used, the maximum downlink transmission power is allocated for each RB. However, SFR reduces the transmission power allocated for RBs used by GR UEs. $\text{SINR}_{threshold}$ is a predefined parameter, used to classify active UEs into GR and BR UEs. It can be adjusted by mobile network operators according to network load and UE satisfaction.

Unlike traditional works where the proposed interference mitigation technique is compared to reuse-1 and reuse-m models under ordinary network conditions (*e.g.*, homogeneous UE density and uniform UE distribution), we investigate ICIC techniques under various simulation scenarios. We study the impact of network load (number of UEs per eNodeB) and UE distribution (percentage of GR UEs in the network) on system performance for each of the compared techniques. For instance, we consider homogeneous UE density among all the cells, and we start increasing the number of active UEs per cell. Therefore, we show the impact of network load on UE satisfaction for reuse-1 model and other ICIC schemes. This study allows us to choose the most adequate technique for each network load scenario. In other words, we will be able to select the ICIC technique that improves system performance when the network is highly loaded, as well as the technique that offers a better performance for low load scenarios. In addition, we consider not only uniform UE distributions, but also scenarios where UEs are not uniformly distributed between cell-zones. Thus, we study the impact of UE distribution on the chosen ICIC technique, and we show the evolution of system performance when the percentage of GR UEs changes.

2.5.2 Performance Metrics

In order to compare the performance of the studied techniques, we define the following performance comparison criteria:

Table 2.3: Simulation Parameters

Parameter	**Value**	**Description**
Cell geometry	Hexagonal	A cell is served by an eNodeB
Number of sites	7	—
Inter-eNodeB distance	500 m	Urban area
Operating bandwidth	5 MHz	—
Number of RBs	25	In the 5 MHz bandwidth
Transmission frequency	2 GHz	—
Subcarrier frequency	15 kHz	1 RB = 12 sub-carriers
RB bandwidth	180 kHz	1215 kHz
TTI	1 ms	Transmit Time Interval
Thermal noise density	-174 dBm/Hz	—
Feedback delay	3 ms	3 TTIs
Scheduler	Round Robin	—
Traffic model	Full buffer	—
eNodeB maximum power (P_t)	20 W	43 dBm
Maximum power per RB (P_{RB})	0.8 W	$P_{RB} = \frac{P_t}{\text{nb. of RBs}}$
$\text{SINR}_{\text{threshold}}$	5 dB	UE classification [KHH$^+$12, Fuj11]
SFR power ratio	0.25	$P_{GR} = \frac{P_{RB}}{4}$
Number of UEs per sector	2, 5, 7, 10, 15, 20	Impact of network load
Antenna gain	14 dBi	—
Penetration Loss ($PenL$)	10 dB	—
Pathloss model	$15.3 + 37.6 \log_{10}(D)$	As in [3GP06b, 3GP06c]; D in m
Simulation time	1000 TTIs	—

2.5.2.1 Spectral Efficiency and Energy Efficiency

Let $\mathcal{K}$ denote the set of active UEs in the network, $\mathcal{I}$ the set of eNodeBs, and $\mathcal{N}$ the set of available RBs in each cell. $\overline{R}_k$ is the mean throughput achieved by UE k, and P_n^i the downlink transmission power allocated by cell i to RB n. Spectral efficiency and energy efficiency are therefore defined as follows:

$$\text{Spectral efficiency} = \frac{\sum_{k=1}^{|\mathcal{K}|} \overline{R}_k \text{ [bit/s]}}{\text{Total spectrum [Hz]}}, \tag{2.6}$$

$$\text{Energy efficiency} = \frac{\sum_{k=1}^{|\mathcal{K}|} \overline{R}_k \text{ [bit/s]}}{\sum_{i=1}^{|\mathcal{I}|} \sum_{n=1}^{|\mathcal{N}|} P_n^i \text{ [W]}}. \tag{2.7}$$

2.5.2.2 UE Throughput

In order to investigate the impact of each technique on UE performance in each zone and on the overall system performance, we use the following metrics:

- *Mean throughput per UE* [Mbit/s]
- *Mean throughput per GR UE* [Mbit/s]
- *Mean throughput per BR UE* [Mbit/s]

For each simulation run, mean throughput is the average throughput achieved by UEs throughout the simulation time. These three metrics give an overview about how the throughput of each zone is modified when applying an ICIC technique. Thus, they allow to carry out a more detailed performance comparison using significant throughput information.

2.5.2.3 Fairness Index

Fairness in resource sharing is an important performance comparison parameter. Jain's fairness index [JCH84] is given by:

$$\mathrm{J}(\overline{R}_1, \overline{R}_2, ..., \overline{R}_{|K|}) = \frac{(\sum_{k=1}^{|\mathcal{K}|} \overline{R}_k)^2}{|\mathcal{K}|. \sum_{k=1}^{|\mathcal{K}|} \overline{R}_k^2}, \tag{2.8}$$

where J rates the fairness of a set of throughput values; $|\mathcal{K}|$ is the number of UEs, and $\overline{R}_k$ is the mean throughput of UE k. Jain's fairness index ranges from $\frac{1}{|\mathcal{K}|}$ (worst case) to 1 (best case). It reaches its maximum value when all UEs receive the same throughput. An efficient ICIC technique reduces the difference between the mean GR throughput and the mean BR throughput, and increases Jain's fairness index.

2.5.2.4 UE Satisfaction

We define a satisfaction throughput threshold as the reference value for performance comparison. It is the minimum throughput value required to guarantee an acceptable

quality of service. A UE is qualified as satisfied if its average throughput is higher than satisfaction threshold; otherwise, this UE will be considered as unsatisfied.

The percentage of unsatisfied UEs among all the active UEs in the network is another parameter for performance comparison. An ICIC technique is better than other state-of-the-art techniques when it shows the lowest percentage of unsatisfied UEs. We also investigate the evolution of this percentage when network load increases.

2.5.2.5 Throughput Cumulative Distribution Function (CDF)

This metric shows UE throughput distribution for the studied ICIC techniques. For a given throughput value, CDF represents the probability to find a UE characterized by a lower throughput. Therefore, when comparing interference mitigation techniques, the best one is the one showing the lowest CDF for all throughput values.

2.6 Simulation Results and Analysis

2.6.1 Spectral Efficiency versus Energy Efficiency

We simulate an LTE network that consists of seven adjacent sites, with 10 UEs randomly placed in each cell. Simulation time is 100 TTIs. Traffic model is full buffer, and all the available RBs are assigned to the active UEs. Consequently, inter-cell interference occur over all the available RBs, since they are permanently used for downlink transmissions, even when the number of UEs per cell is low. Simulations are repeated 100 times, where UE positions and radio conditions are randomly generated each time. The simulation results are illustrated in Fig. 2.8.

The frequency reuse-1 model shows the lowest energy efficiency, since the maximum downlink transmission power is permanently allocated to all the available RBs. However, its spectral efficiency is comparable to that of SFR, and higher than that of FFR and reuse-3 models: reuse-1 makes maximum use of the existing RBs, without any constraint on frequency usage. FFR technique reduces power consumption, and improves energy efficiency in comparison with reuse-1 model. Nevertheless, there is an unused frequency sub-band in each cell; thus, spectral efficiency is reduced.

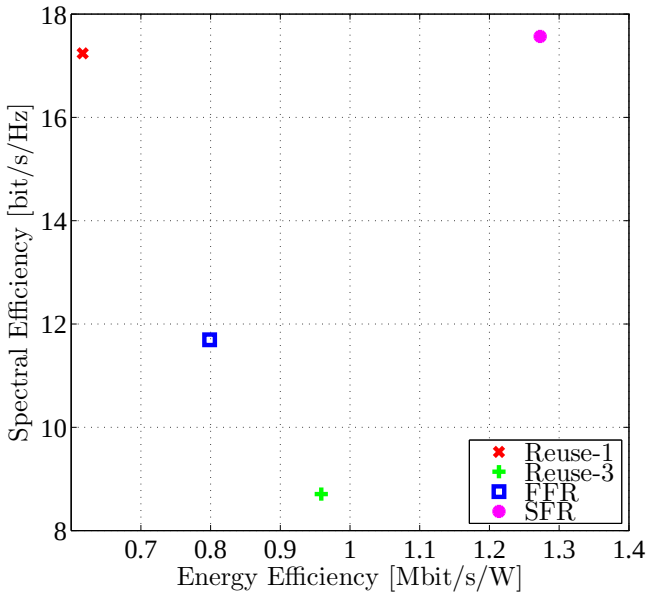

Figure 2.8: Spectral efficiency versus energy efficiency

Reuse-3 model shows the lowest spectral efficiency: only one third of the available spectrum is used in each cell (for a cluster of three adjacent cells), while it increases energy efficiency in comparison with reuse-1 and FFR. SFR improves both spectral and energy efficiencies, in comparison with dense frequency reuse model and other ICIC techniques. It uses a frequency reuse factor of one with restrictions on power allocation; thus, it is able to improve energy efficiency without sacrificing spectral efficiency.

2.6.2 Mean Throughput per Zone

For the same simulated network, we study the impact of each of the compared techniques on UE throughput in GR and BR zones. Mean throughput for GR and BR zones as well as mean throughput per UE are shown in Fig. 2.9.

We notice that FFR technique improves BR UEs throughput, in comparison with reuse-1, reuse-3 and SFR techniques. It prohibits the usage of the same sub-band not only in adjacent BR zones, but also in any other GR zone of the considered cluster. Although ICI is mitigated for BR UEs, frequency sub-bands availability in GR zones is reduced, and FFR reduces the average throughput per UE when compared to the frequency reuse-1 model. The frequency reuse-3 model has a negative impact on system performance, since only one third of the available spectrum is used by active UEs in each cell. Thus, mean throughput per UE reaches its lowest value with reuse-3 model. SFR technique

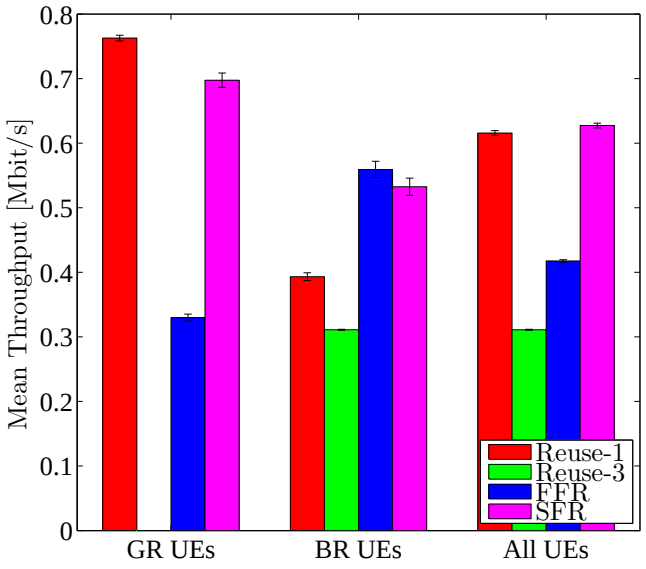

Figure 2.9: Mean Throughput per GR, BR, and all UEs

improves BR UEs throughput without reducing mean throughput per UE for the entire network. The power allocation strategy applied by SFR reduces ICI for BR UEs. Thus, it maximizes the usage of the available spectrum in all network cells, and reduces ICI simultaneously.

2.6.3 Throughput Cumulative Distribution Function

We report throughput CDF for the compared techniques, under the same simulation scenario. It allows us to study throughput distribution among active UEs in the network. CDF for reuse-1, reuse-3, FFR, and SFR techniques is illustrated in Fig. 2.10.

For a given throughput value, CDF represents the probability to find a UE characterized by a lower throughput. The lower the CDF is, the better the quality of service is. We notice that throughput CDF of reuse-3 model is the first to reach the maximum. In other words, the probability to find a UE served with a throughput less than 1 Mbit/s tends to one. FFR improves throughput CDF function in comparison with reuse-3. However, it reaches the maximum before reuse-1 CDF. When using SFR, the number of UEs suffering from bad quality of service is reduced. For relatively low throughput values (less than 1 Mbit/s) throughput CDF for SFR is the lowest curve; thus, it shows the lowest percentage of UEs served with low throughputs. Moreover, SFR curve is the last one to reach its maximum (at 3 Mbit/s approximately). Consequently, when

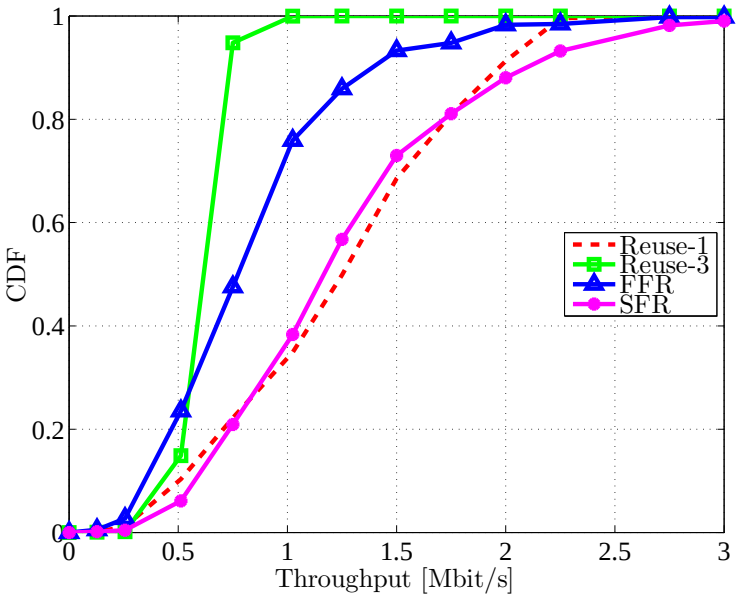

Figure 2.10: Throughput cumulative distribution function

mobile network operators seek to improve throughput CDF for the entire system, SFR is the most adequate technique among the compared ICIC schemes. It succeeds in reducing the percentage of UEs with relatively low throughputs, while also improving the maximum achievable throughput in the network. Through restrictions made on downlink transmission power allocation, SFR reduces ICI for BR UEs, and provides enough bandwidth for GR UEs to achieve higher data rates.

2.6.4 UE Satisfaction versus Network Load

In this paragraph, we compare the percentage of unsatisfied UEs for each technique. The simulated network consists of seven adjacent hexagonal LTE cells. We simulate several scenarios, with increasing number of UEs per cell. The simulation results are illustrated in Fig. 2.11. Satisfaction throughput threshold is set to 512 kbit/s. We assume that the average throughput per UE is required to be higher than 512 kbit/s in order to fulfill its downlink data traffic demands. Otherwise, the UE is considered as an unsatisfied UE.

We notice that reuse-3 model shows the lowest percentage of unsatisfied UEs for low network loads. When each cell is using a disjoint part of the spectrum, ICI problems are almost eliminated. However, the percentage of unsatisfied UEs becomes the highest among all the compared techniques when the network load increases. Only one third of

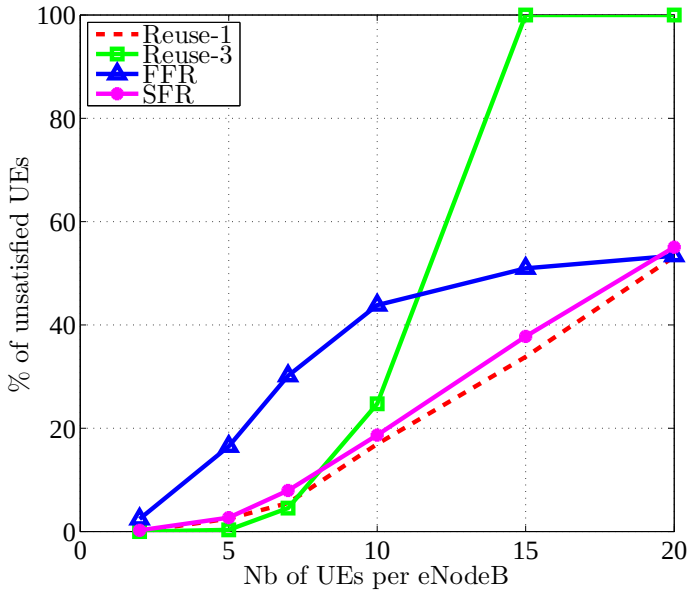

Figure 2.11: UE satisfaction versus network load

the available spectrum is used in each cell; thus, network capacity and UE satisfaction are reduced when network load increases.

Despite of the power reduction over RBs allocated for GR UEs, SFR shows approximately the same percentage of unsatisfied UEs as for reuse-1 model. The power allocation strategy reduces ICI, especially for BR UEs, and GR throughput loss is compensated. Compared to reuse-1 model, FFR increases the percentage of unsatisfied UEs, due to restrictions on RB usage between network cells. A portion of the available spectrum is not allowed to be used in each cell. When network load increases, FFR performance exceeds that of the frequency reuse-3 model. It is a compromise between reuse-1 model and reuse-3 model. In fact, when using FFR, we guarantee that BR UEs of adjacent cells operate on disjoint spectrum. Thus, it makes use of the main advantage of reuse-3 model: ICI is mitigated for BR UEs. Moreover, it avoids the disadvantage of reuse-3 model *i.e.*, the lack of RBs available in each cell, by allowing the usage of reuse-1 model in GR zones of the neighboring cells.

2.6.5 UE Satisfaction versus UE Distribution

In this paragraph, UE positions are generated in a manner that the percentage of GR UEs varies between 20% and 80%. We consider seven adjacent cells with 10 UEs in each cell. For each UE distribution (percentage of GR UEs), simulations are repeated 100 times,

and the obtained results are reported in Fig. 2.12. The particularity of our work is that we compare the performance of different ICIC techniques under both homogeneous and non-homogeneous UE distributions. When UEs are homogeneously distributed between cell zones, half of the active UEs are GR UEs, while the other half are BR UEs.

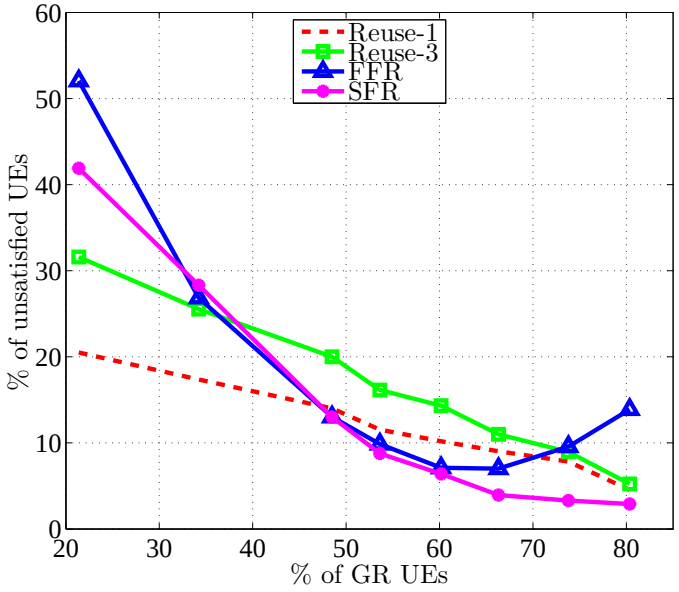

Figure 2.12: UE satisfaction versus percentage of GR UEs

We notice that FFR reduces the percentage of unsatisfied UEs in the network when their distribution is approximately homogeneous between BR and GR zones. It improves system performance in comparison with the frequency reuse-1 model when 50% to 70% of active UEs are GR UEs. However, when the majority of active UEs are either in the BR zone, or in the GR zone, the percentage of unsatisfied UEs exceeds that of reuse-1 model. FFR is a static technique, and RB distribution among GR and BR zones is not dynamically adjusted according to UE distribution. SFR suffers from the same limitation caused by its static aspect. In fact, UE satisfaction is not better than that of the frequency reuse-1 model when the majority of UEs are BR UEs. However, SFR reduces the percentage of unsatisfied UEs when more than 50% of active UEs are GR UEs. The frequency reuse-3 model increases the percentage of unsatisfied UEs when compared to reuse-1 model, for all UE distributions. Restrictions made on RB usage in each cell reduces spectrum profitability, which in turn has a negative impact on the achievable throughput.

We also conclude that static configuration parameters for FFR and SFR can be adjusted

to meet UE distribution between BR and GR zones. The choice of these tuning parameters [HA09, Ass08] is made by mobile network operators according to quality of service requirements and deployment scenarios.

2.6.6 Fairness Index versus UE Distribution

For the same simulation scenario, we study UEs throughput fairness index when the percentage of GR UEs in the network changes. The simulation results are shown in Fig. 2.13.

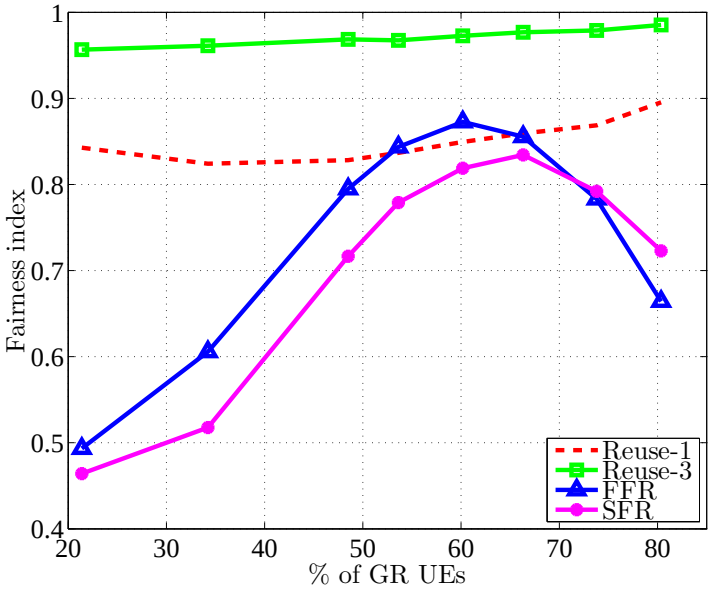

Figure 2.13: Fairness index versus percentage of GR UEs

The frequency reuse-3 model shows permanently the highest throughput fairness index among all the studied techniques. It exceeds Jain's fairness index of reuse-1 model, where BR UEs suffer from ICI, which has a negative impact on their throughput, while GR UEs achieve higher throughputs. The static RB and power distributions between BR and GR zones, applied in FFR and SFR, are not adequate for all UE distributions, especially when the majority of active UEs are homogeneously distributed between cell zones. Although they succeed in reducing ICI, FFR and SFR do not improve throughput fairness among all UEs for these particular scenarios. In fact, the tuning parameters of FFR and SFR techniques, such as the portion of the available spectrum allocated to each cell zone, should be modified to meet UEs throughput demands in each zone. Nevertheless, FFR improves Jain's fairness index in comparison with reuse-1 model when 55% to 65% of UEs

are GR UEs. Thus, FFR tuning parameters should be adjusted according to network load and UE distribution between the different zones.

2.6.7 Spectral Efficiency and Energy Efficiency versus UE Distribution

We also study the impact of UE distribution on spectral efficiency and energy efficiency, for the frequency reuse-1 model, the frequency reuse-3 model, FFR, and SFR techniques. Simulation results are reported in Fig. 2.14 and Fig. 2.15.

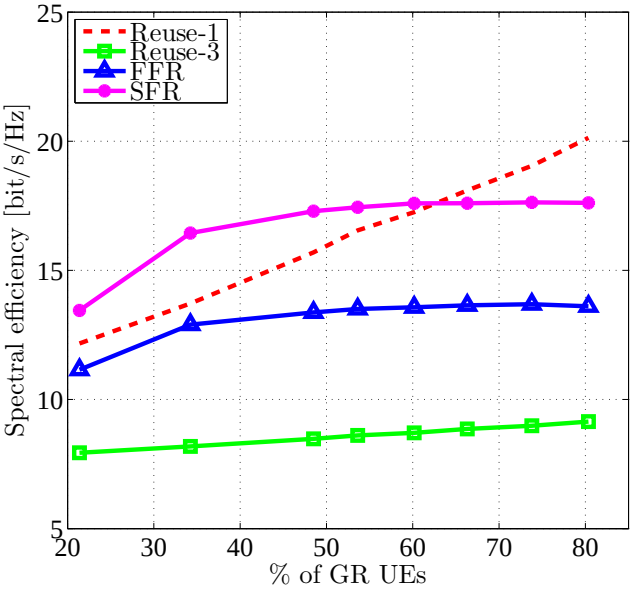

Figure 2.14: Spectral efficiency versus percentage of GR UEs

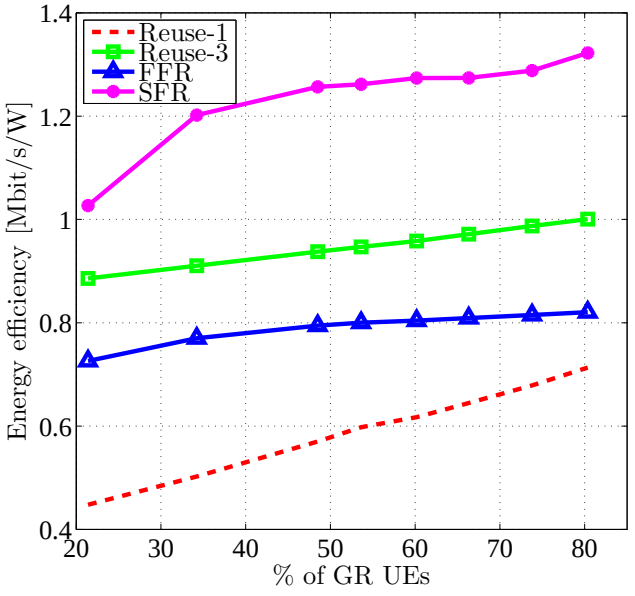

Figure 2.15: Energy efficiency versus percentage of GR UEs

Our results show that SFR has the highest spectral efficiency, since it allows using all the available spectrum in every cell, while imposing restrictions on power allocation for RBs available in each zone. Therefore, it succeeds in reducing ICI while increasing spectral efficiency for all UE distributions, except the case where the majority of UEs are GR UEs: in this case, the frequency reuse-1 model is better since it achieves higher throughputs without the need to reduce downlink transmission power. SFR has also the highest energy efficiency in comparison with the frequency reuse-1 model, the frequency reuse-3 model, and FFR technique.

Energy efficiency for the frequency reuse-3 model exceeds that of the frequency reuse-1 model and FFR technique, since no downlink power consumption is made on unused RBs. Restrictions on RB usage make the frequency reuse-3 model the one with the lowest spectral efficiency: in a cluster of three adjacent cells, only one third of the available spectrum is used in each cell. FFR is a compromise between the frequency reuse-1 model and the frequency reuse-3 model in terms of spectral efficiency and energy efficiency. Indeed, the frequency reuse-1 model is used in GR zones, while the frequency reuse-3 model is used for BR zones of the adjacent cells.

2.7 Conclusion

The increasing demands for data in mobile networks, as well as the exponential growth in mobile applications have lead the mobile network operators to apply dense frequency reuse model to improve spectral efficiency and increase network capacity. However, inter-cell interference problems have a negative impact on UE throughput and system performance. ICIC techniques are proposed to mitigate ICI, and to improve UEs throughput without largely reducing spectral efficiency.

In this chapter, we classified the existing ICIC techniques into several categories, and we surveyed traditional techniques such as the frequency reuse-3 model, FFR, and SFR techniques. These techniques are compared to the frequency reuse-1 model. System-level simulations are made under uniform and non-uniform UE distributions. They allow us to study the performance of each technique, for several parameters: spectral efficiency, energy efficiency, mean throughput per zone, throughput fairness index, and UE satisfaction. The frequency reuse-3 model has the lowest spectral efficiency, while SFR

improves it in comparison with the frequency reuse-1 model. Moreover, we noticed that FFR technique is a compromise between reuse-1 and reuse-3 models in terms of spectral efficiency and energy efficiency. However, FFR and SFR are static ICIC techniques, and they require interventions from mobile network operator to adjust RB allocation and power distribution between cell zones according to UE distribution and quality of service requirements.

In the next chapter, we introduce our proposed centralized multi-cell interference coordination problem. We define the objective function of the joint resource and power allocation problem, under constraints related to resource usage and power allocation. A centralized multi-cell power allocation scheme and a decentralized non-cooperative power allocation scheme are proposed. We investigate the achievable throughput and the spectral efficiency of the proposed techniques, the frequency reuse-1 model, reuse-3 model, FFR, and SFR schemes.

Chapter 3

Centralized versus Decentralized Multi-Cell Resource and Power Allocation

Resource and power allocation techniques are required to alleviate the harmful impact of ICI in multiuser OFDMA networks. Contrarily to the existing techniques that consider single-cell resource and power allocation problem without taking ICI into account, we formulate in this chapter a centralized multi-cell joint resource and power allocation problem. The objective is to maximize system throughput while guaranteeing throughput fairness between UEs. We demonstrate that the joint problem is separable into two independent problems: a resource allocation problem and a power allocation problem. We also propose a decentralized non-cooperative power allocation approach based on game theory. The players are the base stations, and each base station maximizes its own utility function. We investigate the convergence of our proposed centralized and decentralized approaches, and we compare their performance with that of state-of-the-art approaches.

3.1 Introduction

Convex optimization is used to improve the performance of multiuser OFDMA networks, and to alleviate the negative impact of ICI on UE throughput. Resource allocation, power allocation, or joint resource and power allocation problems are usually formulated as nonlinear optimization problems, where the objective consists of maximizing system

throughput, spectral efficiency, or energy efficiency, with constraints on the minimum throughput per UE or other QoS parameters [CTP+07, TLZ08, SAE05]. In fact, improving spectral efficiency is crucial for mobile network operators in order to increase system capacity and UE throughput. Moreover, energy-efficient resource and power allocation is becoming a significant topic for research works [XTL15].

ICIC techniques are essential to improve spectral efficiency, and to increase UE throughput. Moreover, coordinated scheduling, coordinated beamforming, and joint transmission [NBLK14] are seen as important components of ICIC techniques developed for 5G cellular networks. For instance, authors of [HTV14] combine the beamforming technique with resource allocation algorithms in order to improve cell-edge UEs throughput. However, the coordinated approaches generate more sharing of channel information between the network cells. Joint resource and power allocation or distributed power allocation approaches [HRTA14] that guarantee a minimum throughput per UE are among the challenges of 5G networks envisioned to achieve higher data rates, improved end-to-end performance, and reduced energy consumption. The majority of state-of-the-art contributions formulate the resource and power allocation problem for a single cell network [TSAH14, LMB14, XLZ+11], or do not consider the impact of ICI on system performance. For instance, the tradeoff between spectral efficiency and energy efficiency is addressed in [XLZ+11], and a low-complexity suboptimal algorithm is proposed to allocate RBs for practical applications of the tradeoff. However, the system model consists of a single cell OFDMA network, where one subcarrier is assigned to at most one UE. Therefore, ICI problems are not considered.

In this chapter, we formulate the joint resource and power allocation problem for multiuser OFDMA networks, as a centralized optimization problem. We demonstrate that the objective function is separable into two independent optimization problems: a resource allocation problem and a power allocation problem. Our objective is to maximize the achievable throughput for the entire system, while satisfying constraints related to resource usage, SINR, and power allocation. Several adjacent cells share information related to radio conditions and power allocation in order to solve the centralized resource and power allocation problem. We also propose a decentralized power allocation approach that does not rely on centralized controllers. Each base station searches for the power allocation that maximizes its own utility function in a distributed manner. Our major contributions are summarized as follows:

- Propose an original formulation of the centralized joint resource and power allocation problem: instead of considering a single cell OFDMA network, we formulate our problem for a multi-cell OFDMA network. Moreover, ICI problems are taken into account.
- Maximize the mean rate per UE, and ensure a proportional fair rate for all the UEs in the network.
- Prove the convexity of our centralized problem by applying an adequate variable change.
- Decompose the joint resource and power allocation problem into two independent problems.
- Solve the centralized power allocation problem using Lagrange duality theory and subgradient projection method.
- Formulate a novel decentralized super-modular game for resource and power allocation, and propose a best response algorithm to attain the Nash Equilibrium.
- Solve the decentralized power allocation problem using subgradient projection method.
- Validate the convergence of the proposed centralized and decentralized approaches and evaluate their performance in comparison with other state-of-the-art approaches.

3.2 Related Work

Resource and power allocation problem is considered as a centralized optimization problem. For a given multiuser OFDMA system, the optimal solution to this problem consists in maximizing spectral efficiency, energy efficiency, or both. Centralized inter-cell coordination is therefore required to achieve this solution, where the necessary information about SINR, power allocation, and UE radio conditions are sent to a centralized coordination entity.

In [QLS09], the multi-cell optimization problem is decomposed into two distributed optimization problems. The objective of the first problem is to minimize the transmission power allocated for cell-edge UEs, while guaranteeing a minimum throughput for each

UE. RB and power are allocated to cell-edge UEs so that they satisfy their minimum required throughput. The remaining RBs and the remaining transmission power are uniformly allocated to cell-center UEs. At this stage, the second problem aims at finding the resource allocation strategy that maximizes the achievable throughput for cell-center zone. An improved version of this adaptive ICIC technique is proposed in [UH11], where resource allocation for cell-edge UEs is performed depending on their individual channel conditions. Another adjustment is made on resource allocation for cell-edge UEs when the required transmission power exceeds the maximum power of an eNodeB. However, the main disadvantage of this adaptive ICIC technique and the proposed improvement is that they do not consider the impact of ICI between adjacent cells when power allocation is performed. In fact, authors ignore ICI by proposing suboptimal algorithms that solve the optimization problem in a distributed manner: each cell solves its own optimization problem without requesting additional information from its neighboring cells.

Resource and power allocation for a cluster of coordinated OFDMA cells are analyzed in [VZRB15]. Constraints on downlink transmission power are defined to avoid exceeding the maximum power per cell. A global energy efficiency is defined as the ratio between sum-rate and power consumption for the entire network. However, noise-limited regime is considered, and ICI is neglected. The proposed algorithms run in a centralized controller that collects channel measurements from several eNodeBs, and calculates resource and power allocation for the entire cluster of coordinated eNodeBs.

Energy-efficient resource allocation for OFDMA systems is studied in [XLZ+12], where generalized and individual energy efficiencies are defined for the downlink and the uplink of the OFDMA system, respectively. Properties of the energy efficiency objective function are analyzed, then a low-complexity suboptimal algorithm is introduced to reduce the computational burden of the optimal solution. Subcarrier assignment is made easier using heuristic algorithms. Within the same context, link adaptive transmission is exploited to maximize energy efficiency, measured by the *throughput per Joule* metric [MHL10]. Energy efficiency is maximized by adapting both overall transmit power and power allocation according to channel states. Iterative algorithms are used to reach the optimal link adaptation solution. In [LPCVC14, LXCL14] the objective is to minimize the required transmission power while satisfying UE rates constraints. Therefore, resource allocation is performed in a manner that improves energy efficiency for the entire system. Authors of [YLY+14] consider the joint resource allocation, power allocation,

and Modulation and Coding Scheme (MCS) selection problem. Their objective is to maximize the achievable throughput in a proportional fair manner between UEs. The joint optimization problem is separated into resource allocation and power allocation problems, and suboptimal algorithms are proposed. Another low complexity suboptimal resource allocation algorithm is proposed in [AHSS14]. The objective consists in maximizing the achievable throughput, under constraints related to resource usage in the different cells. Cooperation between adjacent cells is needed. Performance comparisons with the frequency reuse-1 model and other static ICIC techniques are done using system level simulations of an LTE network.

The majority of state-of-the-art contributions that formulate spectral efficiency or energy efficiency problems as centralized optimization problems, neglect the impact of ICI on system performance [TSAH14, LMB14, XLZ+11], or introduce suboptimal approaches to solve resource and power allocation problems [NKL14, ZCL+14, SA14]. Moreover, performance comparisons are not made with other distributed heuristic ICIC algorithms, that are usually characterized by a lower computational complexity. In our work, we consider the multi-cell resource and power allocation problem, where the objective is to maximize system throughput while guaranteeing throughput fairness between the different UEs. Moreover, ICI is taken into account when solving the centralized resource and power allocation problem. We also formulate a decentralized non-cooperative power allocation approach based on game theory. The players are the cells, and each cell seeks maximizing its own utility function independently of the other cells in the network. We investigate the convergence of both centralized and decentralized approaches, and we compare their performance with that of the frequency reuse-1 model, the frequency reuse-3 model, FFR, and SFR techniques.

3.3 System Model and Problem Formulation

3.3.1 System Model

We consider the downlink of a multiuser OFDMA system that consists of I adjacent cells and K active UEs. Let $\mathcal{I} = \{1, 2, ..., I\}$ denote the the set of cells, and $\mathcal{K} = \{1, 2, ..., K\}$ the total set of active UEs. We also define $K(i)$ as the number of UEs served by cell i. Thus, we have $\sum_{i=1}^{I} K(i) = K$. The total bandwidth available in each cell equals B,

and $\mathcal{N} = \{1, 2, ..., N\}$ denotes the set of available RBs in each cell. The bandwidth per RB is therefore given by $W = \frac{B}{N}$.

In OFDMA networks, system spectrum is divided into several channels, where each channel consists of a number of consecutive orthogonal OFDM subcarriers [WLP+10]. An RB is the smallest scheduling unit. It consists of 12 consecutive subcarriers in the frequency domain, and seven OFDM symbols with normal cyclic prefix in the time domain [DPS11] (or six OFDM symbols with extended cyclic prefix). Resources are allocated to UEs each Transmit Time Interval (TTI), which is equal to 1 ms. When the frequency reuse-1 model is applied along with homogeneous power allocation, each RB is allocated the same downlink transmission power $\frac{P_{max}}{N}$, where P_{max} denotes the maximum downlink transmission power per cell.

The signal to interference and noise ratio for a UE k attached to cell i and allocated RB n is given by:

$$\sigma_{k,i,n} = \frac{\pi_{i,n} G_{k,i,n}}{N_0 + \sum_{i' \neq i} \pi_{i',n} G_{k,i',n}}, \tag{3.1}$$

where $\pi_{i,n}$ is the downlink transmission power allocated by cell i to RB n, $G_{k,i,n}$ denotes channel gain for UE k attached to cell i and allocated RB n, and N_0 is the thermal noise power. Indexes i and i' refer to useful and interfering signals respectively.

Notations, symbols, parameters, and variables used within this chapter are reported in Table 3.1.

3.3.2 Problem Formulation

3.3.2.1 Centralized Multi-Cell Optimization Problem

We define $\theta_{k,n}$ as the percentage of time during which UE k is associated with RB n. $\theta_{k,n}, \forall k \in \mathcal{K}, \forall n \in \mathcal{N}$, and $\pi_{i,n}, \forall i \in \mathcal{I}, \forall n \in \mathcal{N}$, are the optimization variables of the joint resource and power allocation problem. Our objective is to manage resource and power allocation in a manner that maximizes system throughput and guarantees throughput fairness between the different UEs. The peak rate of UE k when associated with RB n on cell i is given by:

$$\rho_{k,i,n} = \log\left(1 + \frac{\pi_{i,n} G_{k,i,n}}{N_0 + \sum_{i' \neq i} \pi_{i',n} G_{k,i',n}}\right), \tag{3.2}$$

Table 3.1: Sets, parameters, and variables

i	Index of cell
k	Index of UE
n	Index of RB
$\mathcal{I}$	Set of cells
$\mathcal{K}$	Total set of UEs
$\mathcal{K}(i)$	Set of UEs associated to cell i
$\mathcal{N}$	Set of RBs
B	Total bandwidth
W	Bandwidth per RB
$\rho_{k,i,n}$	Peak rate achieved by UE k associated with RB n on cell i
$\pi_{i,n}$	Transmit power of cell i on RB n
$G_{k,i,n}$	Channel gain for UE k over RB n on cell i
N_0	Thermal noise density
$\theta_{k,n}$	Percentage of time UE k is associated with RB n
η	Total system achievable mean rate
$\sigma_{k,i,n}$	SINR for UE k over RB n on cell i
P_{max}	Maximum DL transmission power per cell
π_{min}	Minimum DL transmission power per RB
$\mathcal{I}'(i)$	Set of neighboring cells for cell i

and the mean rate of UE k is given by:

$$\sum_{n\in\mathcal{N}}(\theta_{k,n}.\rho_{k,i,n}) \quad = \sum_{n\in\mathcal{N}}\left(\theta_{k,n}.\log\left(1+\frac{\pi_{i,n}G_{k,i,n}}{N_0+\sum_{i'\neq i}\pi_{i',n}G_{k,i',n}}\right)\right). \tag{3.3}$$

Our centralized multi-cell joint resource and power allocation problem seeks rate maximization in a proportional fair manner. We make use of the logarithmic function that is intimately associated with the concept of proportional fairness [Kel97]. Our joint resource and power allocation problem is formulated in the following:

$$\underset{\boldsymbol{\theta},\boldsymbol{\pi}}{\text{maximize}} \quad \eta = \sum_{i\in\mathcal{I}}\sum_{k\in\mathcal{K}(i)}\log\left(\sum_{n\in\mathcal{N}}\theta_{k,n}.\log\left(1+\frac{\pi_{i,n}G_{k,i,n}}{N_0+\sum_{i'\neq i}\pi_{i',n}G_{k,i',n}}\right)\right) \tag{3.4a}$$

$$\text{subject to} \quad \sum_{k\in\mathcal{K}(i)}\theta_{k,n}\leq 1,\ \forall n\in\mathcal{N}, \tag{3.4b}$$

$$\sum_{n\in\mathcal{N}}\theta_{k,n}\leq 1,\ \forall k\in\mathcal{K}(i), \tag{3.4c}$$

$$\sum_{n\in\mathcal{N}}\pi_{i,n}\leq P_{max},\ \forall i\in\mathcal{I}, \tag{3.4d}$$

$$\pi_{i,n}\geq\pi_{min},\ \forall i\in\mathcal{I},\forall n\in\mathcal{N}, \tag{3.4e}$$

$$0\leq\theta_{k,n}\leq 1,\ \forall k\in\mathcal{K}(i),\forall n\in\mathcal{N}. \tag{3.4f}$$

The objective function η ensures a proportional fair rate for all the active UEs in the network. Constraints (3.4b) ensure that an RB is used at most 100% of the time, and constraints (3.4c) ensure that a UE shares its time on the available RBs. Constraints (3.4d) guarantee that the total downlink transmission power allocated to the available RBs does not exceed the maximum transmission power P_{max} for each cell i, and constraints (3.4e) represent the minimum power constraint of the transmit power allocated to each RB. $\theta_{k,n}$ and $\pi_{i,n}$ are the optimization variables of the joint resource and power allocation problem.

3.3.2.2 Upper Bound of the Objective Functions Difference

In order to reduce the complexity of the joint resource and power allocation problem (3.4), we prove that this problem is separable into two independent problems: a resource allocation problem and a power allocation problem. Given Jensen's inequality and the concavity of the log function, we have:

$$\log\left(\frac{\sum_{n\in\mathcal{N}}\theta_{k,n}.\rho_{k,i,n}}{|\mathcal{N}|}\right) \geq \frac{\sum_{n\in\mathcal{N}}\log\left(\theta_{k,n}.\rho_{k,i,n}\right)}{|\mathcal{N}|} \tag{3.5a}$$

$$\Rightarrow \log\left(\sum_{n\in\mathcal{N}}\theta_{k,n}.\rho_{k,i,n}\right) \geq \frac{\sum_{n\in\mathcal{N}}\log\left(\theta_{k,n}.\rho_{k,i,n}\right)}{|\mathcal{N}|} + \log\left(|\mathcal{N}|\right), \tag{3.5b}$$

the objective function η can be written as:

$$\begin{aligned}\eta &= \sum_{i\in\mathcal{I}}\sum_{k\in\mathcal{K}(i)}\log\left(\sum_{n\in\mathcal{N}}\theta_{k,n}.\rho_{k,i,n}\right)\\ &\geq \frac{1}{|\mathcal{N}|}\sum_{i\in\mathcal{I}}\sum_{k\in\mathcal{K}(i)}\sum_{n\in\mathcal{N}}\log\left(\theta_{k,n}.\rho_{k,i,n}\right) + |\mathcal{K}|.\log\left(|\mathcal{N}|\right).\end{aligned} \tag{3.6}$$

Since $\frac{1}{|\mathcal{N}|}$ and $|\mathcal{K}|.\log\left(|\mathcal{N}|\right)$ are constant terms, maximizing the objective function of problem (3.4) is achieved by maximizing the following term:

$$\sum_{i\in\mathcal{I}}\sum_{k\in\mathcal{K}(i)}\sum_{n\in\mathcal{N}}\log\left(\theta_{k,n}.\rho_{k,i,n}\right) = \sum_{i\in\mathcal{I}}\sum_{k\in\mathcal{K}(i)}\sum_{n\in\mathcal{N}}\left(\log\left(\theta_{k,n}\right) + \log\left(\rho_{k,i,n}\right)\right). \tag{3.7}$$

In order to decompose the joint problem into two independent problems, we evaluate the gap between the original objective function η and the function given in (3.7). We

demonstrate an upper bound on the following difference:

$$0 \leq \log\left(\sum_{n\in\mathcal{N}} \theta_{k,n}.\rho_{k,i,n}\right) - \sum_{n\in\mathcal{N}} \log\left(\theta_{k,n}.\rho_{k,i,n}\right) \leq B. \tag{3.8}$$

Let $\phi_n = \theta_{k,n}.\rho_{k,i,n} > 0$, and suppose that $a \leq \phi_n \leq b$. Thus, there exists $0 \leq \lambda_n \leq 1$ such that $\phi_n = \lambda_n a + (1-\lambda_n)b$.

Theorem 3.1. *The best upper global bound of* $\left(\log\left(\sum_{n\in\mathcal{N}}\phi_n\right) - \sum_{n\in\mathcal{N}}\log\left(\phi_n\right)\right)$ *is:* $B = \max_p \left(\log\left(ap + b\left(|\mathcal{N}| - p\right)\right) - p\log\left(a\right) - \left(|\mathcal{N}| - p\right)\log\left(b\right)\right)$, *where* $p = \sum_{n\in\mathcal{N}}\lambda_n$.

Proof:

$$\begin{aligned}
&\log\left(\sum_{n\in\mathcal{N}}\phi_n\right) - \sum_{n\in\mathcal{N}}\log\left(\phi_n\right)\\
&= \log\left(\sum_{n\in\mathcal{N}}\left(\lambda_n a + \left(1-\lambda_n\right)b\right)\right) - \sum_{n\in\mathcal{N}}\log\left(\lambda_n a + \left(1-\lambda_n\right)b\right)\\
&\leq \log\left(\sum_{n\in\mathcal{N}}\left(\lambda_n a + \left(1-\lambda_n\right)b\right)\right) - \sum_{n\in\mathcal{N}}\left(\lambda_n\log\left(a\right) + \left(1-\lambda_n\right)\log\left(b\right)\right)\\
&= \log\left(a\left(\sum_{n\in\mathcal{N}}\lambda_n\right) + b\left(|\mathcal{N}| - \sum_{n\in\mathcal{N}}\left(\lambda_n\right)\right)\right) - \log\left(a\right)\left(\sum_{n\in\mathcal{N}}\lambda_n\right) - \log\left(b\right)\left(|\mathcal{N}| - \sum_{n\in\mathcal{N}}\left(\lambda_n\right)\right).
\end{aligned}$$

Taking $p = \sum_{n\in\mathcal{N}}\lambda_n$ and $q = |\mathcal{N}| - \sum_{n\in\mathcal{N}}\lambda_n$, we have $0 \leq p \leq |\mathcal{N}|$, $0 \leq q \leq |\mathcal{N}|$, and $p + q = |\mathcal{N}|$. Consequently, we have:

$$\begin{aligned}
&\log\left(\sum_{n\in\mathcal{N}}\phi_n\right) - \sum_{n\in\mathcal{N}}\log\left(\phi_n\right)\\
&\leq \log\left(ap + bq\right) - p\log\left(a\right) - q\log\left(b\right)\\
&\leq \max_p\left(\log\left(ap + b\left(|\mathcal{N}| - p\right)\right) - p\log\left(a\right) - \left(|\mathcal{N}| - p\right)\log\left(b\right)\right) \quad = B.
\end{aligned}$$

For fixed a and b, let us denote:

$$g(p) = \log(ap + b(|\mathcal{N}| - p)) - p\log(a) - (|\mathcal{N}| - p)\log(b).$$

g is defined, differentiable, and concave on $[0, |\mathcal{N}|]$. Its first derivative is given by:

$$g'(p) = \frac{a-b}{ap + b(|\mathcal{N}| - p)} - \log(a) + \log(b).$$

$g(p)$ attains its maximal value B for a p_0 that satisfies: $g'(p_0) = 0$. Thus, we have $B = g(p_0)$, where p_0 is given by:

$$p_0 = \frac{1}{\log(a) - \log(b)} + \frac{b.|\mathcal{N}|}{b-a}.$$

3.4 Problem Decomposition

We tackle ICIC as an optimization problem, where we intend to maximize the mean rate of active UEs in a multiuser OFDMA system. We consider a system of I cells, having $K(i)$ UEs per cell i. According to (3.7), and due to the absence of binding constraints, the optimization problem (3.4) is linearly separable into two independent problems: a power allocation problem and a resource allocation problem.

3.4.1 Centralized Multi-Cell Power Allocation Problem

In the first problem, the optimization variable $\boldsymbol{\pi}$ is considered, and the problem is formulated as follows:

$$\underset{\boldsymbol{\pi}}{\text{maximize}} \quad \eta_1 = \sum_{i\in\mathcal{I}} \sum_{k\in\mathcal{K}(i)} \sum_{n\in\mathcal{N}} \log\left(\log\left(1 + \frac{\pi_{i,n} G_{k,i,n}}{N_0 + \sum_{i'\neq i} \pi_{i',n} G_{k,i',n}}\right)\right) \tag{3.9a}$$

$$\text{subject to} \quad \sum_{n\in\mathcal{N}} \pi_{i,n} \leq P_{max},\ \forall i \in \mathcal{I}, \tag{3.9b}$$

$$\pi_{i,n} \geq \pi_{min},\ \forall i \in \mathcal{I}, \forall n \in \mathcal{N}. \tag{3.9c}$$

Problem (3.9) consists in finding the optimal power allocation for the available RBs. In the following, we introduce a variable change that allows to formulate problem (3.9) as a convex optimization problem.

Theorem 3.2. *The logarithmic function of the sum of exponential functions is convex.*

Proof: Let $f(x) = \log\left(\sum_{j=1}^{J} \exp x_j\right)$.
The Hessian of the log-sum-exp function is given by:

$\nabla^2 f(x) = \frac{1}{S(x)^2}\left(S(x)\mathbf{diag}\left(s\left(x\right)\right) - s\left(x\right)s\left(x\right)^T\right)$,
where $s(x) = (\exp(x_1), \exp(x_2), ..., \exp(x_J))$, and $S(x) = \sum_{j=1}^{J} s_j(x)$.
To verify that $\nabla^2 f(x) \geq 0$ we must show that for every $z \in \mathbf{R}^J$, we have $z^T \nabla^2 f(x) z \geq 0$.
We have:

$$\begin{aligned} S(x)^2.z^T\nabla^2 f(x)z &= z^T\left(S\left(x\right)\mathbf{diag}\left(s\left(x\right)\right) - s\left(x\right)s\left(x\right)^T\right)z \\ &= \left(\sum_{j=1}^{J} s_j\left(x\right)z_j^2\right)\left(\sum_{j=1}^{J} s_j\left(x\right)\right) - \left(\sum_{j=1}^{J} s_j\left(x\right)z_j\right)^2 \geq 0, \end{aligned}$$

due to Cauchy-Schwartz inequality. Thus, $f(x)$ is convex on $\mathbf{R}^J$.

The power allocation problem (3.9) can be written as follows:

$$\underset{\boldsymbol{\rho}}{\text{maximize}} \quad \eta_1 = \sum_{i\in\mathcal{I}}\sum_{k\in\mathcal{K}(i)}\sum_{n\in\mathcal{N}} \log(\rho_{k,i,n}) \tag{3.10a}$$

$$\text{subject to} \quad \rho_{k,i,n} \leq \log\left(1 + \frac{\pi_{i,n}G_{k,i,n}}{N_0 + \sum_{i'\neq i}\pi_{i',n}G_{k,i',n}}\right),\ \forall i \in \mathcal{I}, \forall k \in \mathcal{K}(i), \forall n \in \mathcal{N}, \tag{3.10b}$$

$$\sum_{n\in\mathcal{N}} \pi_{i,n} \leq P_{max},\ \forall i \in \mathcal{I}, \tag{3.10c}$$

$$\pi_{i,n} \geq \pi_{min},\ \forall i \in \mathcal{I}, \forall n \in \mathcal{N}. \tag{3.10d}$$

To show that the optimization problem (3.10) is a convex optimization problem, we need to show that the objective function is concave and the inequality constraint functions define a convex set. Let us consider the following variable change:

$$\widehat{\rho}_{k,i,n} = \log(\exp(\rho_{k,i,n}) - 1),\ \forall\, i \in \mathcal{I}, \forall\, k \in \mathcal{K}(i), \forall n\ \in \mathcal{N}, \tag{3.11a}$$

$$\widehat{\pi}_{i,n} = \log(\pi_{i,n}),\ \forall\, i \in \mathcal{I}, \forall\, n \in \mathcal{N}. \tag{3.11b}$$

Hence, the original variables are given by:

$$\rho_{k,i,n} = \log(\exp(\widehat{\rho}_{k,i,n}) + 1),\ \forall\, i \in \mathcal{I}, \forall\, k \in \mathcal{K}(i), \forall n\ \in \mathcal{N}, \tag{3.12a}$$

$$\pi_{i,n} = \exp(\widehat{\pi}_{i,n}),\ \forall\, i \in \mathcal{I}, \forall\, n \in \mathcal{N}. \tag{3.12b}$$

After applying the variable change on UE peak rate constraints (3.10b), these constraints can be written as follows:

$$
\begin{aligned}
&\rho_{k,i,n} \leq \log\left(1+\frac{\pi_{i,n}G_{k,i,n}}{N_0+\sum_{i'\neq i}\pi_{i',n}G_{k,i',n}}\right),\ \forall i\in\mathcal{I},\forall k\in\mathcal{K}(i),\forall n\in\mathcal{N}\\
&\Rightarrow \log(\exp(\widehat{\rho}_{k,i,n})+1) \leq \log\left(1+\frac{\exp(\widehat{\pi}_{i,n})G_{k,i,n}}{N_0+\sum_{i'\neq i}\exp(\widehat{\pi}_{i',n})G_{k,i',n}}\right)\\
&\Rightarrow \exp(\widehat{\rho}_{k.i.n})+1 \leq 1+\frac{\exp(\widehat{\pi}_{i,n})G_{k,i,n}}{N_0+\sum_{i'\neq i}\exp(\widehat{\pi}_{i',n})G_{k,i',n}}\\
&\Rightarrow \frac{\exp(\widehat{\rho}_{k.i.n}).\left(N_0+\sum_{i'\neq i}\exp(\widehat{\pi}_{i',n})G_{k,i',n}\right)}{\exp(\widehat{\pi}_{i,n})G_{k,i,n}} \leq 1\\
&\Rightarrow \log\left(\exp(\widehat{\rho}_{k.i.n}-\widehat{\pi}_{i,n})\frac{N_0}{G_{k,i,n}}+\sum_{i'\neq i}\exp(\widehat{\rho}_{k.i.n}+\widehat{\pi}_{i',n}-\widehat{\pi}_{i,n})\frac{G_{k,i',n}}{G_{k,i,n}}\right)\leq 0,\\
&\quad \forall i\in\mathcal{I},\forall k\in\mathcal{K}(i),\forall n\in\mathcal{N},
\end{aligned}
$$

these constraints are the logarithmic of the sum of exponential functions. According to Theorem 3.2, they are convex functions. When we apply the variable change on power constraints (3.10c), we obtain the following:

$$
\begin{aligned}
&\sum_{n\in\mathcal{N}}\pi_{i,n}\leq P_{max},\ \forall i\in\mathcal{I}\\
&\Rightarrow \sum_{n\in\mathcal{N}}\exp(\widehat{\pi}_{i,n})\leq P_{max}\\
&\Rightarrow \frac{\sum_{n\in\mathcal{N}}\exp(\widehat{\pi}_{i,n})}{P_{max}}\leq 1\\
&\Rightarrow \log\left(\sum_{n\in\mathcal{N}}\exp(\widehat{\pi}_{i,n})\right)-\log(P_{max})\leq 0,\ \forall i\in\mathcal{I}.
\end{aligned}
$$

Since $\log(\sum \exp)$ is convex, the constraints at hand are therefore convex. Using the variable change, the power allocation problem (3.10) can be written as follows:

$$\underset{\widehat{\boldsymbol{\rho}}}{\text{maximize}} \quad \eta_1 = \sum_{i\in\mathcal{I}} \sum_{k\in\mathcal{K}(i)} \sum_{n\in\mathcal{N}} \log\left(\log(\exp(\widehat{\rho}_{k,i,n}) + 1)\right) \tag{3.13a}$$

$$\text{subject to} \quad \log\left(\exp(\widehat{\rho}_{k.i.n} - \widehat{\pi}_{i,n})\frac{N_0}{G_{k,i,n}} + \sum_{i'\neq i} \exp(\widehat{\rho}_{k.i.n} + \widehat{\pi}_{i',n} - \widehat{\pi}_{i,n})\frac{G_{k,i',n}}{G_{k,i,n}}\right) \leq 0,$$

$$\forall i \in \mathcal{I}, \forall k \in \mathcal{K}(i), \forall n \in \mathcal{N}, \tag{3.13b}$$

$$\log\left(\sum_{n\in\mathcal{N}} \exp(\widehat{\pi}_{i,n})\right) - \log(P_{max}) \leq 0, \ \forall i \in \mathcal{I}, \tag{3.13c}$$

$$\widehat{\pi}_{i,n} \geq \log(\pi_{min}), \ \forall i \in \mathcal{I}, \forall n \in \mathcal{N}. \tag{3.13d}$$

The objective function of problem (3.13) is concave in $\widehat{\boldsymbol{\rho}}$, and constraints (3.13b), (3.13c), and (3.13d) are convex functions. Thus, the power allocation problem is a convex optimization problem.

3.4.2 Centralized Resource Allocation Problem

The optimization variable $\boldsymbol{\theta}$ is considered in the second optimization problem that is given in the following:

$$\underset{\boldsymbol{\theta}}{\text{maximize}} \quad \eta_2 = \sum_{i\in\mathcal{I}} \sum_{k\in\mathcal{K}(i)} \sum_{n\in\mathcal{N}} \log(\theta_{k,n}) \tag{3.14a}$$

$$\text{subject to} \quad \sum_{k\in\mathcal{K}(i)} \theta_{k,n} \leq 1, \ \forall n \in \mathcal{N}, \tag{3.14b}$$

$$\sum_{n\in\mathcal{N}} \theta_{k,n} \leq 1, \ \forall k \in \mathcal{K}(i), \tag{3.14c}$$

$$0 \leq \theta_{k,n} \leq 1, \ \forall k \in \mathcal{K}(i), \forall n \in \mathcal{N}. \tag{3.14d}$$

As demonstrated for the power allocation problem (3.9), we prove that problem (3.14) is indeed a convex optimization problem in $\boldsymbol{\theta}$. The objective function (3.14a) of the resource allocation problem (3.14) is concave in $\boldsymbol{\theta}$, since the log function is concave for $\boldsymbol{\theta} \in]0; 1]$. Moreover, constraints (3.14b), (3.14c), and (3.14d) are linear and separable constraints. Hence, the resource allocation problem (3.14) is a convex optimization problem, and it is separable into $\mathcal{I}$ subproblems. For each cell i, the ith optimization problem is written

as follows:

$$\underset{\boldsymbol{\theta}}{\text{maximize}} \quad (\eta_2)_i = \sum_{k\in\mathcal{K}(i)} \sum_{n\in\mathcal{N}} \log(\theta_{k,n}) \tag{3.15a}$$

$$\text{subject to} \quad \sum_{k\in\mathcal{K}(i)} \theta_{k,n} \leq 1,\ \forall n \in \mathcal{N}, \tag{3.15b}$$

$$\sum_{n\in\mathcal{N}} \theta_{k,n} \leq 1,\ \forall k \in \mathcal{K}(i), \tag{3.15c}$$

$$0 \leq \theta_{k,n} \leq 1,\ \forall k \in \mathcal{K}(i), \forall n \in \mathcal{N}. \tag{3.15d}$$

Resource and power allocation problems are convex optimization problems that aim at maximizing the total achievable rate for the entire system, while taking into account constraints related to power allocation and resource usage.

We identify two different resource and power allocation scenarios, based on the amount of collaboration between the different cells:

1. Centralized resource and power allocation.
2. Decentralized non-cooperative resource and power allocation.

The centralized resource and power allocation scenario is when the optimization problem is solved for the entire system, after collecting the necessary information from all the cells. It assumes that a central entity has the complete knowledge of resource and power allocation within all the cells: $\theta_{k,n}$ and $\pi_{i,n}$ values are known $\forall i \in \mathcal{I}$, $\forall k \in \mathcal{K}$, $\forall n \in \mathcal{N}$. The main advantage of this scenario is that it offers the resource and power allocation that maximize the achievable throughput for the entire network. In other words, it leads to the optimal spectral efficiency, at the expense of additional signaling messages to be exchanged between the cells and the central entity, as well as an exponentially increasing computational complexity.

When distributed non-cooperative resource and power allocation scenario is considered, the optimization problem is solved locally for each cell, and information about resource and power allocation in the neighboring cells is not requested. The term $\sum_{i'\neq i} \pi_{i',n} G_{k,i',n}$ that reflects ICI caused by the neighboring cells, is unknown for cell i. Thus, each cell i maximizes its achievable rate $\sum_{k\in\mathcal{K}(i)} \log\left(\sum_{n\in\mathcal{N}} \theta_{k,n}.\rho_{k,i,n}\right)$ without taking into account the impact of simultaneous transmissions made by its neighboring cells on the same

resources. This assumption reduces the efficiency of this approach in comparison with cooperative and centralized scenarios. However, it is interesting when the network size increases, since it does not generate any additional signaling traffic.

3.5 Centralized Resource and Power Allocation

3.5.1 Solving the Centralized Power Allocation Problem

3.5.1.1 Lagrange-Based Method

Since the power allocation problem (3.13) is proven to be a convex optimization problem, we can make use of Lagrange duality properties, which also lead to decomposability structures [PC06]. Lagrange duality theory links the original problem, called *primal problem*, with a dual maximization problem. The primal problem (3.13) is relaxed by transferring the constraints to the objective in the form of weighted sum. The Lagrangian is formed by relaxing the coupling constraints (3.13b) and (3.13c) in (3.13):

$$\begin{aligned} L(\widehat{\boldsymbol{\rho}}, \widehat{\boldsymbol{\pi}}, \boldsymbol{\lambda}, \boldsymbol{\nu}) = & \sum_{i\in\mathcal{I}} \sum_{k\in\mathcal{K}(i)} \sum_{n\in\mathcal{N}} \log(\log(\exp(\widehat{\rho}_{k,i,n}) + 1)) \\ & - \sum_{i\in\mathcal{I}} \sum_{k\in\mathcal{K}(i)} \sum_{n\in\mathcal{N}} \lambda_{k,i,n} (\log(\exp(\widehat{\rho}_{k.i.n} - \widehat{\pi}_{i,n}) \frac{N_0}{G_{k,i,n}} \\ & + \sum_{\substack{i'\in\mathcal{N} \\ i'\neq i}} \exp(\widehat{\rho}_{k.i.n} + \widehat{\pi}_{i',n} - \widehat{\pi}_{i,n}) \frac{G_{k,i',n}}{G_{k,i,n}})) \\ & - \sum_{i\in\mathcal{I}} \nu_i (\log(\sum_{n\in\mathcal{N}} \exp(\widehat{\pi}_{i,n})) - \log(P_{max})). \end{aligned} \tag{3.16}$$

The optimization variables $\widehat{\boldsymbol{\rho}}$ and $\widehat{\boldsymbol{\pi}}$ are called the primal variables. $\lambda_{k,i,n}$ and ν_i are the *Lagrange multipliers* or *prices* associated with the (k,i,n)-th inequality constraint (3.13b) and with the i-th inequality constraint (3.13c), respectively. $\boldsymbol{\lambda}$ and $\boldsymbol{\nu}$ are also termed the *dual variables*.

After relaxing the coupling constraints, the optimization problem separates into two levels of optimization: lower level and higher level. At the lower level, $L(\widehat{\boldsymbol{\rho}}, \widehat{\boldsymbol{\pi}}, \boldsymbol{\lambda}, \boldsymbol{\nu})$ is the objective function to be maximized. $\widehat{\rho}_{k,i,n}$ and $\widehat{\pi}_{i,n}$ are the optimization variables to

be found, and the primal problem is given by:

$$\begin{aligned}
\underset{\widehat{\boldsymbol{\rho}},\widehat{\boldsymbol{\pi}}}{\text{maximize}} \qquad & L(\widehat{\boldsymbol{\rho}},\widehat{\boldsymbol{\pi}},\boldsymbol{\lambda},\boldsymbol{\nu}) = \sum_{i\in\mathcal{I}}\sum_{k\in\mathcal{K}(i)}\sum_{n\in\mathcal{N}}\log(\log(\exp(\widehat{\rho}_{k,i,n})+1)) \\
& - \sum_{i\in\mathcal{I}}\sum_{k\in\mathcal{K}(i)}\sum_{n\in\mathcal{N}}\lambda_{k,i,n}(\log(\exp(\widehat{\rho}_{k.i.n}-\widehat{\pi}_{i,n})\frac{N_0}{G_{k,i,n}} \\
& + \sum_{\substack{i'\in\mathcal{N}\\ i'\neq i}}\exp(\widehat{\rho}_{k.i.n}+\widehat{\pi}_{i',n}-\widehat{\pi}_{i,n})\frac{G_{k,i',n}}{G_{k,i,n}})) \\
& - \sum_{i\in\mathcal{I}}\nu_i(\log(\sum_{n\in\mathcal{N}}\exp(\widehat{\pi}_{i,n}))-\log(P_{max})) \qquad (3.17a) \\
\text{subject to} \qquad & \widehat{\pi}_{i,n}\geq\log(\pi_{min}),\ \forall i\in\mathcal{I},\forall n\in\mathcal{N}. \qquad (3.17b)
\end{aligned}$$

In order to solve the primal optimization problem (3.17), we use the subgradient projection method. It starts with some initial feasible values of $\widehat{\rho}_{k,i,n}$ and $\widehat{\pi}_{i,n}$ that satisfy the constraints (3.17b). Then, the next iteration is generated by taking a step along the subgradient direction of $\widehat{\rho}_{k,i,n}$ and $\widehat{\pi}_{i,n}$. For the primal optimization variables, iterations of the subgradient projection are given by:

$$\widehat{\rho}_{k,i,n}(t+1) = \widehat{\rho}_{k,i,n}(t) + \delta(t)\frac{\partial L}{\partial\widehat{\rho}_{k,i,n}}, \forall k\in\mathcal{K}(i),\forall i\in\mathcal{I},\forall n\in\mathcal{N}, \qquad (3.18a)$$

$$\widehat{\pi}_{i,n}(t+1) = \widehat{\pi}_{i,n}(t) + \delta(t)\frac{\partial L}{\partial\widehat{\pi}_{i,n}}, \forall i\in\mathcal{I},\forall n\in\mathcal{N}. \qquad (3.18b)$$

The scalar $\delta(t)$ is a step size that guarantees the convergence of the optimization problem (3.17). The partial derivatives of the objective function $L(\widehat{\boldsymbol{\rho}},\widehat{\boldsymbol{\pi}},\boldsymbol{\lambda},\boldsymbol{\nu})$ with respect to $\widehat{\rho}_{k,i,n}$ and $\widehat{\pi}_{i,n}$, are given in the following:

$$\frac{\partial L}{\partial\widehat{\rho}_{k,i,n}} = \frac{\exp(\widehat{\rho}_{k,i,n})}{(\exp(\widehat{\rho}_{k,i,n})+1)\log(\exp(\widehat{\rho}_{k,i,n})+1)} - \lambda_{k,i,n}, \forall k\in\mathcal{K}(i),\forall i\in\mathcal{I},\forall n\in\mathcal{N}, \qquad (3.19a)$$

$$\frac{\partial L}{\partial\widehat{\pi}_{i,n}} = \sum_{k\in\mathcal{K}(i)}\lambda_{k,i,n} - \nu_i\frac{\exp(\widehat{\pi}_{i,n})}{\sum_{n\in\mathcal{N}}\exp(\widehat{\pi}_{i,n})},\ \forall i\in\mathcal{I},\forall n\in\mathcal{N}. \qquad (3.19b)$$

At the higher level, we have the master dual problem in charge of updating the dual variables $\boldsymbol{\lambda}$ and $\boldsymbol{\nu}$ by solving the dual problem:

$$\begin{aligned} \underset{\boldsymbol{\lambda},\boldsymbol{\nu}}{\text{minimize}} \quad & \max_{\widehat{\boldsymbol{\rho}},\widehat{\boldsymbol{\pi}}}(L(\widehat{\boldsymbol{\rho}},\widehat{\boldsymbol{\pi}},\boldsymbol{\lambda},\boldsymbol{\nu})) && \text{(3.20a)} \\ \text{subject to} \quad & \boldsymbol{\lambda} \geq 0, && \text{(3.20b)} \\ & \boldsymbol{\nu} \geq 0. && \text{(3.20c)} \end{aligned}$$

The dual function $g(\boldsymbol{\lambda},\boldsymbol{\nu}) = \max_{\widehat{\boldsymbol{\rho}},\widehat{\boldsymbol{\pi}}}(L(\widehat{\boldsymbol{\rho}},\widehat{\boldsymbol{\pi}},\boldsymbol{\lambda},\boldsymbol{\nu}))$ is differentiable. Thus, the master dual problem (3.20) can be solved using the following gradient method:

$$\begin{aligned} \lambda_{k,i,n}(t+1) = \lambda_{k,i,n}(t) + \delta(t)(\log(\exp(\widehat{\rho}^{\star}_{k.i.n} - \widehat{\pi}^{\star}_{i,n})\frac{N_0}{G_{k,i,n}} \\ + \sum_{\substack{i' \in \mathcal{N} \\ i' \neq i}} \exp(\widehat{\rho}^{\star}_{k.i.n} + \widehat{\pi}^{\star}_{i',n} - \widehat{\pi}^{\star}_{i,n})\frac{G_{k,i',n}}{G_{k,i,n}})), \forall k \in \mathcal{K}(i), \forall i \in \mathcal{I}, \forall n \in \mathcal{N}, \end{aligned} \tag{3.21a}$$

$$\nu_i(t+1) = \nu_i(t) + \delta(t)(\log(\sum_{n \in \mathcal{N}} \exp(\widehat{\pi}^{\star}_{i,n})) - \log(P_{max})), \forall i \in \mathcal{I}, \forall n \in \mathcal{N}, \tag{3.21b}$$

where t is the iteration index, and $\delta(t)$ is the step size at iteration t. Appropriate choice of the step size [Chi05] leads to convergence of the dual algorithm. $\widehat{\pi}^{\star}_{i,n}$ and $\widehat{\rho}^{\star}_{k,i,n}$ denote the solution to the primal optimization problem (3.17). When $t \to \infty$ the dual variables $\boldsymbol{\lambda}(t)$ and $\boldsymbol{\nu}(t)$ converge to the dual optimal $\boldsymbol{\lambda}^*$ and $\boldsymbol{\nu}^*$, respectively. The difference between the optimal primal objective and the optimal dual objective, called *duality gap*, reduces to zero at optimality, since the problem (3.13) is convex and the KKT conditions are satisfied.

We define $\Delta\widehat{\boldsymbol{\rho}}, \Delta\widehat{\boldsymbol{\pi}}, \Delta\boldsymbol{\lambda}$, and $\Delta\boldsymbol{\nu}$ as the differences between the optimization variables obtained at the current iteration and their values at the previous iteration. They are given by:

$$\Delta\widehat{\boldsymbol{\rho}}(t+1) = \|\widehat{\boldsymbol{\rho}}(t+1) - \widehat{\boldsymbol{\rho}}(t)\|, \tag{3.22a}$$

$$\Delta\widehat{\boldsymbol{\pi}}(t+1) = \|\widehat{\boldsymbol{\pi}}(t+1) - \widehat{\boldsymbol{\pi}}(t)\|, \tag{3.22b}$$

$$\Delta\boldsymbol{\lambda}(t+1) = \|\boldsymbol{\lambda}(t+1) - \boldsymbol{\lambda}(t)\|, \tag{3.22c}$$

$$\Delta\boldsymbol{\nu}(t+1) = \|\boldsymbol{\nu}(t+1) - \boldsymbol{\nu}(t)\|. \tag{3.22d}$$

Algorithm 1 Dual algorithm for centralized power allocation

1: Parameters: the utility function $L(\widehat{\boldsymbol{\rho}}, \widehat{\boldsymbol{\pi}}, \boldsymbol{\lambda}, \boldsymbol{\nu})$, P_{max}, and π_{min}.
2: Initialization: set $t = t_{primal} = t_{dual} = 0$, and $\pi_{i,n} \geq \pi_{min}, \forall i \in \mathcal{I}, \forall n \in \mathcal{N}$, such as $\sum_{n \in \mathbb{N}} \pi_{i,n} \leq P_{max}, \forall i \in \mathcal{I}$. Calculate $\widehat{\pi}_{i,n}(0)$ and $\widehat{\rho}_{k,i,n}(0)$ accordingly, $\forall k \in \mathcal{K}(i), \forall i \in \mathcal{I}, \forall n \in \mathcal{N}$.
3: Set $\lambda_{k,i,n}(0)$ and $\nu_i(0)$ equal to some non negative value, $\forall k \in \mathcal{K}(i), \forall i \in \mathcal{I}, \forall n \in \mathcal{N}$.
4: $(\widehat{\boldsymbol{\pi}}^{\star}(t+1), \widehat{\boldsymbol{\rho}}^{\star}(t+1)) \leftarrow$ PrimalProblem$(\boldsymbol{\nu}^{\star}(t), \boldsymbol{\lambda}^{\star}(t))$
5: $(\boldsymbol{\nu}^{\star}(t+1), \boldsymbol{\lambda}^{\star}(t+1)) \leftarrow$ DualProblem$(\widehat{\boldsymbol{\pi}}^{\star}(t+1), \widehat{\boldsymbol{\rho}}^{\star}(t+1))$
6: **if** $(\Delta\widehat{\boldsymbol{\pi}}^{\star}(t+1) > \epsilon)$ **or** $(\Delta\widehat{\boldsymbol{\rho}}^{\star}(t+1) > \epsilon)$ **or** $(\Delta\boldsymbol{\nu}^{\star}(t+1) > \epsilon)$ **or** $(\Delta\boldsymbol{\lambda}^{\star}(t+1) > \epsilon)$ **then**
7: $t \leftarrow t+1$
8: **go to** 4
9: **end if**

3.5.1.2 Iterative Algorithm for Centralized Multi-Cell Power Allocation

The procedure for solving the centralized power allocation problem is described in Algorithm 1. Initially, the primal optimization variables $\widehat{\rho}_{k,i,n}$ and $\widehat{\pi}_{i,n}$ as well as the dual variables $\lambda_{k,i,n}$ and ν_i start with some initial feasible values. t, t_{primal}, and t_{dual} denote the number of rounds required for the centralized power allocation problem to converge, the number of iterations for the primal problem, and the number of iterations for the dual problem, respectively. At each round t, we start by updating the primal optimization variables, using the PrimalProblem function given in Algorithm 2. The solution to the primal optimization problem at the current round t is denoted by $\widehat{\pi}^{\star}_{i,n}(t+1)$ and $\widehat{\rho}^{\star}_{k,i,n}(t+1)$. The PrimalProblem function updates $\widehat{\pi}_{i,n}(t_{primal}+1)$ and $\widehat{\rho}_{k,i,n}(t_{primal}+1)$, and increments t_{primal} until $\Delta\widehat{\boldsymbol{\pi}}(t_{primal}+1)$ and $\Delta\widehat{\boldsymbol{\rho}}(t_{primal}+1)$ become less than ϵ.

Then, the solution to the dual optimization problem at the current round t, denoted by $\nu^{\star}_i(t+1)$ and $\lambda^{\star}_{k,i,n}(t+1)$ is calculated using the DualProblem function given in Algorithm 3. ν_i and $\lambda_{k,i,n}$ are updated using the obtained primal solution $\widehat{\pi}^{\star}_{i,n}(t+1)$ and $\widehat{\rho}^{\star}_{k,i,n}(t+1)$, until $\Delta\boldsymbol{\nu}(t_{dual}+1)$ and $\Delta\boldsymbol{\lambda}(t_{dual}+1)$ become less than ϵ. An additional round of calculations is performed, and t is incremented as long as $\Delta\widehat{\boldsymbol{\pi}}^{\star}(t+1)$ or $\Delta\widehat{\boldsymbol{\pi}}^{\star}(t+1)$ or $\Delta\boldsymbol{\nu}^{\star}(t+1)$ or $\Delta\boldsymbol{\lambda}^{\star}(t+1)$ is greater than ϵ. Otherwise, the obtained solution at the current round is the optimal solution to the centralized power allocation problem.

Algorithm 2 Primal problem function

function PRIMALPROBLEM($\boldsymbol{\nu}^\star(t), \boldsymbol{\lambda}^\star(t)$)
  for $i = 1$ to $|\mathcal{I}|$ **do**
    for $n = 1$ to $|\mathcal{N}|$ **do**
      $\widehat{\pi}_{i,n}(t_{primal}+1) \leftarrow \max\left(\log(\pi_{min}); \widehat{\pi}_{i,n}(t_{primal}) + \delta(t)\frac{\partial L}{\partial \widehat{\pi}_{i,n}}\right)$
      for $k = 1$ to $|\mathcal{K}(i)|$ **do**
        $\widehat{\rho}_{k,i,n}(t_{primal}+1) \leftarrow \widehat{\rho}_{k,i,n}(t_{primal}) + \delta(t)\frac{\partial L}{\partial \widehat{\rho}_{k,i,n}}$
      end for
    end for
  end for
  if $(\Delta\widehat{\boldsymbol{\pi}}(t_{primal}+1) > \epsilon)$ **or** $(\Delta\widehat{\boldsymbol{\rho}}(t_{primal}+1) > \epsilon)$ **then**
    $t_{primal} \leftarrow t_{primal} + 1$
    go to 2
  end if
  return $\widehat{\boldsymbol{\pi}}(t_{primal}+1), \widehat{\boldsymbol{\rho}}(t_{primal}+1)$
end function

Algorithm 3 Dual problem function

function DUALPROBLEM($\widehat{\boldsymbol{\pi}}^\star(t+1), \widehat{\boldsymbol{\rho}}^\star(t+1)$)
  for $i = 1$ to $|\mathcal{I}|$ **do**
    $\nu_i(t_{dual}+1) \leftarrow \max(0; \nu_i(t_{dual}) + \delta(t)(\log(\sum_{n\in\mathcal{N}} \exp(\widehat{\pi}^\star_{i,n}(t+1))) - \log(P_{max})))$
    for $n = 1$ to $|\mathcal{N}|$ **do**
      for $k = 1$ to $|\mathcal{K}(i)|$ **do**
        $\lambda_{k,i,n}(t_{dual}+1) \leftarrow \max(0; \lambda_{k,i,n}(t_{dual}) + \delta(t)(\log(\exp(\widehat{\rho}^\star_{k.i.n}(t+1) - \widehat{\pi}^\star_{i,n}(t+1))\frac{N_0}{G_{k,i,n}} + \sum_{\substack{i'\in\mathcal{N}\\ i'\neq i}} \exp(\widehat{\rho}^\star_{k.i.n}(t+1) + \widehat{\pi}^\star_{i',n}(t+1) - \widehat{\pi}^\star_{i,n}(t+1))\frac{G_{k,i',n}}{G_{k,i,n}})))$
      end for
    end for
  end for
  if $(\Delta\boldsymbol{\nu}(t_{dual}+1) > \epsilon)$ **or** $(\Delta\boldsymbol{\lambda}(t_{dual}+1) > \epsilon)$ **then**
    $t_{dual} \leftarrow t_{dual} + 1$
    go to 2
  end if
  return $\boldsymbol{\nu}(t_{dual}+1), \boldsymbol{\lambda}(t_{dual}+1)$
end function

3.5.2 Solving the Resource Allocation Problem

In this subsection, we search for the optimal solution to the resource allocation problem (3.15). For each cell i, the problem (3.15) is a convex optimization problem, as proven previously.

Theorem 3.3. *For each cell i, the optimal solution to the resource allocation problem* (3.15) *is given by:* $\theta_{k,n} = \frac{1}{\max(|\mathcal{K}(i)|, |\mathcal{N}|)}, \forall k \in \mathcal{K}(i), \forall n \in \mathcal{N}$.

Proof: We consider the objective function (3.15a), which can be written as follows:

$$\begin{aligned}(\eta_2)_i &= \sum_{k\in\mathcal{K}(i)}\sum_{n\in\mathcal{N}}\log(\theta_{k,n}) \\ &= \log\left(\prod_{\substack{k\in\mathcal{K}(i)\\ n\in\mathcal{N}}}\theta_{k,n}\right).\end{aligned} \tag{3.23}$$

Since log function is monotonically increasing, the maximization of $(\eta_2)_i$ becomes equivalent to the maximization of the term $\prod_{\substack{k\in\mathcal{K}(i)\\ n\in\mathcal{N}}}\theta_{k,n}$. We consider the following cases:

1. Let us assume that:

$$\sum_{k\in\mathcal{K}(i)}\theta_{k,n} < \sum_{n\in\mathcal{N}}\theta_{k,n},\ \forall\ k\ \in\mathcal{K}(i),\ \forall\ n\in\ \mathcal{N}. \tag{3.24}$$

We suppose that $\theta_{k,n}, \forall\ k\in\mathcal{K}(i), \forall\ n\in\mathcal{N}$ is an optimal solution to the resource allocation problem (3.15) *i.e.*, this solution maximizes the objective function (3.15a). For this solution, we assume that:

$$\exists\ k\ \in\ \mathcal{K}(i)\ /\ \sum_{n\in\mathcal{N}}\theta_{k,n}\ <\ 1. \tag{3.25}$$

We define $\epsilon\ >\ 0$ as follows:

$$\epsilon = 1 - \sum_{n\in\mathcal{N}}\theta_{k,n},$$

and we demonstrate that this solution is not an optimal solution to problem (3.15) using the proof by contradiction. In fact, we define another set of $\theta'_{k,n}$ values as given in the following:

$$\theta'_{k,n} = \begin{cases} \theta_{k,n}, & \forall\ n\in\mathcal{N},\ n\neq n_1, \forall\ k\in\mathcal{K}(i) \\ \theta_{k,n}+\epsilon, & \text{if } n = n_1, \forall\ k\in\mathcal{K}(i). \end{cases}$$

Therefore, we have:

$$\prod_{\substack{k\in\mathcal{K}(i)\\ n\in\mathcal{N}}} \theta'_{k,n} = \prod_{\substack{k\in\mathcal{K}(i)\\ n\in\mathcal{N}}} \theta_{k,n} + \epsilon \cdot \prod_{\substack{k\in\mathcal{K}(i)\\ n\in\mathcal{N}}} \theta_{k,n}$$
$$> \prod_{\substack{k\in\mathcal{K}(i)\\ n\in\mathcal{N}}} \theta_{k,n},$$

and the assumption made in (3.25) is false, since it does not maximize the objective function (3.15a). Consequently, we have:

$$\sum_{n\in\mathcal{N}} \theta_{k,n} = 1, \forall\ k\ \in\ \mathcal{K}(i)$$
$$\Rightarrow \quad \sum_{k\in\mathcal{K}(i)} \sum_{n\in\mathcal{N}} \theta_{k,n} = |\mathcal{K}(i)|.$$

Since the sum of all the $\theta_{k,n}$ variables is constant, the term $\prod_{\substack{k\in\mathcal{K}(i)\\ n\in\mathcal{N}}} \theta_{k,n}$ reaches its maximum when all the variables $\theta_{k,n}$ are equal *i.e.*,

$$\theta_{k,n} = \frac{|\mathcal{K}(i)|}{|\mathcal{K}(i)| \cdot |\mathcal{N}|} = \frac{1}{|\mathcal{N}|}, \forall\ k \in \mathcal{K}(i), \forall\ n \in \mathcal{N},$$

which is an optimal solution to the resource allocation problem (3.15). According to (3.24):

$$\sum_{k\in\mathcal{K}(i)} \theta_{k,n} < \sum_{n\in\mathcal{N}} \theta_{k,n},\ \forall\ k\ \in \mathcal{K}(i),\ \forall\ n \in\ \mathcal{N}$$
$$\Rightarrow \qquad \frac{|\mathcal{K}(i)|}{|\mathcal{N}|} < 1$$
$$\Rightarrow \qquad |\mathcal{K}(i)| < |\mathcal{N}|.$$

2. Similarly, when:

$$\sum_{n\in\mathcal{N}} \theta_{k,n} < \sum_{k\in\mathcal{K}(i)} \theta_{k,n},\ \forall\ k\ \in \mathcal{K}(i),\ \forall\ n \in\ \mathcal{N}, \tag{3.26}$$

We suppose that a given set of $\theta_{k,n}$ values $\forall\ k\ \in\ \mathcal{K}(i), \forall\ n\ \in\ \mathcal{N}$ is an optimal solution to the resource allocation problem (3.15). For this solution, we assume that:

$$\exists\ n\ \in\ \mathcal{N}\ /\ \sum_{k\in\mathcal{K}(i)} \theta_{k,n}\ <\ 1. \tag{3.27}$$

We define $\xi > 0$ as follows:

$$\xi = 1 - \sum_{k \in \mathcal{K}(i)} \theta_{k,n},$$

and we demonstrate that this solution is not an optimal solution to problem (3.15) using the proof by contradiction. In fact, we define another set of $\theta^{"}_{k,n}$ variables as given in the following:

$$\theta^{"}_{k,n} = \begin{cases} \theta_{k,n}, & \forall\, n \in \mathcal{N}, \forall\, k \in \mathcal{K}(i), k \neq k_1 \\ \theta_{k,n} + \xi, & \text{if } k = k_1, \forall\, n \in \mathcal{N}. \end{cases}$$

Therefore, we have:

$$\begin{aligned} \prod_{\substack{k \in \mathcal{K}(i) \\ n \in \mathcal{N}}} \theta^{"}_{k,n} &= \prod_{\substack{k \in \mathcal{K}(i) \\ n \in \mathcal{N}}} \theta_{k,n} + \xi \cdot \prod_{\substack{k \in \mathcal{K}(i) \\ n \in \mathcal{N}}} \theta_{k,n} \\ &> \prod_{\substack{k \in \mathcal{K}(i) \\ n \in \mathcal{N}}} \theta_{k,n}, \end{aligned}$$

and the assumption made in (3.27) is false, since it does not maximize the objective function (3.15a). Consequently, we have:

$$\begin{aligned} & \sum_{k \in \mathcal{K}(i)} \theta_{k,n} = 1, \forall\, n \in \mathcal{N} \\ \Rightarrow \quad & \sum_{n \in \mathcal{N}} \sum_{k \in \mathcal{K}(i)} \theta_{k,n} = |\mathcal{N}|. \end{aligned}$$

Since the sum of the $(|\mathcal{K}(i)| \cdot |\mathcal{N}|)$ variables $\theta_{k,n}$ is constant, the term $\prod_{\substack{k \in \mathcal{K}(i) \\ n \in \mathcal{N}}} \theta_{k,n}$ reaches its maximum when all the variables $\theta_{k,n}$ are equal *i.e.*,

$$\theta_{k,n} = \frac{|\mathcal{N}|}{|\mathcal{K}(i)| \cdot |\mathcal{N}|} = \frac{1}{|\mathcal{K}(i)|}, \forall\, k \in \mathcal{K}(i), \forall\, n \in \mathcal{N},$$

which is an optimal solution to the resource allocation problem (3.15). According to (3.26):

$$\begin{aligned} & \sum_{n \in \mathcal{N}} \theta_{k,n} < \sum_{k \in \mathcal{K}(i)} \theta_{k,n},\ \forall\, k \in \mathcal{K}(i),\ \forall\, n \in \mathcal{N} \\ \Rightarrow \quad & \frac{|\mathcal{N}|}{|\mathcal{K}(i)|} < 1 \\ \Rightarrow \quad & |\mathcal{N}| < |\mathcal{K}(i)|. \end{aligned}$$

When the number of active UEs is less than the number of available resources, $\theta_{k,n} = \frac{1}{|\mathcal{N}|}, \forall k \in \mathcal{K}(i), \forall n \in \mathcal{N}$, and we obtain:

$$\begin{aligned} \sum_{k \in \mathcal{K}(i)} \theta_{k,n} &= \frac{|\mathcal{K}(i)|}{|\mathcal{N}|} \quad \leq 1, \forall n \in \mathcal{N}, \\ \sum_{n \in \mathcal{N}} \theta_{k,n} &= \frac{|\mathcal{N}|}{|\mathcal{N}|} \quad = 1, \forall k \in \mathcal{K}(i). \end{aligned}$$

Thus, the available resources are not fully used over time, and each UE is permanently served. Otherwise, the optimal solution is: $\theta_{k,n} = \frac{1}{|\mathcal{K}(i)|}, \forall k \in \mathcal{K}(i), \forall n \in \mathcal{N}$. This corresponds to the scenario where the number of active UEs is greater than the number of RBs. We obtain:

$$\begin{aligned} \sum_{k \in \mathcal{K}(i)} \theta_{k,n} &= \frac{|\mathcal{K}(i)|}{|\mathcal{K}(i)|} \quad = 1, \forall n \in \mathcal{N}, \\ \sum_{n \in \mathcal{N}} \theta_{k,n} &= \frac{|\mathcal{N}|}{|\mathcal{K}(i)|} \quad \leq 1, \forall k \in \mathcal{K}(i). \end{aligned}$$

In this case, each RB is fully used over time, while UEs are not permanently served over time.

3.6 Decentralized Resource and Power Allocation

3.6.1 Problem Formulation and Decomposition

We have shown that the power allocation problem can be solved optimally in a centralized fashion. In this section we investigate the decentralized resource and power allocation approach. Base stations of the LTE/LTE-A networks are autonomous entities, and each cell performs resource and power allocation independently of the other cells. Each cell i maximizes its own utility function, which is given by:

$$\begin{aligned} &\sum_{k \in \mathcal{K}(i)} \sum_{n \in \mathcal{N}} \log \left(\theta_{k,n} . \log \left(1 + \frac{\pi_{i,n} G_{k,i,n}}{N_0 + \sum_{i' \neq i} \pi_{i',n} G_{k,i',n}} \right) \right) \\ &= \sum_{k \in \mathcal{K}(i)} \sum_{n \in \mathcal{N}} \log(\theta_{k,n}) + \sum_{k \in \mathcal{K}(i)} \sum_{n \in \mathcal{N}} \log \left(\log \left(1 + \frac{\pi_{i,n} G_{k,i,n}}{N_0 + \sum_{i' \neq i} \pi_{i',n} G_{k,i',n}} \right) \right). \end{aligned} \tag{3.28}$$

The decentralized joint resource and power allocation problem is therefore separable into two independent problems: a resource allocation problem and a power allocation problem. The resource allocation problem is solved in a distributed manner as demonstrated in the previous section. We propose a decentralized power allocation approach based on game theory, where the cells are the decision makers or players of the game. We define a multi-player game $\mathcal{G}$ between the $|\mathcal{I}|$ cells. The cells are assumed to make their decisions without knowing the decisions of each other.

The formulation of this non-cooperative game $G = \langle \mathcal{I}, S, U \rangle$ can be described as follows:

- A finite set of cells $\mathcal{I} = (1, ..., |\mathcal{I}|)$.
- For each cell i, the space of pure strategies is S_i given by what follows:

$$S_i = \{\pi_i \in R^{|\mathcal{N}|} \text{such as } \pi_{i,n} \geq \pi_{min}, \forall i \in \mathcal{I}, \forall n \in \mathcal{N} \text{and} \sum_{n \in \mathcal{N}} \pi_{i,n} \leq P_{max}, \forall i \in \mathcal{I}\}.$$

  An action of a cell i is the amount of power $\pi_{i,n}$ allocated to the RB n, and the strategy chosen by cell i is then $\pi_i = (\pi_{i,1}, ..., \pi_{i,N})$. A *strategy profile* $\pi = (\pi_1, ..., \pi_{|\mathcal{I}|})$ specifies the strategies of all players and $S = S_1 ... S_{|\mathcal{I}|}$ is the set of all strategies.

- A set of utility functions $U = (U_1(\pi), U_2(\pi), ..., U_I(\pi))$ that quantify players' utility for a given strategy profile π, where a given utility U_i for cell i is such as:

$$U_i = \sum_{k \in \mathcal{K}(i)} \sum_{n \in \mathcal{N}} \log \left(\log \left(1 + \frac{\pi_{i,n} G_{k,i,n}}{N_0 + \sum_{i' \neq i} \pi_{i',n} G_{k,i',n}} \right) \right). \tag{3.29}$$

For every i, U_i is concave with respect to π_i and continuous with respect to $\pi_l, l \neq i$. Hence, a Nash Equilibrium (NE) exists [Ros65]. We note that the objective function η_1 of the centralized power allocation problem (3.13) is equivalent to the sum of the utility functions U_i of the I cells.

3.6.2 Super-Modular Games

Super-modular games exhibit strategic complementarity *i.e.*, the marginal utility for a player in playing a higher strategy increases when the opponents also play higher strategy [Top98]. These games encompass many applied models, and they are characterized by

the existence of pure strategy NE. Before presenting the properties of a super-modular game, we list first some definitions.

Definition 3.4. If U_i is twice differentiable, it is said to be super-modular if:

$$\frac{\partial U_i}{\partial \pi_l \partial \pi_i} \geq 0,$$

for all $l \in \mathcal{I} - \{i\}$ and $\forall\, \pi_i \in S_i$.

According to [Top79], a game is super-modular if $\forall i \in \mathcal{I}$:

1. The strategy space S_i is a compact sublattice of $\mathbb{R}^N$.
2. The utility function U_i is super-modular.

In [Top79, Yao95], proof is given for the following two results in a S-modular game:

- If each cell i initially uses either its lowest or largest policy in S_i, then a best response algorithm converges monotonically to an equilibrium that may depend on the initial state.
- If we start with a feasible policy, then the sequence of best responses monotonically converges to an equilibrium: it monotonically increases in all components in the case of maximizing in a super-modular game.

Proposition 3.5. *The game $\mathcal{G}$ is a super-modular game.*

Proof: To prove the super-modularity of the present game, we need to verify the conditions in 3.6.2. First, the strategy space S_i is clearly a compact convex set of $\mathbb{R}^N$. Hence, it suffices to verify the super-modularity of the utility function as there are no constraint policies for $\mathcal{G}$:

$$\frac{\partial U_{i,n}}{\partial \pi_{l,n} \partial \pi_{i,n}} = \frac{1}{\log\left(1+\sigma_{k,i,n}\right)} \frac{G_{k,i,n} G_{k,l,n}}{\left(N_0 + \sum_{i' \neq i} \pi_{i',n} G_{k,i',n}\right)^2} \left(\frac{\sigma_{k,i,n}}{\log\left(1+\sigma_{k,i,n}\right)} - 1 \right).$$

As $\frac{x}{\log(1+x)} > 1$ for $x > 0$, $\frac{\partial U_{i,n}}{\partial \pi_{l,n} \partial \pi_{i,n}} \geq 0$, $\forall l \in \mathcal{I} - \{i\}$ and $\forall n \in \mathcal{N}$.

To attain the NE of the game, we implement a best response algorithm where in each round t, cell i strives to find, in parallel for every RB $n \in \mathcal{N}$, the following optimal power

level as a response to $\pi_{-i}(t-1)$:

$$\pi_i^*(t) = \arg \quad \max_{\pi_i} U_i(\pi_i, \pi_{-i}), s.t.\, \pi_i^* \in S_i.$$

The resulting optimization problem for each cell i is as follows:

$$\underset{\boldsymbol{\pi}_i}{\text{maximize}} \; U_i \tag{3.30a}$$

$$\text{subject to:} \sum_{n \in \mathcal{N}} \pi_{i,n} \leq P_{max}, \tag{3.30b}$$

$$\pi_{i,n} \geq \pi_{min}, \forall n \in \mathcal{N}. \tag{3.30c}$$

3.6.3 Solving the Decentralized Power Allocation Problem

We use the subgradient projection method to solve the decentralized power allocation problem (3.30). It is an iterative method that starts with some initial feasible vector $\boldsymbol{\pi}_i$ that satisfies constraints (3.30b) and (3.30c), and generates the next iteration by taking a step along the subgradient direction of U_i at $\boldsymbol{\pi}_i$. For each cell i, iterations of the subgradient projection are given by:

$$\pi_{i,n}(t+1) = \pi_{i,n}(t) + \delta(t) \frac{\partial U_i}{\partial \pi_{i,n}}, \forall n \in \mathcal{N}, \tag{3.31}$$

where the partial derivative of the objective function U_i with respect to $\pi_{i,n}$ is given by:

$$\frac{\partial U_i}{\partial \pi_{i,n}} = \sum_{k \in \mathcal{K}(i)} \frac{G_{k,i,n}}{(N_0 + F_{i,n}) \left(1 + \frac{\pi_{i,n} G_{k,i,n}}{N_0 + F_{i,n}}\right) \log\left(1 + \frac{\pi_{i,n} G_{k,i,n}}{N_0 + F_{i,n}}\right)}, \tag{3.32a}$$

$$F_{i,n} = \sum_{\substack{i' \in \mathcal{I} \\ i' \neq i}} \pi_{i',n} G_{k,i',n}, \forall n \in \mathcal{N}. \tag{3.32b}$$

The scalar $\delta(t) > 0$ is a small step size (*e.g.*, $\delta(t) = 0.001$) chosen appropriately [Chi05] to guarantee the convergence of the decentralized power allocation problem (3.30). Before updating the variables $\pi_{i,n}(t+1)$, we make sure that $\pi_{i,n}(t+1) \geq \pi_{min}$ in order to satisfy the constraints (3.30c). Moreover, if constraints (3.30b) are not satisfied, we perform a projection on the feasible set P_{max}, which is straightforward for a simplex [Pal05]. Then, we calculate the power difference $\Delta\pi_i$, which is the difference between

Algorithm 4 Decentralized power allocation

1: Parameters: the utility function $U_i, \forall i \in \mathcal{I}$, the maximum power per cell P_{max}, and the minimum power per RB π_{min}.
2: Initialization: set $t = 0$, $t_i = 0, \forall i \in \mathcal{I}$, and $\pi_{i,n}(0)$ to some positive value $\geq \pi_{min}, \forall i \in \mathcal{I}, \forall n \in \mathcal{N}$, such as $\sum_{n \in \mathcal{N}} \pi_{i,n}(0) \leq P_{max}, \forall i \in \mathcal{I}$.
3: **for** $i = 1$ to $|\mathcal{I}|$ **do**
4: **for** $n = 1$ to $|\mathcal{N}|$ **do**
5: $\pi_{i,n}(t_i + 1) \leftarrow \max\left(\pi_{min}; \pi_{i,n}(t_i) + \delta(t_i) \frac{\partial U_i}{\partial \pi_{i,n}}\right)$
6: **end for**
7: **if** $\sum_{n=1}^{|\mathcal{N}|} \pi_{i,n}(t_i + 1) > P_{max}$ **then**
8: Perform projection on simplex P_{max}
9: **end if**
10: **if** $\Delta\pi_i(t_i + 1) > \epsilon$ **then**
11: $t_i \leftarrow t_i + 1$
12: **go to** 4
13: **end if**
14: $\pi^*_{i,n}(t + 1) \leftarrow \pi_{i,n}(t_i + 1), \forall n \in \mathcal{N}$
15: **end for**
16: **if** $\Delta\pi^*(t + 1) > \epsilon$ **then**
17: $t \leftarrow t + 1$
18: **go to** 3
19: **end if**

the power allocation vectors of the current and the previous iterations. It is given by:

$$\Delta\pi_i(t + 1) = \|\pi_i(t + 1) - \pi_i(t)\|. \tag{3.33}$$

For each cell i, iterations are performed until satisfying the satisfaction criterion *i.e.*, when $\Delta\pi_i < \epsilon$, where $\epsilon > 0$ is a very small scalar.

As described in Algorithm 4, each cell i calculates $\pi_{i,n}(t_i + 1), \forall n \in \mathcal{N}$, where t_i is the iteration number for cell i. The obtained power values are updated in accordance with the constraints (3.30b) and (3.30c). This procedure is repeated and the number of iterations t_i is incremented until $\Delta\pi_i(t_i + 1)$ becomes less than ϵ. The number of rounds required for all the cells to converge is denoted by t. An additional round of power calculation is performed for all the cells and t is incremented as long as $\Delta\pi^*(t + 1) > \epsilon$, where $\pi^*(t)$ is the power allocation vector obtained at the end of round t.

3.7 Performance Evaluation

In this section, we evaluate the convergence and the performance of the proposed centralized joint resource and power allocation problem, and the decentralized power allocation approach.

3.7.1 Centralized Resource and Power Allocation

To verify the convergence of the centralized solution, we consider a multi-user OFDMA network, such as LTE/LTE-A networks, that consists of seven adjacent hexagonal cells, with one UE served by each cell. System bandwidth equals 5 MHz, and traffic model is full buffer. UE positions and radio conditions are randomly generated, and the initial power allocation for each RB equals the minimum downlink transmission power per RB. Thus, we have an initial feasible power vector that satisfies constraints (3.17b):

$$\pi_{i,n} = \pi_{min}, \forall i \in \mathcal{I}, \forall n \in \mathcal{N}.$$

The primal optimization variables $\widehat{\rho}_{k,i,n}$ and $\widehat{\pi}_{i,n}$ are calculated accordingly. System bandwidth equals 5 MHz. Thus, 25 RBs are available in each cell. The maximum transmission power per cell P_{max} is set to 43 dBm or 20 W. At the first iteration, the dual variables $\lambda_{k,i,n}(0), \forall k \in \mathcal{K}(i), \forall i \in \mathcal{I}, \forall n \in \mathcal{N}$, and $\nu_i(0), \forall i \in \mathcal{I}$, are assigned initial non negative values. Then the primal variables are updated using the subgradient projection iterates (3.18a) and (3.18b), and the obtained solution is denoted $\widehat{\rho}^{\star}_{k,i,n}(\boldsymbol{\lambda}(t), \boldsymbol{\nu}(t))$ and $\widehat{\pi}^{\star}_{i,n}(\boldsymbol{\lambda}(t), \boldsymbol{\nu}(t))$. The dual variables $\boldsymbol{\lambda}$ and $\boldsymbol{\nu}$ are then updated using the gradient iterates (3.21a) and (3.21b), respectively. The same procedure is repeated until convergence of the primal and the dual variables. The evolution of $\widehat{\pi}_{i,1}$ along with the number of iterations is shown in Fig. 3.1, where $\widehat{\pi}_{i,1}$ is the logarithm of the transmission power allocated by the cell i to the RB 1. In addition, the number of primal iterations and the number of dual iterations per round are shown in Fig. 3.2.

We notice that for the centralized power allocation approach, the primal problem requires approximately 6000 iterations to converge. As shown in Fig. 3.2, 1100 rounds are required to reach the optimal values of the primal and the dual variables. The zoomed box within Fig. 3.1 shows the evolution of $\widehat{\pi}_{i,n}$ versus the number of primal iterations for a given round t. The values of $\widehat{\pi}_{i,n}$ are calculated using the dual variables obtained at the

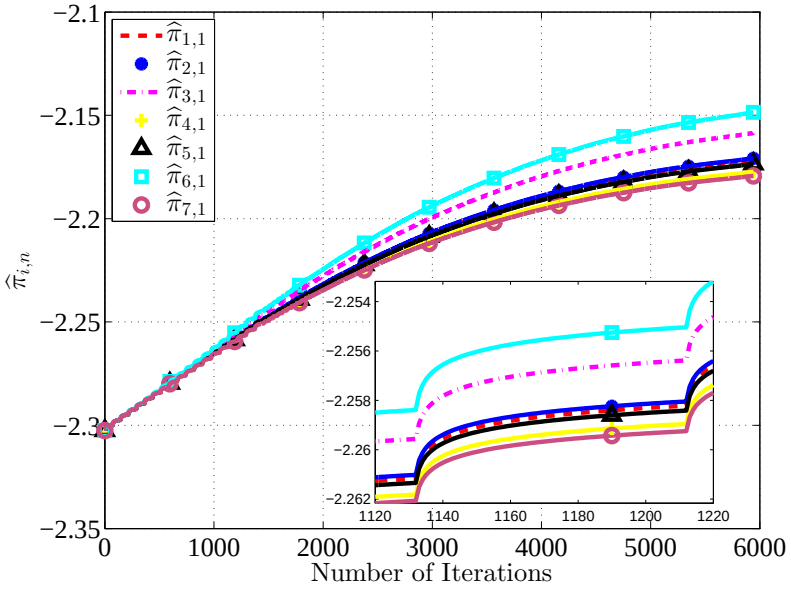

Figure 3.1: Convergence of the primal variables $\widehat{\pi}_{i,n}$

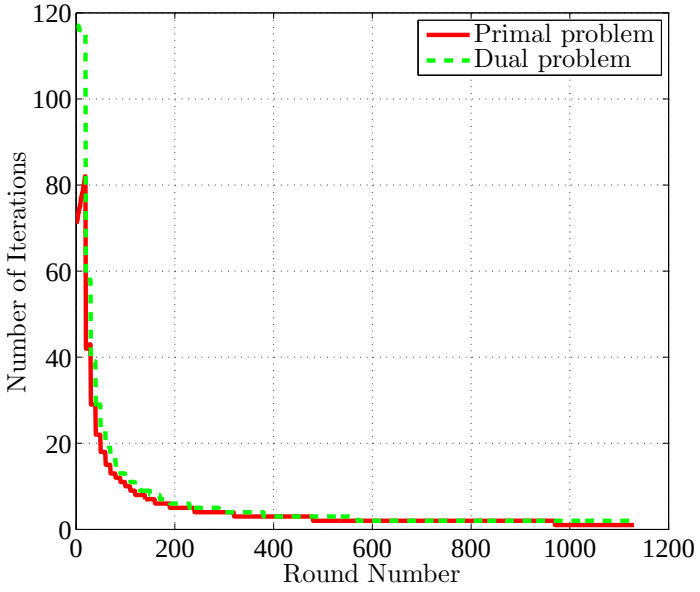

Figure 3.2: Number of primal and dual iterations per round

round $(t-1)$. We also notice that the number of primal iterations and the number of dual iterations decreases with the number of rounds. When t increases, the impact of Lagrange prices $\lambda_{k,i,n}(t)$ and $\nu_i(t)$ on the primal variables calculation is reduced, and the number of primal iterations required for the primal problem to converge becomes lower. The same behavior is noticed for the number of dual iterations when the number of rounds increases.

For the same simulated scenario, we also show the dual variables $\lambda_{k,i,n}$ and ν_i versus

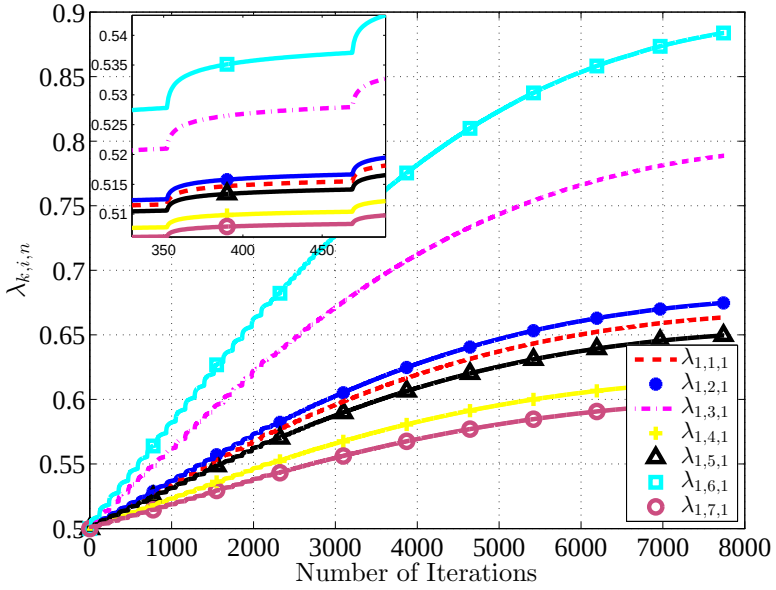

Figure 3.3: Lagrange prices $\lambda_{k,i,n}$

the number of dual iterations in Fig. 3.3 and Fig. 3.4, respectively. We notice that approximately 8000 iterations are required for the dual problem to converge. At a given round t, the Lagrange prices $\lambda_{k,i,n}$ and ν_i are updated using the most recent values of the primal variables. The zoomed boxes within Fig. 3.3 and Fig. 3.4 show the evolution of $\lambda_{k,i,n}$ and ν_i versus the number of iterations, respectively. These values are updated until $\Delta\lambda_{k,i,n}$ and $\Delta\nu_i$ become less than ϵ. Convergence of the centralized power allocation problem occurs when two conditions are satisfied: first, the difference between the updated primal variables at round t and their values at round $(t-1)$ is less than ϵ. Second, the difference between the updated primal variables at round t and their values at round $(t-1)$ is less than ϵ.

3.7.2 Decentralized Power Allocation

The same scenario in 3.7.1 is also simulated to evaluate the performance and convergence of the decentralized power allocation approach. The evolution of the downlink transmission power allocated by all the cells to a given RB, along with the number of iterations is shown in Fig. 3.5.

The initial value of the downlink transmission power allocated to each RB equals π_{min} (0.1 W). This allocation satisfies the constraints of the minimal downlink transmission power per RB and that of the maximum transmission power per cell. Each cell i seeks

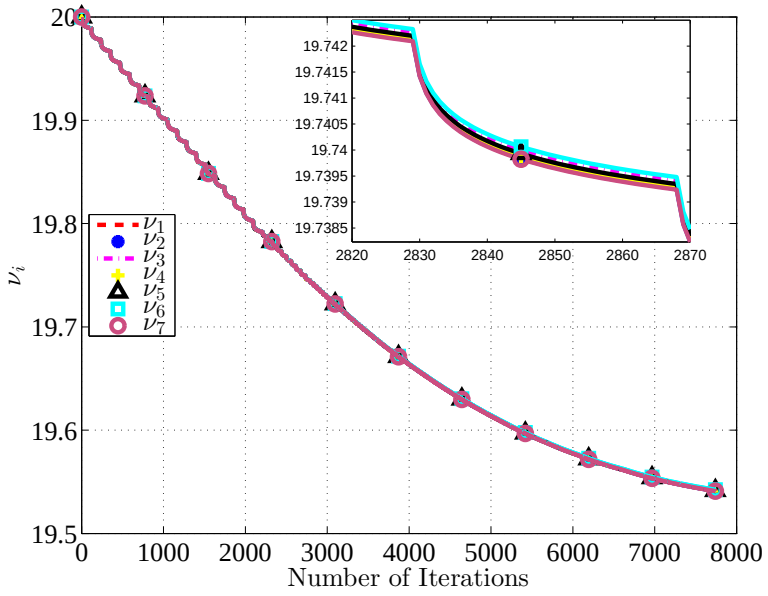

Figure 3.4: Lagrange prices ν_i

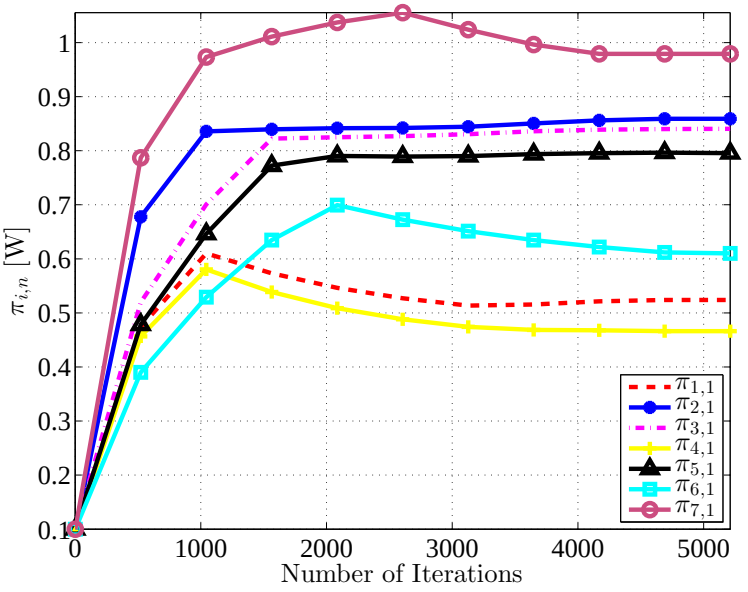

Figure 3.5: $\pi_{i,n}$ versus the number of iterations for the decentralized approach

maximizing its own utility function U_i by adjusting the transmission power allocated to the available RBs. It also estimates the interference due to the usage of the same RBs by the neighboring cells, and it uses this estimation to calculate SINR values of the UEs within its coverage area. As shown in Fig. 3.5, each cell starts increasing the downlink transmission power allocated to its RBs, and then the transmission power converges after a given number of iterations. At convergence, the partial derivative of the objective function U_i with respect to $\pi_{i,n}$ becomes negligible. The difference between the updated power allocation vector $(\pi_{i,1}, \pi_{i,2}, ..., \pi_{i,N})$ at iteration $(t+1)$ and the power vector at

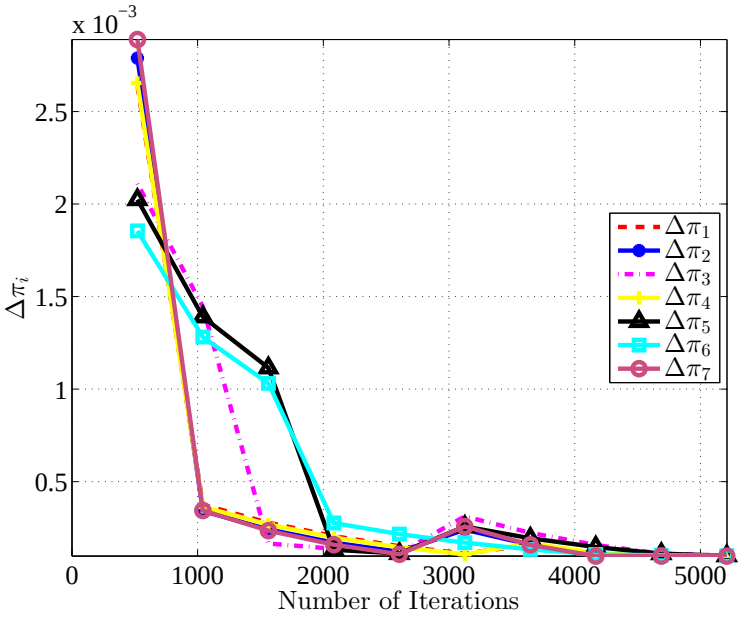

Figure 3.6: $\Delta\pi_i$ versus the number of iterations for the decentralized approach

iteration t becomes less than ϵ.

We also show the evolution of the power vector difference $\Delta\pi_i, \forall i \in \mathcal{I}$, defined in (3.33) along with the number of iterations in Fig. 3.6.

The results show that $\Delta\pi_i$ decreases when the number of iterations increases. The impact of the subgradient projection iterations on the downlink transmission power $\pi_{i,n}$ becomes smaller as more iterations are performed. Power convergence is achieved when $\Delta\pi_i$ becomes less than ϵ. In fact, the utility function of each cell i is maximized, and the amount by which the downlink transmission power $\pi_{i,n}$ is modified becomes negligible.

3.7.3 Comparison with State-of-the-Art Resource Allocation Approaches

We also compare the performance of our proposed centralized and decentralized resource and power allocation approaches with that of state-of-the-art resource and power allocation approaches such as the frequency reuse-1 model, the frequency reuse-3 model, FFR, and SFR techniques [YAL+15]. Simulation scenario is the same as in 3.7.1. The frequency reuse-1 model allows the usage of the same frequency spectrum simultaneously in all the network cells. Moreover, homogeneous power allocation is performed, and the

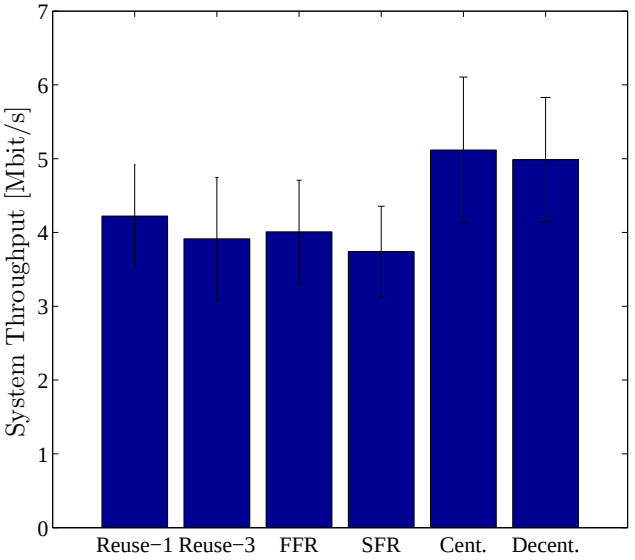

Figure 3.7: System throughput for several resource allocation approaches

downlink transmission power allocated to each RB is given by:

$$\pi_{i,n} = \frac{P_{max}}{N}, \forall i \in \mathcal{I}, \forall n \in \mathcal{N}. \tag{3.34}$$

In the frequency reuse-3 model, one third of the available spectrum is used in each cell in a cluster of three adjacent cells. Interference problems are eliminated, but the spectral efficiency is largely reduced. FFR and SFR techniques divide each cell into a cell-center and a cell-edge zones, and set restrictions on resource usage and power allocation in each zone. For all the compared techniques, resource allocation is performed according to Theorem 3.3.

3.7.3.1 System Throughput

For several simulation runs, we show the total system throughput for all the strategies under the same simulation scenarios. Simulation results, including the 95% confidence interval, are illustrated in Fig. 3.7.

The centralized resource allocation approach offers the highest system throughput among all the compared techniques. In fact, it searches for the optimal resource and power allocation while taking into account restrictions on resource usage between the active UEs and on the downlink transmission power allocation. System throughput for the decentralized approach is slightly lower than that of the centralized approach, since resource

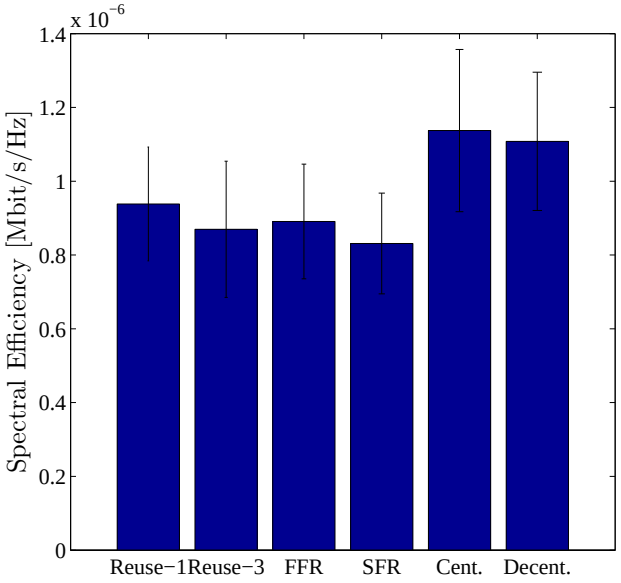

Figure 3.8: Spectral efficiency for several resource allocation approaches

and power allocation is performed locally by each cell without getting the necessary information about resource usage and power allocation from the neighboring cells. The achievable throughput is greater than that of the frequency reuse-3 model, FFR, and SFR techniques. Although the restrictions made on resource usage by these techniques mitigate ICI, the achievable throughput is reduced since the available spectrum in each cell or in each cell zone, is reduced.

3.7.3.2 Spectral Efficiency

We also investigate the impact of the compared techniques on the spectral efficiency. Simulation results are shown in Fig. 3.8.

Our proposed centralized resource allocation approach offers the highest spectral efficiency, since the optimal resource and power allocation is guaranteed. The spectral efficiency of our decentralized approach is slightly lower than that of the centralized approach, due to the lack of information about resource usage in the neighboring cells. Nevertheless, the spectral efficiency for both the centralized and the decentralized approaches is higher than that of FFR and SFR techniques. In fact, the static restrictions made on resource allocation between cell zones, and the quantified transmission power levels allocated to the available RBs do not allow to perform flexible resource allocation in a manner that satisfies UE needs in each cell.

3.7.4 Centralized Versus Decentralized Complexity Comparison

We evaluate the computational complexity of our centralized and decentralized resource and power allocation approaches. For the centralized and decentralized approaches, resource allocation is performed according to Theorem 3.3, and it is equivalent to one operation. The complexity of each approach equals the number of required operations multiplied by the complexity of a single operation, which is denoted by T_{op}. The complexity of the centralized approach's algorithm is given by:

$$O\left[\left(\mathrm{nb}_{\mathrm{primal}}|\mathcal{N}|(1+k)+\mathrm{nb}_{\mathrm{dual}}\left(1+k|\mathcal{N}|\right)\right)|\mathcal{I}|T_{op}\right]. \tag{3.35}$$

Similarly, the decentralized approach complexity is given as follows:

$$O(\mathrm{nb}_{\mathrm{iterations}}|\mathcal{I}||\mathcal{N}|T_{op}), \tag{3.36}$$

where $\mathrm{nb}_{\mathrm{primal}}$ is the number of primal iterations and $\mathrm{nb}_{\mathrm{dual}}$ is the number of dual iterations required for convergence of the centralized approach. k is the number of UEs per cell, and $\mathrm{nb}_{\mathrm{iterations}}$ is the number of iterations required for convergence of the decentralized approach.

We notice that the decentralized approach complexity is independent of the number of UEs per cell, contrarily to that of the centralized approach. The complexity of both techniques depends of the number of cells in the system and the number of resources available in each cell. Moreover, the computational complexity of the centralized and decentralized approaches are evaluated under the same simulation scenario as in 3.7.1. Simulation results are given in Fig. 3.9. The mean number of operations required for the centralized and decentralized approaches are given in Table 3.2.

Table 3.2: Mean number of operations per approach

Approach	**Number of operations**
Centralized	$3.02 \cdot 10^8$
Decentralized	$8.84 \cdot 10^5$

According to the results illustrated in Fig. 3.9, and reported in Table 3.2, the number of operations required for the centralized resource and power allocation approach largely exceeds that of the decentralized approach. In fact, the centralized approach maximizes the objective function for the entire network, contrarily to the decentralized approach

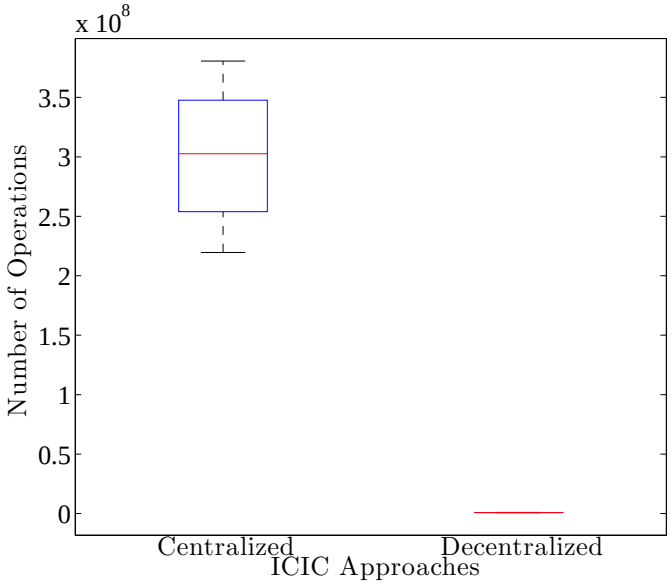

Figure 3.9: Computational complexity of the centralized and decentralized approaches

where each cell maximizes its objective function independently of the other cells. Therefore, the centralized approach guarantees the optimal solution at the expense of a high computational complexity.

3.8 Conclusion

The resource and power allocation problem is a challenging problem for present and future mobile networks. Several state-of-the-art techniques consider the joint resource and power allocation problem, and formulate it as nonlinear optimization problems. The objective is maximizing system throughput, spectral efficiency, or energy efficiency under constraints related to the minimum throughput per UE, QoS parameters, and the maximum transmission power. However, the main disadvantage of these techniques is that they do not consider the impact of ICI when solving the multi-cell optimization problem. Indeed, each cell solves its own resource and power allocation problem without taking into account resource usage and power allocation in the neighboring cells.

In this chapter, we formulated the joint resource and power allocation problem for multiuser OFDMA networks as a centralized optimization problem, where the objective consists in maximizing system throughput while guaranteeing throughput fairness between UEs. The joint problem is then decomposed into two independent problems: a resource allocation problem and a power allocation problem. Contrarily to the majority

of the state-of-the-art approaches, ICI is not neglected, and the impact of the simultaneous transmissions in the neighboring cells is taken into account when managing the resource and power allocation. Moreover, we introduced a decentralized power allocation approach based on game theory. The players are the cells, and each cell aims at maximizing its own utility function regardless of the decisions made by the other cells. Simulation results prove the convergence of the dual variables, and show the positive impact of our proposed centralized and decentralized resource allocation approaches on system performance.

In the next chapter, we investigate autonomous resource and power allocation techniques for multiuser OFDMA networks. These techniques are characterized by a low computation complexity, and they do not generate any additional signaling traffic in comparison with the centralized approaches.

Chapter 4

Heuristic Downlink Power Control Algorithm and Autonomous ICIC for Multiuser OFDMA Networks

Although centralized interference mitigation techniques find the optimal resource and power allocation for the entire multiuser OFDMA network, the centralized approach is characterized by a high computational complexity, and generates additional signaling overhead. For these reasons, autonomous ICIC approaches are fostered. In this chapter, we introduce a heuristic downlink power control algorithm that adjusts power allocation on the downlink of multiuser OFDMA networks. It operates in a distributed manner at each base station. We investigate the impact of the proposed heuristic algorithm on UE throughput and on system power consumption. System performance is compared with the frequency reuse-1 model. Simulation results show that the proposed algorithm largely reduces the downlink power consumption without degrading system performance. It also increases cell-edge UEs throughput that are mainly affected by ICI problems. To further improve system performance, we propose an autonomous dynamic ICIC technique based on CQI feedbacks sent by the UEs to the base stations. It aims at reducing downlink inter-cell interference problems, and achieving throughput fairness for all the UEs without any cooperation between network cells. Contrarily to static FFR and SFR schemes, our technique dynamically allocates resources according to user demands in each cell zone. System level simulations are done to compare the performance of the proposed technique

with the frequency reuse-1 model and other state-of-the-art techniques. The obtained results show that the proposed technique improves energy efficiency, reduces the percentage of unsatisfied UEs, and increases Jain's throughput fairness index in comparison with frequency reuse-1 model and other ICIC techniques.

4.1 Introduction

The main objective of ICIC techniques is to increase the throughput of cell-edge UEs that suffer the most from interference problems. For instance, FFR modifies the frequency resources distribution within each cell in order to reduce interference. Instead of using all the available bandwidth in the neighboring cells, FFR allocates disjoint spectrum for edge zones at neighboring cells. Hence, reuse-3 model is used for cell-edge zones, while reuse-1 is used for cell-center zones. Other frequency reuse-based ICIC techniques modify the transmission power allocated to each band of the available spectrum on the downlink. For example, SFR [Hua05] allocates lower power for cell-center RBs while cell-edge RBs get higher transmission power.

LTE networks are meant to be self-organizing, where operators seek to minimize ICI while reducing the amount of cooperation required between LTE cells. Cooperative ICIC techniques benefit from the communication between network entities to coordinate RBs distribution in the different cells, to reduce ICI and to improve system performance. However, the cooperation between different base stations increases computational complexity, and generates an additional signaling load. Autonomous ICIC techniques do not require any cooperation between base stations, and they are characterized by a lower complexity. Each base station performs RB allocation locally, and there is no need for additional signaling messages.

Before introducing our autonomous ICIC technique, we investigate the impact of power allocation on system performance. Regardless of the resource allocation strategy used, the power allocation mechanism adjusts the transmission power on the different frequency resources in order to increase system throughput. Downlink transmission power is an important issue in distributed networks with dense frequency reuse schemes. The excessive use of downlink power causes interference problems to the neighboring cells. Thus, it degrades system performance, and lowers spectrum profitability. Several works have proposed power allocation algorithms for multiuser OFDMA [PSC12] networks such as LTE.

For instance, authors of [BPVG06] investigate a power allocation algorithm that tries to minimize the requested power under user rate constraints in a non-collaborative system. In addition, [AkI08] introduces a hybrid algorithm that combines adaptive modulation along with power control (*i.e.*, power is increased when the order of the modulation scheme is reduced and vice versa).

ICIC is also the objective in [FFSY09], where the authors use a proportional fair scheduler along with an open loop power control strategy to reduce ICI on the uplink of multi-user OFDMA system. Their objective is to reduce SINR variation in order to increase average UE throughput and cell-edge UE throughput on the uplink. Power is allocated to each UE depending on the number of used RBs, on cell-specific characteristics, and on path loss parameters. Authors of [PB08] introduce a cooperation between base stations of the OFDMA cellular systems in order to couple the resources allocated by the source and relay base stations for a UE. They also propose a distributed power control algorithm that operates independently of the information received from neighboring cells. The influence of cooperation and power control is tested over four different schedulers.

In multiuser OFDMA networks, interference mainly affects cell-edge UEs that receive high interfering signals due to their proximity to the neighboring cells. We propose a heuristic power control algorithm that operates along with the scheduler deployed at each base station. The objective of this algorithm is to avoid power wastage especially for cell-center UEs (that are close to the base stations) or UEs having good radio conditions. Numerous scheduling techniques can be combined with our power control algorithm such as Proportional Fair, Round Robin, Maximum SNR, and many others. Particularly, our heuristic power control algorithm computes power allocation to the different resource blocks once they are allocated to UEs. Power allocation problem is tackled as a method to reduce ICI in dense frequency reuse networks, where all the available frequency resources are simultaneously used in adjacent cells. Power control does not only reduce the power levels of interfering signals (signals usually belonging to cell-center UEs), but it can also increase the power levels on resource blocks that suffer of bad radio conditions (usually RBs allocated for cell-edge UEs). Therefore, it can be considered as an ICIC technique.

4.2 Downlink Power Control in LTE

We particularly focus on the downlink of LTE networks, where frequency reuse-1 model is used along with homogeneous power allocation for all the available RBs. In LTE, downlink Reference Signal (RS) exists only in the physical layer. There are two types of RS: cell specific and user specific. The former is transmitted every sub-frame, and it spans the operating bandwidth. However, the latter is only transmitted within the resource blocks allocated to a specific UE. RSs are inserted every six sub-carriers in the frequency domain [3GP12b, Roe11]. Each RB contains two RSs in the first and the fifth OFDM symbols.

The power level for the RS is signaled within system information to the device. It is cell-specific [3GP09], and it ranges between -60 dBm and +50 dBm per 15 kHz. It is a requirement that the LTE base station transmits all reference signals with constant power over the entire bandwidth. RS is an important element for downlink power allocation, which can be done on a 1 ms basis. In fact, it delivers the reference point for the downlink power.

Authors of [XKM13] propose a downlink power control algorithm based on CQI feedbacks. UEs with different types of service are studied. The downlink power allocated for all the RBs is initialized with the minimum transmission power. For voice-over-IP and data UEs, transmission power is increased until their data requirements are met. However, an additional offset throughput is set upon the minimum data rate requirement for web UEs. The base station stops increasing the transmission power when the additional throughput is achieved.

The transmission power allocated for frequency resources on the downlink affects UEs in the neighboring cells. Thus, downlink power control is also used to reduce interference. For example, authors of [SQ09] noticed that high transmission power for cell-center UEs in 4G systems degrades the performance of cell-edge UEs in the neighboring cells. Therefore, an adaptive power control is proposed to reduce ICI. It aims to ensure the same SINR at the receiver. A distributed power control strategy is used in [KW11] to reduce ICI especially when there is a lack of cooperation between base stations. Power control algorithms were already proposed in [SV09, WKSV10], where they lead to dynamic Soft Frequency Reuse schemes. In addition, authors of [WCLM99, CKKL04] have proposed

dynamic subcarrier, bit and power allocation for multiuser OFDM systems. In fact, frequency resources, modulation order and transmission power are dynamically assigned depending on channel conditions. This flexibility allows to reduce the transmission power while guaranteeing the required bitrates and bit error rate for all the users. Therefore, it is more advantageous than static access schemes such as time division multiple access and frequency division multiple access. Moreover, authors of [KLL03] divided the resource and power allocation problem into two steps. The objective is to minimize total transmission power with constraints on bit-error rate and transmission rate for UEs. In the first step, SINR is used to determine the number of subcarriers to be allocated for each UE. The second step of the algorithm finds the best assignment of subcarriers to UEs.

4.3 System Model

We consider an LTE network of seven adjacent base station sites, each with three hexagonal sectors as shown in Fig. 4.1.

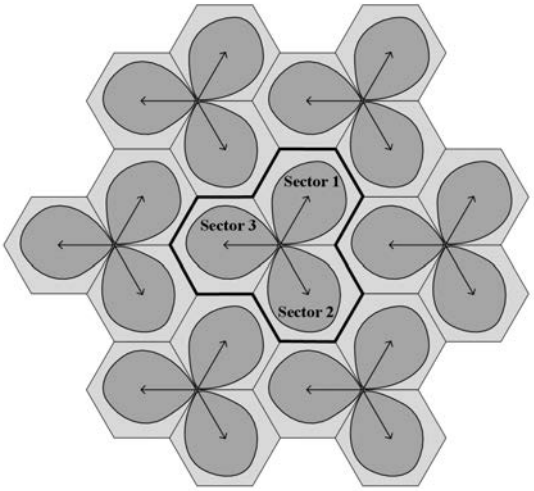

Figure 4.1: LTE network layout

Many state-of-the-art techniques use the distance between eNodeB and UE to classify UEs into cell-edge and cell-center UEs. In our work, we use mean wideband SINR values to perform UE classification. Therefore, there is no need to find the exact position of each UE in the network, and mobile operators are no longer required to solve this localization problem. SINR-based classification is more realistic, since we might have cell-center UEs characterized by a weak useful signal (due to high interference or bad radio conditions) and cell-edge UEs having relatively high SINR values.

Let P denote the maximum downlink transmission power of a cell and N the number of available RBs in this cell. When using frequency reuse-1 model, homogeneous power allocation is applied, and each RB gets the same downlink transmit power P_{RB} given by:

$$P_{RB} = \frac{P}{N}. \tag{4.1}$$

SFR reduces downlink transmission power allocated to the GR UEs in order to minimize ICI for BR UEs using the protected band in adjacent sectors. P_{GR} denotes transmission power allocated to a GR RB:

$$P_{GR} = \alpha P_{RB}, \tag{4.2}$$

$$0 \ < \ \alpha \ < \ 1. \tag{4.3}$$

Where α is the SFR power ratio. The downlink transmission power allocated to the RBs used in the BR zone is identical to the frequency reuse-1 model. The only constraint on power allocation is that the downlink transmission power allocated by a cell i to all the RBs does not exceed its maximum transmission power:

$$\sum_{n=1}^{N} P_n^i \leq P. \tag{4.4}$$

On the downlink of a multiuser OFDMA system, such as LTE, UEs can measure the separate levels for different dominant sources of interference [KHQT13a]. For a downlink transmission to a UE in a sector, interference is caused by all the sectors allocating simultaneously the same RB for another UE. We consider a UE k attached to cell i and allocated RB n. The corresponding SINR is therefore given by:

$$SINR_{k,n}^i = \frac{P_n^i \cdot G_{k,i,n}}{\sum\limits_{j \neq i} P_n^j \cdot G_{k,j,n} + P_{TN}}, \tag{4.5}$$

Table 4.1: List of Symbols

n	index of RB
k	index of UE
i	index of serving cell
j	index of interfering cell
N	number of RBs
K	number of users
P	maximum downlink transmission power per cell
P_{RB}	maximum power per RB
P_{GR}	downlink power per GR RB
P_{TN}	thermal noise power
α	SFR power ratio
β_{GR}	ratio of RBs with lower power
P_n^i	downlink power allocated by cell i to the RB n
$G_{k,i,n}$	channel gain for UE k on RB n in cell i
$SINR_{k,\,n}^i$	SINR for UE k on RB n in cell i
$R_{k,\,n}^i$	data rate achieved by UE k on RB n in cell i
$SINR_{th}$	SINR threshold used to classify UEs
CQI_n^k	narrowband CQI for UE k on RB n
Δ_{th}	throughput difference to borrow RBs

where P_n^i is the downlink transmission power allocated by cell i to the RB n, $G_{k,i,n}$ is channel gain for UE k served by eNodeB i on RB n, and P_{TN} is the thermal noise power on the considered RB. Channel gain includes all key fading components *i.e.*, path loss, shadowing and multipath that UE k experiences on RB n. Index i refers to the serving base station, while index j refers to the remaining cells, whose transmissions are causing interference problems.

Let $R_{k,\,n}^i$ denote the achievable rate on RB n for UE k in the cell i, then:

$$R_{k,\,n}^i = f(SINR_{k,\,n}^i). \tag{4.6}$$

Where $f(.)$ is the adaptive modulation and coding function that maps SINR to rate. For convenience, notation used in this chapter are listed in Table 4.1.

LTE requires the transmission of UE feedback in order to adapt the transmission to

the current channel conditions. In this context, CQI is a four-bit value sent from the UE to its serving eNodeB. It reflects the level of SINR of a certain frequency band in downlink channels [AHS14, XKM13]. It indicates the highest modulation and coding scheme that guarantees a block error rate lower than 10% for physical downlink shared channel transmissions. Channel state reports are configured by the network to be either periodically delivered with a certain periodicity or aperiodically delivered when explicitly requested by the network. In LTE, several reporting modes are supported. For example, wideband CQI feedbacks reflect the average channel quality across the entire cell bandwidth while specific reports require the transmission of one CQI per configured sub-band (narrowband CQI feedbacks).

4.4 Heuristic Power Control Algorithm

We propose a distributed heuristic power control algorithm that avoids power wastage especially for cell-center UEs that usually have good radio conditions, and increases downlink transmission power on RBs allocated to cell-edge UEs that suffer the most from interference and path loss problems. Cell-edge UEs denote UEs with bad radio conditions. The downlink channel dependent scheduling in LTE requires specific information to be sent by the terminals to the network. Such information is transmitted through Channel State Reports that contain CQI feedback.

We use CQI feedbacks as an entry to solve the downlink power allocation problem. In this context, we propose a distributed heuristic downlink power control algorithm that computes downlink power allocation on the different resources according to CQI values received from UEs. The heuristic power control algorithm is compared with the scenario where no power control is applied *i.e.*, the scheduler allocates permanently the maximum downlink transmission power for each RB.

In the proposed algorithm, the scheduler of each base station (*e.g.*, Proportional Fair, Round Robin, or Best CQI) performs both RB and power allocation each TTI, independently of the other base stations in the network. The algorithm minimizes downlink transmission power without degrading the performance of cell-center UEs. In addition, transmission power allocated for RBs having low SINR values is increased to benefit from the available spectrum. If the received CQI feedback is higher than a predefined

Algorithm 5 Downlink power control

1: Each user sends CQI feedback about all available RBs to the serving cell
2: **for each** $RB \in RB\_pool$ **do**
3: **if** $((CQI < CQI_{threshold})$ & $(P_{t-TTI} < P_{max\,perRB}))$ **then**
4: $P_t \leftarrow P_{t-TTI} + Power\_Control\_Step$
5: **else if** $((CQI > CQI_{threshold})$ & $(P_{t-TTI} > P_{min\,perRB}))$ **then**
6: $P_t \leftarrow P_{t-TTI} - Power\_Control\_Step$
7: **end if**
8: **end for**

$CQI_{threshold}$, downlink transmission power is reduced as long as it is higher than a predefined minimum power P_{min}. However, if CQI feedback is lower than $CQI_{threshold}$, downlink transmission power is increased as long as it is lower than the maximum allowed transmission power P_{max}, where:

$$P_{max} = \frac{\text{Sector Maximum Downlink Power}}{\text{Number of Available RBs}} = P_{RB}. \tag{4.7}$$

The minimum transmission power P_{min} is a predefined parameter that guarantees an acceptable data rate over the considered RB. $CQI_{threshold}$ can take one of fifteen possible integer values since $1 \leq CQI \leq 15$. When $CQI_{threshold}$ equals 15, the power control algorithm allocates the maximum downlink transmission power for each RB. Moreover, P_{max}, given in (4.7), guarantees that the maximum transmission power allocated for all the RBs is always less than or equals the maximum transmission power of the cell. Algorithm 5 describes how downlink transmission power attributed for each RB is adjusted by the scheduler according to the last received CQI feedback. In fact, information about channel quality are sent by the UEs to their serving cells. The received CQI feedbacks are monitored by the scheduler of each cell. Every TTI, the transmission power allocated to each RB is adjusted according to the CQI value and to the transmission power allocated to this RB at the previous TTI: $P_{\text{t - TTI}}$. If the received CQI is less than $CQI_{threshold}$ and $P_{\text{t - TTI}}$ is less than the maximum transmission power per RB, the transmission power allocated to this RB is incremented by a power control step. Otherwise, the transmission power at TTI t is decremented by a power control step when the received CQI exceeds $CQI_{threshold}$, as long as the transmission power allocated to the concerned RB is greater than the minimum transmission power per RB. The power control step is a predefined parameter that allows controlling the granularity of the proposed algorithm. A very small power control step results in delaying the improvement of system performance, while a big step size creates additional oscillations in the downlink power allocation.

4.5 Simulation Environment

In order to study the performance of our power control algorithm, several LTE system level simulations are performed. Comparison parameters are: downlink transmission power and mean UE throughput. We simulate our proposed algorithm using a MATLAB based LTE downlink system level simulator [IWR10], and we compare its performance to other power control strategies.

We adapted the chosen LTE downlink system level simulator before performing the required simulations. In fact, SINR calculations were made assuming the maximum downlink transmission power is attributed permanently for all the RB. In addition, no downlink power control mechanism was implemented. Therefore, we adjusted the MATLAB open-source code of the simulator to ensure that the effective power levels on each RB are taken into account when calculating SINR levels. We choose the proportional fair scheduler to implement the proposed power control algorithm. Note that this algorithm can also be integrated within other schedulers such as round robin or best CQI. Simulation parameters for the simulated LTE system and the power control algorithm are summarized in Table 4.2.

The simulated network consists of several adjacent hexagonal LTE cells, where inter-eNodeB distance equals 500 m. eNodeB spacing corresponds to dense networks deployed in urban areas. In each cell, 25 RBs are available and fully used, since the operating bandwidth equals 5 MHz. Traffic model is full buffer *i.e.*, all the available spectrum is permanently allocated for active UEs. The scheduling period in LTE equals one TTI (1 ms), where power and RB allocation are periodically performed by the scheduler located at each eNodeB.

4.6 Performance Evaluation of the Downlink PC Algorithm

4.6.1 Downlink Transmission Power

First, we simulate a basic scenario where an LTE system contains one cell-center UE and one cell-edge UE in two adjacent cells. The objective of the simulation is to show the impact of our proposed heuristic algorithm on the downlink transmission power for

Table 4.2: Simulation Parameters

Parameter	**Value**	**Description**
Cell geometry	Hexagonal	A cell is served by an eNodeB
Inter-eNodeB distance	500 m	Urban area
Operating bandwidth	5 MHz	—
Number of RB	25	In the 5 MHz bandwidth
Transmission frequency	2 GHz	—
Subcarrier frequency	15 kHz	1 RB = 12 sub-carriers
TTI	1 ms	Transmit Time Interval
Pathloss model	TS 25.814	Same as in HSDPA
Thermal noise density	-174 dBm/Hz	—
Feedback delay	3 ms	3 TTIs
Scheduler	Proportional Fair	—
Traffic model	Full buffer	—
eNodeB max. power	10 W	—
Max. power per RB	0.4 W	$\frac{eNodeB\,max.\,power}{Number\,of\,RB}$
Power control step	0.04 W	$\frac{Max.\,power\,per\,RB}{10}$
Min. power per RB	0.16	$4 * Power\_Control\_Step$
$CQI_{threshold}$	7	$1 \leq CQI \leq 15$

cell-center and cell-edge UEs. Simulation time equals 500 TTIs which is equivalent to 500 ms. We report the variation of the total downlink transmission power allocated for each UE along with time. These variations are illustrated in Fig. 4.2.

According to Fig. 4.2, we notice that the downlink transmission power allocated for the cell-center UE is reduced after receiving the corresponding CQI feedback at the serving base station. In fact, the power control algorithm implemented at the scheduler will decrease the downlink power allocated for the RBs used by this UE, since the received CQI is higher than the predefined $CQI_{threshold}$. Downlink power is decreased as long as the received CQI is higher than the predefined threshold, until it reaches the minimum downlink transmission power. The oscillations observed for the downlink transmission power of cell-edge UE are due to successive increase and decrease in the downlink transmission power. Consequently, this power reduction will affect the current CQI value that will also decrease. Thus, downlink power value along with time is subject to oscillations that are ruled by the received CQI feedback values. To reduce these oscillations, we

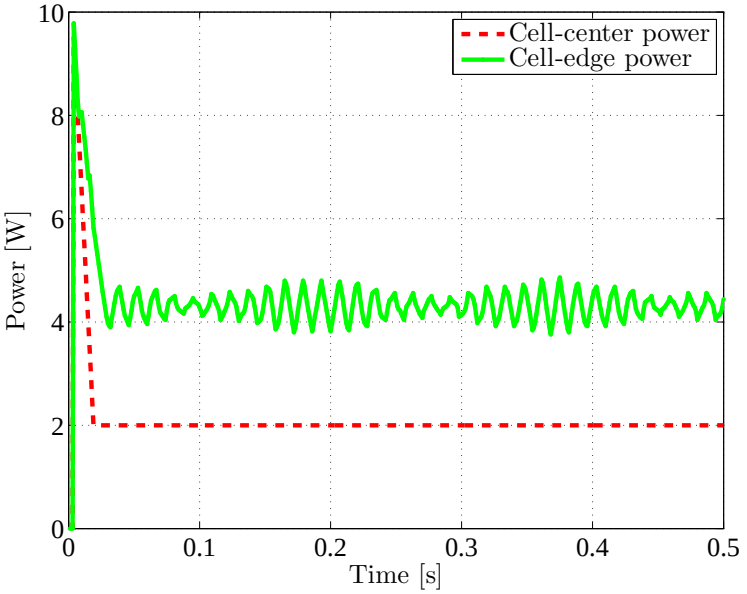

Figure 4.2: Downlink transmission power versus time

define a CQI interval around $CQI_{threshold}$ where we tolerate CQI variations *i.e.*, where we do not modify the allocated downlink power.

4.6.2 System Performance

Using the same parameters as in the previous subsection, we simulate the LTE system with 10 UEs randomly placed in each cell. Therefore, the simulated system contains 70 UEs. The heuristic power control algorithm adjusts downlink transmission power according to CQI feedbacks received from UEs. Simulations are repeated 100 times where UE positions and radio conditions are randomly generated each time. Performance parameters, such as mean throughput per UE and system power consumption, are averaged over the 100 simulation runs. The majority of UEs in the central cell of the system are cell-edge UEs, while they are cell-center UEs in the other cells. Simulation results are reported in Fig. 4.3 to 4.6.

In Fig. 4.3, we report the mean throughput per UE with and without the power control heuristic algorithm. It shows that system throughput is slightly reduced when using our algorithm. In fact, downlink transmission power for resource blocks having good radio conditions (CQI relatively high) is decreased; however, the transmission power allocated to RB characterized by low CQI feedback values is increased to compensate throughput

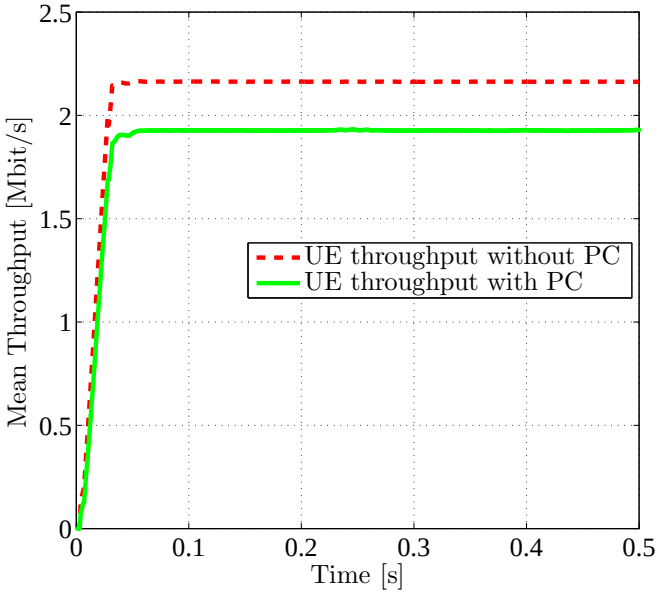

Figure 4.3: Mean throughput versus time

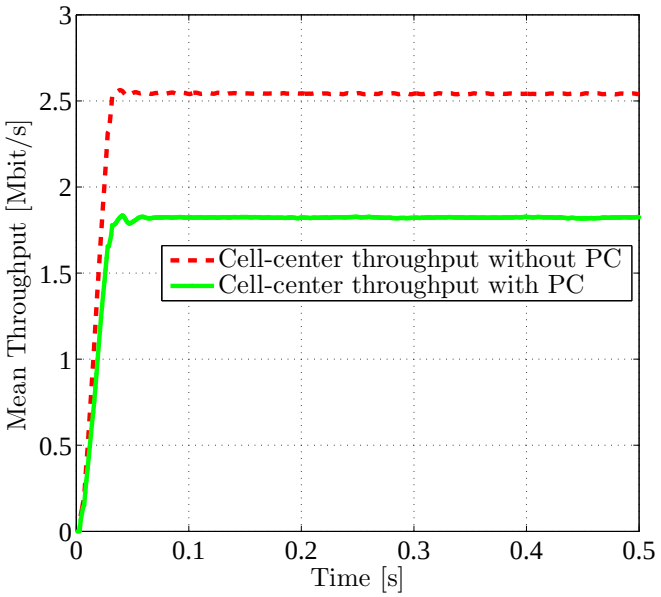

Figure 4.4: Cell-center UEs throughput versus time

loss that might occur due to propagation loss and ICI problems. Globally, the mean throughput per UE is slightly reduced.

Figure 4.4 shows the impact of downlink transmission power adjustments on cell-center UEs. These UEs are characterized by a lower path loss. In addition, they are less affected by inter-cell interference, since the interfering signals will experience important degradation before reaching these UEs. For these reasons, resources allocated for cell-center UEs show relatively high CQI feedback values. Hence, downlink power allocated

for these resources is decreased, and the mean throughput per cell-center UE is reduced.

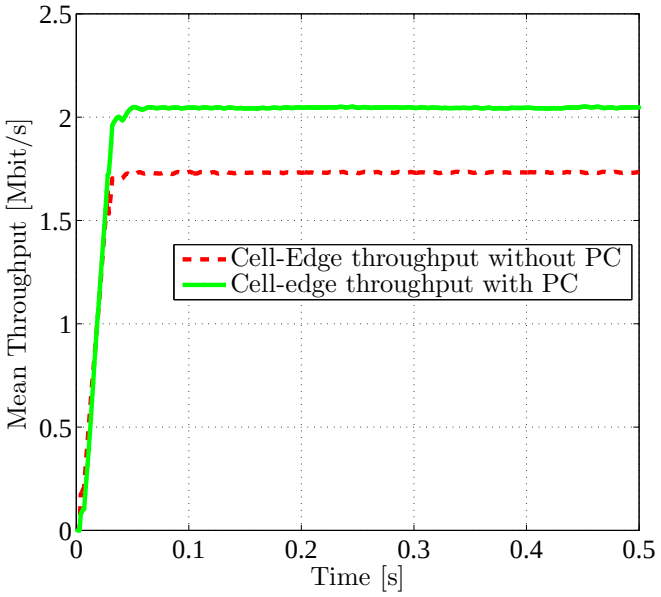

Figure 4.5: Cell-edge UEs throughput versus time

Simulation results reported in Fig. 4.5 show the average throughput per cell-edge UE with and without the power control algorithm. We notice that mean throughput per cell-edge UE is increased when applying the algorithm. In fact, these UEs suffer the most from inter-cell interference problems for two reasons: first, their signal path loss is important; second, they are highly affected by interfering signals transmitted by the neighboring cells. Since resource blocks allocated for cell-edge UEs are characterized by low CQI values (due to propagation loss and inter-cell interference), the power allocated for these RBs is increased. Thus, the signal loss caused by free space propagation is reduced. Furthermore, resource blocks used by cell-center UEs in the neighboring cells have higher CQI values. When reducing the downlink transmission power allocated to these RBs, the amount of inter-cell interference that affects cell-edge UEs operating on the same RBs in the neighboring cells is reduced. These power adjustments improve channel quality and SINR of cell-edge UEs, allowing them to get higher throughputs and better performance.

Figure 4.6 shows that our heuristic power control algorithm largely reduces the required downlink transmission power. Indeed, the simulated LTE system consumes only 22 W instead of 70 W, which is the transmission power consumed when no downlink power control is applied. Thus, the total downlink transmission power is reduced by 68%. Combining these results with the results obtained in Fig. 4.3 (system throughput is

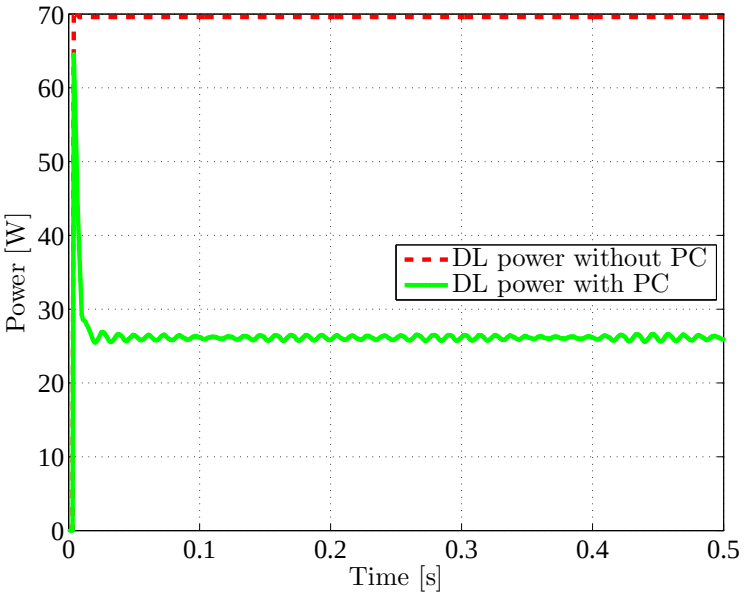

Figure 4.6: System power consumption versus time

slightly reduced) allows us to exhibit the main advantage of our algorithm: we avoid power wastage and we improve cell-edge UEs throughput.

Note that in the special case where all UEs are located at the edge of the cells, downlink transmission power is increased until we reach the maximum transmission power. Thus, the percentage of cell-edge UEs has an important impact on power consumption.

4.7 Autonomous Dynamic ICIC Technique

The heuristic power control algorithm that we introduced at the beginning of this chapter operates in a distributed manner at the scheduler of each base station, regardless of the resource allocation strategy used. To further protect UEs having low SINR values from ICI problems, we also introduce an autonomous distributed dynamic ICIC technique that aims at improving the quality of service for BR UEs and increasing throughput fairness among all the active UEs in the network. Our technique dynamically adjusts RB allocation depending on UE demands in each cell zone. It operates on the downlink of multiuser OFDMA networks, such as LTE, where frequency reuse-1 model implies severe restricting ICI problems, and it does not require any cooperation between network base stations. Thus, no additional signaling overhead is generated.

Algorithm 6 RB classification

1: All UEs send CQI feedbacks to the base station
2: **for each** $RB \in RB\_pool$ **do**
3: $\quad \mathrm{CQI}_n(\mathrm{t}) \leftarrow \frac{\sum_{k=1}^{K} \mathrm{CQI}_n^k(\mathrm{t})}{K}$
4: $\quad \overline{\mathrm{CQI}}_n(\mathrm{t}) \leftarrow \gamma \overline{\mathrm{CQI}}_n(\mathrm{t\text{-}1}) + (1-\gamma)\mathrm{CQI}_n(\mathrm{t})$
5: **end for**

The cooperation between adjacent base stations is possible by exchanging the necessary information over the X2 interface [Raz13] that interconnects adjacent eNodeBs. Drawbacks of such cooperation are basically an additional signaling load due to messages exchanged between eNodeBs and an additional time delay in order to solve the resource and power allocation problem in a cooperative manner. Our proposed ICIC technique is an autonomous distributed method where the existence of a central controller is not required.

Information about channel quality at the UE is transmitted regularly to the eNodeB. CQI is calculated by the UE based on the SINR of the received common pilot [EDB07]. It is expressed as a recommended transport block size, and it is received after a predefined number of TTIs, since the uplink transmission channel is shared by several UEs. We assume that CQI degradation is caused by interference problems due to the usage of the same resources in adjacent cells. For a given RB, the block error rate increases when it is simultaneously used in adjacent cells, due to ICI that causes SINR degradation. Mean narrowband CQI feedbacks are information concerning the link quality for specific RBs. They are sent by the active UEs to the network, and they are used to classify RBs allocated to each zone, as shown in Algorithm 6. First, we calculate the mean CQI value for a RB n over the K active UEs at time t. Then, the average CQI over time is calculated for each RB. γ is a real coefficient less than one, and it is used to give more weight to the recently received CQI feedbacks. Thus, the algorithm becomes more responsive to recent modifications in the radio conditions, and to the latest received CQI feedbacks. RBs originally allocated to the GR zone and characterized by high CQI values are potential candidates to be moved to the cell-edge zone when needed *i.e.*, when BR UEs are not satisfied. Moreover, BR resources having low CQI values are most probably the ones to be used in the GR zone if GR UEs are not satisfied.

Algorithm 7 shows how our autonomous dynamic ICIC technique periodically adjusts RB allocation between cell zones. Initially, RB and power allocation are performed

Algorithm 7 Autonomous dynamic ICIC

```
Allocate RBs and power according to SFR
Every T TTIs:
if (R_GR − R_BR > Δ_th) then
    Borrow the RB with the highest CQI from GR to BR zone
else if (R_BR − R_GR > Δ_th) then
    Borrow the RB with the lowest CQI from BR to GR zone
else
    Keep the same RB distribution
end if
```

according to the SFR technique: one third of the available bandwidth is allocated to the BR UEs and used at the maximum downlink transmission power; while the remaining bandwidth is allocated to the GR UEs at a lower transmit power, as shown in Fig. 4.7. After receiving the first narrowband CQI feedbacks from active UEs, eNodeB starts calculating mean CQI values for each RB available in the cell. $\overline{R_{GR}}$ and $\overline{R_{BR}}$ denote the mean throughput per GR UE and BR UE respectively. A throughput threshold Δ_{th} is defined and used to decide whether UEs of a specific zone are more satisfied than UEs in the other zone or not.

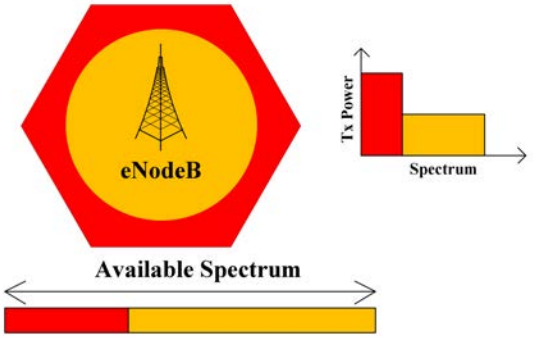

Figure 4.7: Initial RB and power allocation

The scheduler of each base station locally performs periodic interventions, every T TTIs. The intervention period T is greater than the scheduling period (one TTI), so that the scheduler has enough time to receive UE feedbacks, to calculate the mean throughput for each zone, and to monitor the impact of the latest modifications on mean UE throughput per zone. If mean throughput per GR UE exceeds by Δ_{th} the mean BR throughput, then BR UEs are considered to be unsatisfied. As mentioned earlier in this section, GR RBs are classified according to their mean CQI feedbacks. According to the proposed ICIC technique, BR zone borrows one RB from the RBs allocated to the GR zone in order to

satisfy throughput demands of its UEs, as shown in Fig. 4.8. The borrowed RB is the one having the highest CQI feedback value, since it will be allocated to the disadvantaged UEs (having bad radio conditions and low SINR). However, downlink transmission power allocated to this RB is maintained (according to the SFR scheme) to avoid additional interference for BR UEs of the neighboring cells. In fact, power allocation mask is kept the same as for SFR, since there is no cooperation between network entities to coordinate RB distribution in each cell. A local power increase decision that raises ICI level is therefore avoided.

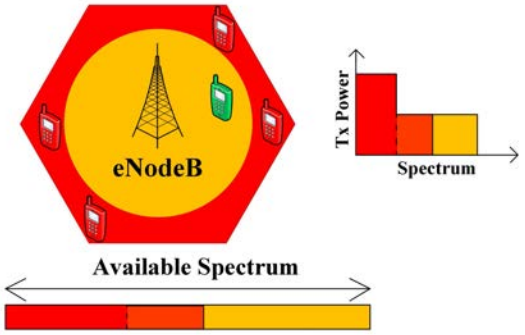

Figure 4.8: BR UEs unsatisfied

Similarly, if mean throughput per BR UE exceeds by Δ_{th} the mean GR throughput, then GR throughput requirements are not satisfied. Consequently, BR RB characterized by the lowest mean CQI feedback is selected, and it is borrowed by the GR zone. This scenario is illustrated in Fig. 4.9. Since GR UEs usually have good radio conditions and high SINR, GR zone can borrow RBs with low CQI values. Resources with higher CQI feedback values are reserved for BR UEs. Downlink transmission power allocated to the borrowed RB is maintained since it does not have a negative impact on BR UEs in the neighboring cells.

Δ_{th} allows to avoid unnecessary modifications of RB allocation between cell zones when the difference between mean GR throughput and mean BR throughput is low. It is a tuning parameter that could be adjusted by mobile network operators according to quality of service requirements. For instance, if we tolerate a throughput difference of 128 kbit/s per UE between GR and BR zones, then no intervention is performed as long as the absolute value of GR and BR throughput difference is less than 128 kbit/s. In this case, RB distribution between cell zones is kept the same.

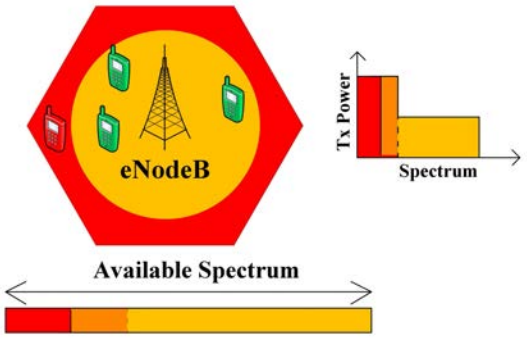

Figure 4.9: GR UEs unsatisfied

Time scale of the proposed autonomous ICIC technique is greater than the scheduling period in LTE (one TTI), *i.e.*, when intervention period elapses, restrictions on RB usage in each zone are updated according to UEs needs. Therefore, base station schedulers have enough time to measure the impact of RB borrowing on UE throughput in each zone. It also allows to avoid oscillations in RB borrowing, that might occur when mean throughput per GR and BR zones have close values. Interventions occur every T ms in a distributed manner, to decide whether to change or not RB distribution locally between cell zones. Static ICIC techniques, such as FFR and SFR, are not adapted for non-uniform user distributions between the different network cells. In addition, they do not adjust RB distribution between cell zones, especially when user density is not geographically homogeneous within the same cell.

4.8 Simulation Environment

4.8.1 Simulation Parameters

Simulations are performed to evaluate the performance of the proposed autonomous dynamic ICIC technique to be compared with the frequency reuse-1 model and traditional state-of-the-art ICIC techniques. LTE system level simulator generates sites with three hexagonal sectors per site. We implemented an algorithm that adjusts downlink transmission power allocated to each RB. It is used when adjusting power allocation according to SFR technique and according to our proposed autonomous ICIC technique. We have implemented our proposed ICIC technique and another state-of-the-art ICIC technique, called Adaptive ICIC [QLS09]. It considers the resource and power allocation problem

for each cell independently of the other cells. For the cell-edge zone, the objective is to minimize the transmission power under constraints related to the minimum throughput per UE. For the cell-center zone, the objective consists in maximizing the achievable throughput under constraints related to resource usage. The adaptive ICIC technique operates as follows:

- UEs are divided into cell-edge and cell-center UE groups.
- RB and power allocation to the cell-edge group is performed. After that, the RB and power allocation to the cell-center group is performed based on the assignment results of the cell-edge UE group.
- The RBs and power allocation to cell-edge UEs is performed using a waterfilling-based power allocation algorithm, so that all the cell-edge UEs satisfy the predetermined target throughput.
- The RB and power allocation problem is subject to constraints related to the minimum throughput per UE, and to the maximum downlink transmission power.
- Each cell solves its own optimization problem with minimal exchange of information between the cells.

Therefore, we are able to compare our autonomous technique with the frequency reuse-1 model, FFR, SFR, and adaptive ICIC techniques.

The simulated LTE network consists of several adjacent hexagonal cells, where each cell is served by an eNodeB. Inter-eNodeB distance equals 500 m, which corresponds to the distance separating two adjacent eNodeBs in urban areas. Operating bandwidth, transmission frequency, and other parameters for the simulated LTE system are the same as given in Table 4.2. Downlink transmission power allocated to the GR RBs is defined by an SFR power ratio ($\alpha < 1$). Satisfaction throughput threshold is a predefined parameter used to measure the percentage of satisfied UEs *i.e.*, UEs having their mean throughput higher than this threshold. In our simulations, it equals 512 kbit/s. We assume that the minimum throughput required to guarantee an acceptable QoS for the active UEs equals 512 kbit/s. The intervention period T for our autonomous ICIC technique equals 25 TTIs, which is greater than the scheduling period (1 TTI).

4.8.2 Performance Metrics

4.8.2.1 Spectral Efficiency and Energy Efficiency

Spectral efficiency is an important metric for performance comparison, due to the scarcity of the frequency spectrum. Another important concern for mobile network operators is energy efficiency. Indeed, the integration of a power allocation algorithm that reduces ICI will increase cell-edge UEs throughput, and reduce system power consumption.

We define the spectral efficiency as the aggregate system throughput divided by the available spectrum; it indicates the throughput per Hertz. Similarly, energy efficiency gives the aggregate system throughput per Watt:

$$\text{Spectral efficiency [bit/s/Hz]} = \frac{\sum_{k=1}^{K} R_k[bit/s]}{\text{Available spectrum [Hz]}}, \tag{4.8}$$

$$\text{Energy efficiency [bit/s/W]} = \frac{\sum_{k=1}^{K} R_k[bit/s]}{\text{Total power consumption [W]}}, \tag{4.9}$$

where K is the number of active UEs, and R_k is the mean throughput of UE k. An efficient ICIC technique for a mobile network operator is a technique that increases spectral efficiency, energy efficiency, or both.

4.8.2.2 Mean Throughput per UE

Since each cell is divided into GR and BR zones, we define two additional throughput metrics: mean throughput per GR UE and mean throughput per BR UE.

We have performance improvements for the LTE system due to an increase in GR UEs throughput only. However, BR throughput is reduced, and the objective of ICIC is not achieved. For this reason, BR and GR UEs' throughput are introduced to investigate user performance in each zone. They also show the impact of ICIC techniques on system performance using detailed throughput information.

4.8.2.3 Throughput Cumulative Distribution Function

Throughput CDF shows UE throughput distribution for the different ICIC techniques. For each throughput value, CDF represents the probability to find a UE characterized

by a lower throughput. When comparing ICIC techniques, the best one is the one that shows the lowest CDF for all throughput values.

4.8.2.4 UE Satisfaction

We define a satisfaction throughput threshold as the reference throughput for performance comparison. We assume that a UE is satisfied when his average throughput exceeds this threshold. In fact, it is the minimum throughput that guarantees an acceptable quality of service. UEs having a mean throughput lower than the satisfaction threshold are qualified as unsatisfied.

For each ICIC technique, we compute the percentage of unsatisfied users in the network. We investigate the evolution of user satisfaction when the percentage of GR UEs changes *i.e.*, when the majority of active UEs are GR UEs or BR UEs or when UEs are equally distributed between cell zones. We also study the impact of network load (number of UEs per eNodeB) on user satisfaction for each of the studied ICIC techniques.

4.8.2.5 Fairness Index

Throughput fairness is an important performance comparison parameter. It gives insights about the gap between BR and GR UEs performance. Jain's fairness index [JCH84] is given by:

$$J(R_1,\, R_2,\, ...,\, R_K) = \frac{(\sum_{k=1}^{K} R_k)^2}{K \cdot \sum_{k=1}^{K} R_k^2}. \tag{4.10}$$

Where J rates the fairness of a set of throughput values; K is the number of active UEs, and R_k is the throughput of UE k. Jain's fairness index ranges from $\frac{1}{K}$ (worst case) to 1 (best case). It reaches its maximum value when all UEs receive the same throughput.

4.9 Simulation Results

Extensive simulations are done to compare the performance of the proposed autonomous dynamic ICIC technique with frequency reuse-1 model, FFR, SFR, and adaptive ICIC

techniques. Results concerning energy efficiency, spectral efficiency, UE satisfaction, mean throughput per zone, and throughput fairness are reported in the current section.

4.9.1 Throughput Threshold Δ_{th}

We study the impact of the throughput threshold Δ_{th}, which is the tolerated throughput difference between the different cell zones, on system performance. We simulate the same network scenarios under different Δ_{th} values, for uniform and non-uniform UE distributions. Our results concerning UE satisfaction versus UE distribution are shown in Fig. 4.10, and results showing the impact of Δ_{th} on throughput fairness are given in Fig. 4.11.

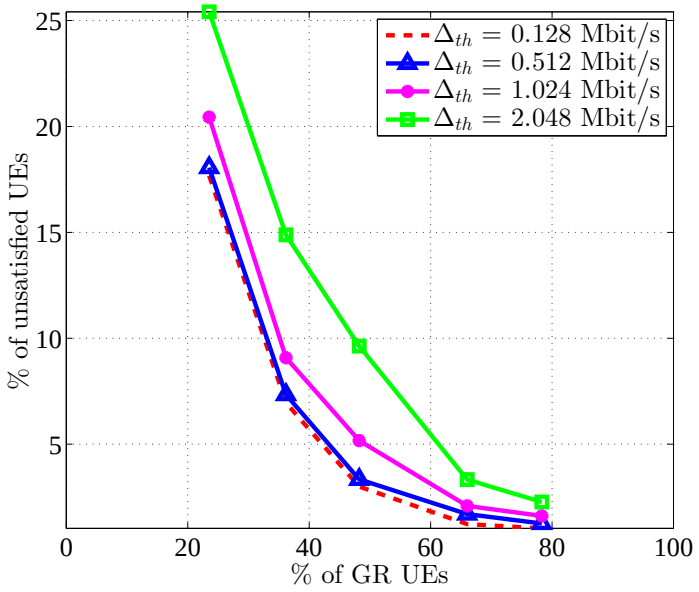

Figure 4.10: UE satisfaction versus UE distribution

According to Fig. 4.10, the lowest percentage of unsatisfied UEs for uniform and non-uniform UE distributions is achieved for Δ_{th} = 128 kbit/s. When we allow a larger throughput difference between cell zones, the number of interventions that occur to adjust RB allocation decreases. Thus, the adjustments made on RB allocation between cell zones are not enough to respond accurately to throughput demands in each zone. The percentage of unsatisfied UEs increases when Δ_{th} increases. If Δ_{th} equals zero, RB allocation between GR and BR zones is modified at each intervention. Although system performance is improved, additional oscillations in RB allocation between cell zones are caused by these consecutive interventions.

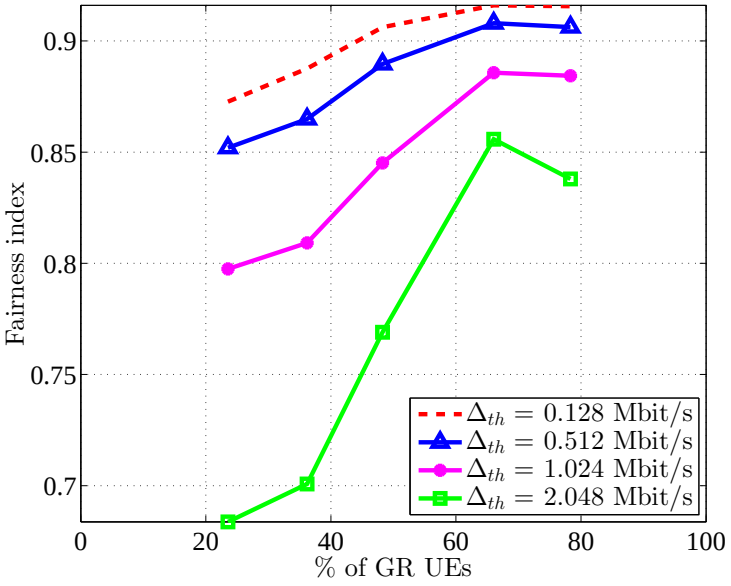

Figure 4.11: Fairness index versus UE distribution

Similarly, our autonomous ICIC technique offers the highest fairness index when Δ_{th} equals 128 kbit/s, as shown in Fig. 4.11. When Δ_{th} increases, the tolerated throughput difference between cell zones increases. Thus, the higher the throughput threshold Δ_{th} is, the lower the fairness index is. This result is valid independently of the UE distribution between cell-center and cell-edge zones. The optimal Δ_{th} value is therefore selected for the rest of the simulations.

4.9.2 Spectral Efficiency versus Energy Efficiency

We simulate a cluster of seven adjacent hexagonal LTE cells with 10 UEs randomly placed in each cell. Simulations are repeated 100 times, and mean results are shown in Fig. 4.12.

Simulation results reported in Fig. 4.12 show that the frequency reuse-1 model presents the lowest energy efficiency. In fact, RBs are simultaneously used in the adjacent cells, and all the active UEs experience ICI problems that mainly affect those located at the edge of the cell. The downlink transmission power is always set to the maximum, since no power control is used. Thus, reuse-1 model has the lowest energy efficiency in comparison with other ICIC techniques.

FFR increases energy efficiency compared to the frequency reuse-1 model. It creates a static group of restricted RBs that are not used in each cell. The unused RBs are

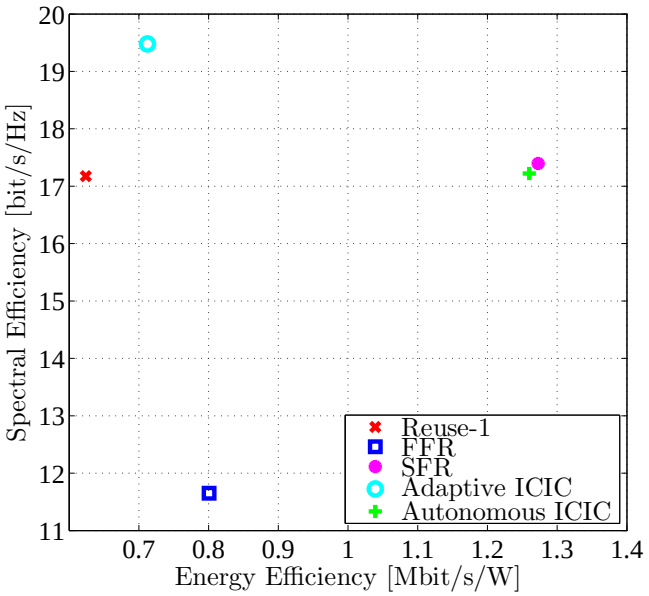

Figure 4.12: Spectral efficiency versus energy efficiency

not allocated any downlink transmission power. Therefore, system power consumption is reduced, which increases energy efficiency. However, FFR shows the lowest spectral efficiency in comparison with other techniques. Restrictions on RB usage reduce the amount of RBs available in each cell; thus, spectral efficiency is reduced. The adaptive ICIC technique improves spectral efficiency in comparison with reuse-1 model, since it increases the achievable throughput for the LTE network. Adjustments made on power allocation also allow a slight improvement of energy efficiency. However, energy efficiency for adaptive ICIC technique is less than that of FFR.

According to simulation results, our proposed autonomous ICIC technique improves both spectral efficiency and energy efficiency in comparison with frequency reuse-1 model and static FFR technique. This RB allocation strategy improves UE throughput, and increases spectral efficiency. Moreover, downlink transmission power allocated to the GR RBs is lower than the maximum transmission power per RB; therefore, the total downlink transmission power is reduced and energy efficiency is improved. Performance results for our dynamic ICIC technique are similar to those of SFR for homogeneous UE distributions.

4.9.3 Mean Throughput per UE

We simulate the same scenario for frequency reuse-1 model, FFR, SFR, adaptive ICIC, and our proposed ICIC technique, and we investigate mean UE throughput as well as mean GR and BR throughputs for all these techniques. When using SFR, one third of the available RBs in each cell are exclusively allocated to BR UEs, and they are used at the maximum downlink transmission power. The remaining spectrum is used by GR UEs at a lower transmission power. Simulations are repeated 100 times, where UE positions and radio conditions are randomly generated each time, and mean results are reported in Fig. 4.13.

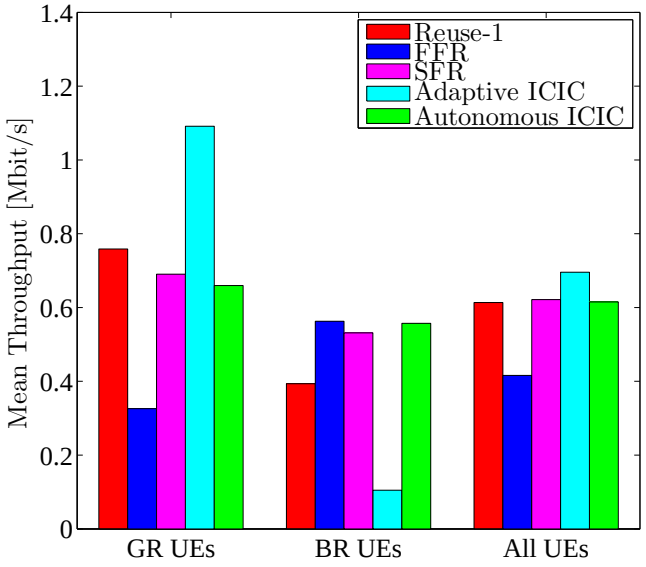

Figure 4.13: Mean throughput per GR, BR and all UEs

Simulation results show that the proposed technique is a compromise between FFR and SFR techniques. The main objective of ICIC is to protect BR UEs that are characterized by low SINR values due to interference problems. FFR guarantees that BR RBs are not reused in GR zones of the adjacent cells; therefore, higher SINR values are reached in comparison with reuse-1 (where RBs are reused at the full downlink transmission power) and SFR (where BR RBs are reused in adjacent cells with a lower transmit power). GR UE throughput is reduced due to restrictions on RB usage, which results in a decrease of the overall mean throughput in comparison with the frequency reuse-1 model. Adaptive ICIC adjusts RB and power allocation between BR and GR zones, in order to satisfy throughput requirements for BR UEs, while minimizing downlink transmission power used in BR zone. Nevertheless, it does not take into account ICI

caused by RBs used in GR zones of the neighboring cells, thus system throughput is improved due to improvements in GR UEs throughput.

SFR improves BR UEs throughput in comparison with reuse-1 without degrading system throughput. In fact, all the spectrum is used in each cell, but power allocation restrictions are imposed to reduce ICI. The drawback of SFR is that RB distribution between cell zones remains static; it does not take into account traffic demands in each zone. Thus, our proposed technique keeps the same downlink power restrictions, but it adapts RB distribution between cell zones in order to reach throughput homogeneity among all the users. This result will be further explained in the following paragraph. BR UEs throughput is improved without reducing mean throughput per user.

4.9.4 Throughput CDF

The same scenario is simulated in order to study throughput CDF for reuse-1 model, FFR, SFR, adaptive ICIC, and our autonomous ICIC technique. Simulations are repeated 100 times, where the positions and the radio conditions of 70 UEs are randomly generated each time. The obtained results are illustrated in Fig. 4.14.

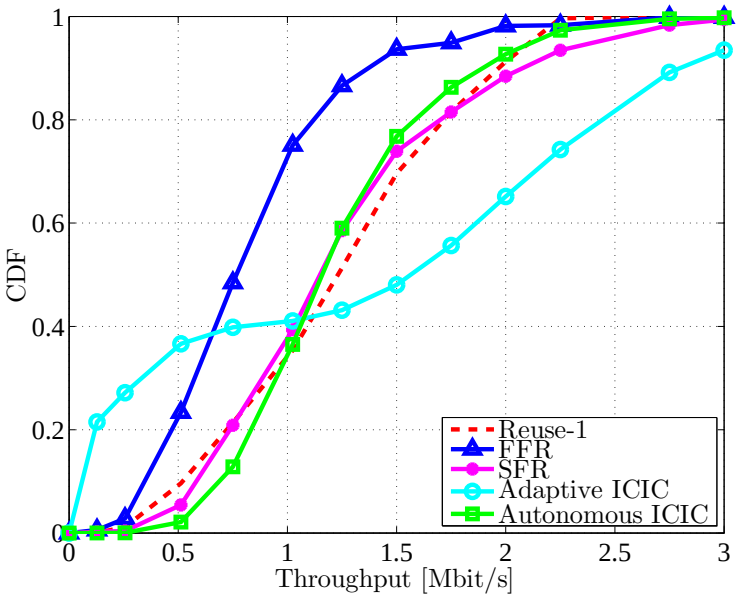

Figure 4.14: Throughput cumulative distribution function

We notice that our ICIC technique has the lowest CDF for throughput values less than 1 Mbit/s. Consequently, the number of UEs suffering of bad quality of service is reduced. CDF of adaptive ICIC technique is the best for throughput values higher than 1 Mbit/s.

Thus, it increases the number of UEs having relatively high throughput. However, restrictions made on RB and power allocation do not succeed in reducing the percentage of UEs having low throughput.

Our autonomous dynamic ICIC technique outperforms reuse-1 model and other state-of-the-art techniques. In fact, our objective is to increase throughput fairness among all the active UEs by reducing the number of RBs allocated to the UEs having relatively high throughputs, in order to improve quality of service for vulnerable UEs.

4.9.5 UE Satisfaction

4.9.5.1 Network Load

We compare the percentage of unsatisfied UEs for the proposed ICIC technique and other state-of-the-art techniques for a scenario of seven adjacent hexagonal LTE cells. We define a throughput threshold as the reference throughput for performance comparison. If the average throughput for a user is higher than the predefined satisfaction throughput threshold, the user is considered satisfied; otherwise, this user is considered as an unsatisfied user.

Satisfaction throughput threshold is set to 512 kbit/s. We assume that this threshold is the minimum throughput required to guarantee an acceptable QoS for the active UEs. Our objective is to show the evolution of the overall UE satisfaction when the network load (or the number of UEs per cell) increases. For each simulation run, UE positions and radio conditions are randomly generated. Mean results are displayed in Fig. 4.15.

These results show that our algorithm is characterized by the lowest percentage of unsatisfied UEs in comparison with reuse-1, FFR and SFR. In fact, our distributed ICIC technique adjusts RBs distribution between GR and BR zones in each cell dynamically, according to user demands in each zone. When the number of UEs per eNodeB is greater than 12, FFR user satisfaction becomes the worst. In fact, RBs are statically distributed between cell zones, regardless of the number of UEs and their actual throughput demands in each zone. In addition, no downlink power allocation is performed to reduce ICI over GR RBs (that are reused according to frequency reuse-1 scheme). Adaptive ICIC technique shows approximately the same percentage of unsatisfied UEs regardless

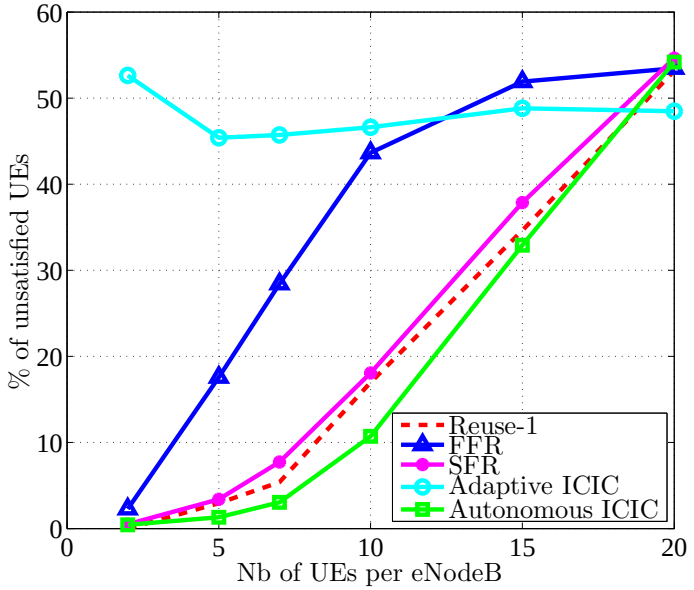

Figure 4.15: UE satisfaction versus network load

of the number of UEs per cell. It outperforms FFR when the number of UEs per eNodeB exceeds 12. Thus, adaptive ICIC is well adapted for high load situations, where the downlink transmission power is allocated to the BR and GR UEs in a manner that improves BR UEs throughput without increasing ICI. Power adjustments made by SFR allow keeping approximately the same percentage of unsatisfied UEs as for frequency reuse-1 model.

4.9.5.2 UE Distribution

We investigate the impact of user distribution between GR and BR zones on system performance. An LTE network of seven adjacent hexagonal cells with 10 UEs per cell is considered. UEs positions are generated in a manner that the percentage of GR UEs existing in the system varies between 20% and 80%. For each user distribution (percentage of GR UEs), simulations are repeated 100 times. Simulation time is 1000 TTIs, and mean results are reported in Fig. 4.16.

Our results show that our autonomous dynamic ICIC technique is characterized by the lowest percentage of unsatisfied UEs, compared to frequency reuse-1 model, FFR, SFR and adaptive ICIC techniques. However, FFR and SFR performance depends on UE distribution in the network. When the majority of UEs are in the BR zone, reuse-1 model outperforms FFR and SFR techniques. In fact, these static ICIC techniques do

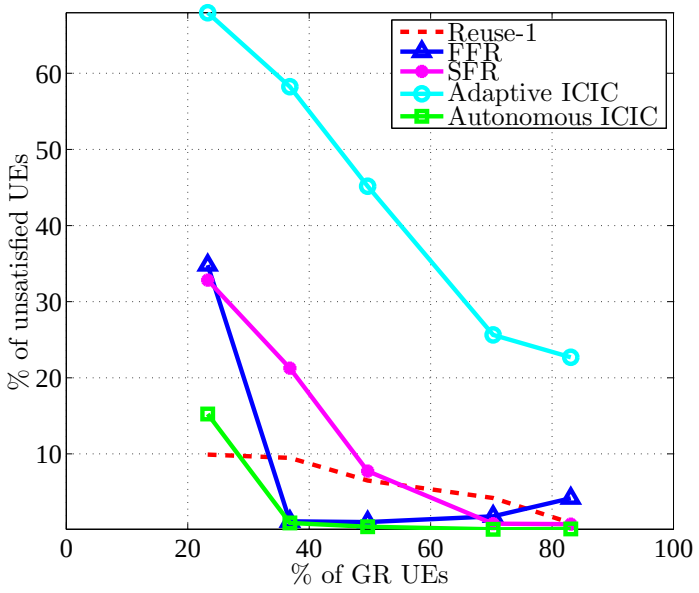

Figure 4.16: UE satisfaction versus percentage of GR UEs

not adapt RB allocation between GR and BR zones according to user demands in each zone. However, they increase user satisfaction when UEs are uniformly distributed in each cell. In fact, RB classification is performed statically, and it is well adapted for user demands when UEs are uniformly distributed between BR and GR zones. Adaptive ICIC technique does not reduce the percentage of unsatisfied UEs, since power allocation problem for cell-edge UEs does not take into account potential interference caused by downlink transmissions for cell-center UEs of the neighboring cells. The main advantage of our technique is that it adapts RB distribution between cell zones in a distributed way (without any cooperation between eNodeBs) in order to increase user satisfaction, and improve system performance.

4.9.6 Fairness Index

We simulate the same scenario as in the previous subsection, and simulation time is 1000 TTIs. ICIC algorithm interventions occur periodically (every 25 TTIs). We generate UEs with uniform and non-uniform distributions between GR and BR zones. Simulation results are shown in Fig. 4.17.

Fairness index gives information about throughput distribution between the different UEs. The difference between mean UEs throughput tends to zero when the fairness index tends to one. Simulation results reported in Fig. 4.17 show that FFR, SFR, and

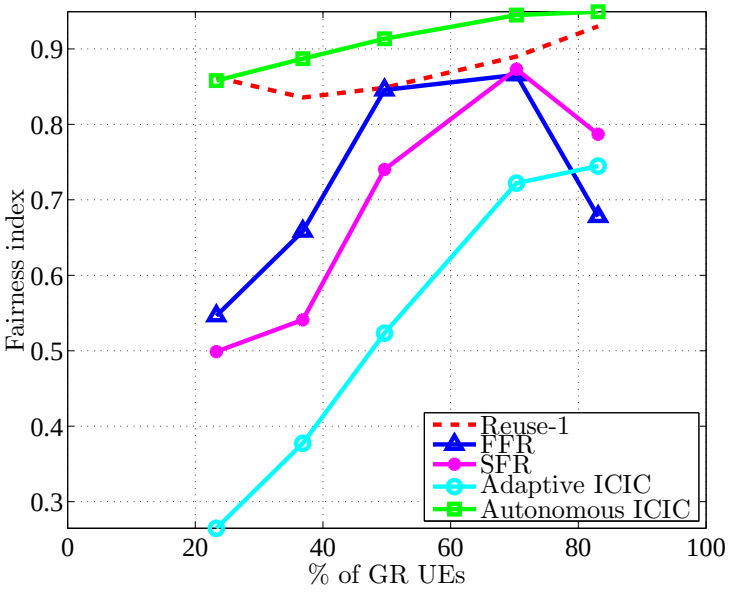

Figure 4.17: Fairness index versus percentage of GR UEs

adaptive ICIC techniques have low fairness index in comparison with frequency reuse-1 model, especially for non-uniform user distributions between cell zones. In fact, static RB classification are not adapted for situations where the majority of UEs served by an eNodeB are located in only one of the two zones. Consequently, throughput discrepancies between UEs increases, and fairness index is reduced. FFR improves throughput fairness in comparison with reuse-1 model only when RB classification between GR and BR zones matches UE demands in these zones. The objective of adaptive ICIC technique is to allocate enough RBs for BR UEs while minimizing the transmission power used in BR zone. Thus, BR UE demands are satisfied, but the remaining transmission power is totally allocated to the cell-center zone, and it allows GR UEs to achieve higher throughputs. Throughput fairness index is therefore reduced. However, the proposed technique adjusts RB allocation according to UE demands, without any cooperation between eNodeBs, while maintaining power allocation constraints to reduce ICI. Therefore, it shows the highest Jain's fairness index compared to SFR, FFR and frequency reuse-1 model.

4.10 Conclusion

In this chapter, we proposed a distributed power control heuristic algorithm that operates on the downlink of multiuser OFDMA networks. It can be implemented within several

schedulers such as proportional fair, round robin or max SINR. The proposed algorithm adjusts the downlink transmission power allocated for each RB according to the received CQI feedbacks. We investigated its performance, and we compared it to the frequency reuse-1 model by simulating an LTE network with randomly placed cell-center and cell-edge UEs. Simulation results show that our algorithm reduces power wastage without degrading system performance. It also improves the performance of cell-edge UEs by decreasing the transmission power on resource blocks allocated to cell-center UEs in the neighboring cells, since they are the main source of interference between neighboring cells. Moreover, the proposed algorithm does not require any cooperation between base stations.

We also introduced an autonomous dynamic downlink ICIC technique for multiuser OFDMA networks. The proposed method is characterized by a low complexity, and it does not generate any additional signaling overhead. RB allocation between GR and BR zones is dynamically adjusted according to user demands in each zone. Simulation results show that our technique improves BR UEs throughput without reducing the average throughput per user. It reduces energy consumption, increases the percentage of satisfied users, and improves throughput fairness among all the users, which are the main goals of mobile network operators.

In the next chapter, we introduce a cooperative resource management and power allocation technique that makes use of the communications between the neighboring base stations. Resource and power allocation are performed in a collaborative manner, using information about UE throughput and resource usage in the neighboring cells. The cooperative approach is a compromise between the centralized approach that offers optimal resource and power allocation at the expense of high signaling overhead, and the autonomous approach where suboptimal resource and power allocation is achieved without generating additional signaling traffic.

Chapter 5

Cooperative Resource Management and Power Allocation for Multiuser OFDMA Networks

In this chapter, we address the compromise between the centralized and the decentralized resource and power allocation approaches by proposing a cooperative distributed interference management algorithm. Signaling messages are exchanged between adjacent cells to adjust resource and power allocation in a collaborative manner. Objectives sought are: increasing user satisfaction, improving system throughput, and increasing both spectral efficiency and energy efficiency. The proposed technique is compared to the frequency reuse-1 model and to other state-of-the-art techniques under uniform and non-uniform user distributions and for different network loads. We consider elastic traffic sessions, and we define UE satisfaction as a function of the achievable throughput. System-level simulation results demonstrate that our cooperative technique succeeds in achieving the desired objectives under various user distributions and for different throughput demands.

5.1 Introduction

LTE/LTE-A networks are meant to be self-organizing networks, where eNodeBs operate autonomously independently of each other. However, it is possible to exchange signaling

messages between eNodeBs over X2 interface that interconnects adjacent cells. Information about channel gain, traffic load, radio conditions, and interference are useful to adjust resource and power allocation in a manner that improves system performance.

ICIC seeks a compromise between spectral efficiency and throughput fairness. In other words, the objective is to improve the quality of service for UEs suffering of severe ICI problems (having low SINR) without reducing system throughput. A dynamic cooperative FFR-based technique is proposed in [RSV10], where interference mitigation is achieved through the exchange of interference related information among neighboring cells. Another cooperative ICIC technique is presented in [YPW08]. It consists in a graph-based dynamic FFR, where an RB allocation algorithm based on the auction method is introduced. It achieves interference mitigation in a multi-cell OFDMA environment via base-station coordination. In this chapter, we introduce a cooperative ICIC algorithm that exploits communications between adjacent cells to reduce ICI problems in multiuser OFDMA networks such as LTE/LTE-A networks. Our technique aims at improving spectral efficiency, energy efficiency, system throughput, and UE satisfaction under various UE distributions and network loads. We define a satisfaction function as well as satisfaction throughput thresholds for each cell in the simulated network. The time scale of the proposed technique is higher than the scheduling period, since it sets RB and power allocation restrictions for the scheduler of each cell. It also adjusts RB distribution between cell-center and cell-edge zones for each network cell. Our technique is compared to the frequency reuse-1 model, FFR, SFR, autonomous ICIC technique proposed in chapter 3.8, and another state-of-the-art ICIC techniques. System-level simulation results show that the proposed technique achieves significant improvements under various UE distributions and network loads.

5.2 System Model

Let K denote the set of active UEs, I denotes the set of LTE/LTE-A cells, and N is the set of RBs available in each cell. We consider a UE k attached to the cell i and allocated RB n. Let $R^i_{k,n}$ denote the achievable rate on RB n for UE k in the cell i, then:

$$R^i_{k,n} = f(\mathrm{SINR}^i_{k,n}). \tag{5.1}$$

Where $f(.)$ is the adaptive modulation and coding function that maps SINR to rate. An LTE/LTE-A network of multiple adjacent hexagonal cells is considered.

LTE/LTE-A networks require the transmission of UE feedback in order to adapt transmission to current channel conditions. In this context, CQI is a four-bit value sent from the UE to the eNodeB [3GP13] that reflects the level of SINR of a given frequency band in downlink channels. It indicates the highest modulation and coding scheme that guarantees a block error rate lower than 10% for physical downlink shared channel transmissions. Several reporting modes are supported: for example, wideband CQI feedbacks reflect the average channel quality across the entire cell bandwidth, while specific reports require the transmission of one CQI per configured sub-band (narrowband CQI feedbacks).

We consider elastic traffic sessions, such as file transfer, web traffic, and email, since these are the traditional data services in mobile networks [ELK13]. Then we define the satisfaction function for each UE k at time t, $S_k(t)$, as a function of the achievable throughput for this UE, $R_k(t)$, and it is given by:

$$S_k(t) = 1 - \exp(-\frac{R_k(t)}{R_S}), \tag{5.2}$$

where R_S is the satisfaction throughput for the considered UE, or the mean throughput beyond which UE satisfaction exceeds 0.63. Satisfaction with respect to R_k has a concave shape; it increases slowly as the throughput exceeds the satisfaction throughput R_S for UE k. Therefore, the satisfaction of an LTE/LTE-A cell i having $K(i)$ UEs is given by:

$$S^i(t) = \frac{\sum_{k=1}^{K(i)} S_k(t)}{K(i)}. \tag{5.3}$$

LTE/LTE-A cells are hexagonal, and each cell exchanges signaling messages with its six neighboring cells. The cell i calculates mean satisfaction function $\overline{S}$ for the considered cluster C that contains K_C UEs:

$$\overline{S} = \frac{\sum_{k=1}^{K_C} S_k(t)}{K_C}. \tag{5.4}$$

5.3 Cooperative Resource and Power Allocation

We introduce a cooperative resource management and power allocation technique for multiuser OFDMA networks, where the adjacent cells exchange signaling messages over X2 interface in order to reduce ICI problems. It is a distributed technique that requires cooperation between adjacent cells to adjust RB and power allocation. Initially, RB and power allocation between the different cells is performed according to the SFR scheme. Thus, the frequency reuse-1 model is chosen to maximize spectral efficiency, while restrictions are made on RB and power allocation between the different cells. Centralized resource and power allocation schemes provide the optimal resource and power allocation solutions. However, these schemes are characterized by a high computation complexity, and they generate an additional signaling overhead. Thus, decentralized cooperative interference coordination schemes are adequate for medium-sized and big-sized networks, where the centralized schemes face severe limitations in terms of signaling and processing load.

Our technique makes use of the signaling messages exchanged between neighboring eNodeBs over X2 interface. Each cell has local information, concerning the SINR of its active UEs, as well as their achievable throughputs and their satisfaction. It also requests information about UE satisfaction from the neighboring cells. Therefore, adjacent eNodeBs adjust power allocation to the different RBs, in order to reduce ICI and to improve UE satisfaction in a collaborative manner. In a second phase, resource allocation between cell zones is autonomously adjusted by each eNodeB in order to satisfy throughput demands in each zone.

As explained previously, an LTE/LTE-A cell is divided into two zones, according to UEs wideband SINR values: GR and BR zones. Initially, one third of the available spectrum in each cell is kept for BR UEs, and the maximum downlink transmission power (π_{max}) is allocated to each RB used in this zone. The remaining bandwidth is used at a lower transmission power (P_{GR}) in the GR zone. BR UEs of adjacent cells operate on different frequency sub-bands, and they receive low power interfering signals from their neighboring cells. The intervention period of our proposed technique is chosen to be higher than the scheduling period (1 ms) and higher than the CQI feedback reception delay, so the scheduler of each cell has enough time to investigate the impact of RB

and power allocation changes on UEs throughput. Each cell performs periodically, every T TTIs, where $T \geq \max(1 \text{ TTI}, \text{CQI feedback delay})$, the following actions:

1. Classify the available RBs according to mean narrowband CQI feedback values.
2. Collect information about mean throughput per UE in the neighboring cells.
3. Request information about resource and power allocation from the neighboring cells.
4. Send *Stop* messages to the neighboring cells.
5. Calculate the local cell satisfaction $S^i(t)$.
6. Calculate mean satisfaction for the neighboring cells $\overline{S}(t)$.
7. When unsatisfied, increase the downlink transmission power allocated to the worst low power RB, and ask the neighboring cells to reduce downlink transmission power allocated to this RB.
8. When satisfied, keep the same resource and power allocation.
9. Send *Release* messages to the neighboring cells.
10. Locally adjust resource allocation between GR and BR zones of the current cell according to throughput demands in each zone.

Our proposed technique exploits the fact that adjacent eNodeBs can exchange information related to UE throughput in each cell. When a given cell decides to perform the cooperative ICIC procedure, it sends *Stop* messages to its neighboring cells to avoid any potential conflict that might occur when adjacent cells take simultaneous power allocation decisions. Since the X2 interface between adjacent eNodeBs is bidirectional, the *Stop* messages contain a time stamp, that allows to avoid any potential deadlock that might occur if two eNodeBs send simultaneous *Stop* messages to each other. Time synchronization between eNodeBs is required. Each cell calculates the mean satisfaction for its active UEs, as well as mean satisfaction for UEs in the neighboring cells. We tolerate a predefined difference (Δ_S^i) between the satisfaction of the local cell and mean satisfaction per cell to reduce the number of interventions performed by each cell. When power adjustments are done, a *Release* message is sent to the neighboring cells, and

RB distribution between GR and BR zones is locally updated according to throughput demands in each zone.

The distributed algorithm operates at the scheduler of each eNodeB as shown in Algorithm 8. $\overline{R_i}(t)$ denotes the mean throughput per UE in cell i; I is the number of cells in the neighboring cells pool $\mathbf{I}$. P_n^i is the downlink transmission power allocated by cell i to the RB n. π_{max} is the power allocated to a BR RB, while P_{GR} is the downlink power per GR RB. $\overline{R}_{GR}$ and $\overline{R}_{BR}$ denote the mean throughput per GR and BR zones, respectively. After receiving narrowband CQI feedbacks from the UEs, each cell calculates mean CQI per RB. The coefficient γ equals 0.5, and it is used to emphasize the last received CQI feedback value, $CQI_n(t)$. Each cell classifies the available RBs according to mean CQI values, then it sends signaling messages to its neighbors so that the downlink transmission power allocated to the different RBs is kept the same.

Our algorithm consists of two phases: in the first phase, the adjacent cells exchange the necessary information required to coordinate power allocation, while in the second phase, each cell locally modifies RB distribution between the different zones. After setting restrictions on power allocation with its neighbors, each cell adjusts RB allocation between GR and BR zones according to UE throughput demands in each zone. The objective behind second phase is to dynamically respond to throughput demands within each cell, even when UE distributions are not homogeneous among GR and BR zones.

Figure 5.1 shows a cluster of seven adjacent hexagonal LTE/LTE-A cells. We assume that the central cell (eNodeB 7) has the highest traffic load, and seeks to improve its mean UE satisfaction. After exchanging the necessary signaling messages with its neighboring cells, eNodeB 7 increases the downlink transmission power allocated to a portion of the available bandwidth that was originally used at a low transmission power. It also orders the concerned neighboring cells (eNodeBs 1, 3, and 5) to reduce their downlink transmission power allocated to this portion of the spectrum. Therefore, eNodeB 7 reduces ICI and improves mean UE satisfaction via collaborative power allocation decisions. Moreover, it autonomously adjusts resource allocation between cell-center and cell-edge zones based on throughput demands in each zone.

Algorithm 8 Cooperative resource and power allocation

Perform RB and power allocation according to SFR
All UEs send CQI feedbacks to the eNodeB
for each $RB \in RB\_pool$ **do**
    $\mathrm{CQI}_n^i(\mathrm{t}) \leftarrow \frac{\sum_{k=1}^{K} \mathrm{CQI}_n^k(\mathrm{t})}{K}$
    $\overline{\mathrm{CQI}_n^i}(\mathrm{t}) \leftarrow \gamma\overline{\mathrm{CQI}_n^i}(\mathrm{t\text{-}1}) + (1-\gamma)\mathrm{CQI}_n(\mathrm{t})$
end for
Every T TTIs:
Cell i sends *Stop* messages to its neighbors
$\mathrm{S}_k(\mathrm{t}) \leftarrow 1 - exp(-\frac{R_k(t)}{R_S})$
$\mathrm{S}^i(\mathrm{t}) \leftarrow \frac{\sum_{k=1}^{K_i} S_k(t)}{K_i}$
$\overline{S}(t) \leftarrow \frac{\sum_{k=1}^{K_C} S_k(t)}{K_C}$
if $(S^i(t) < (1-\Delta_S^i)\overline{S}(t))$ **then**
    Select the low power RB n with the lowest $\overline{\mathrm{CQI}_n^i}(\mathrm{t})$
    $P_n^i \leftarrow \pi_{max}$
    $P_n^j \leftarrow P_{GR}; \forall j \in \mathbf{I}$
else
    Keep the same power allocation mask
end if
Send *Release* messages to the neighboring cells
if $(\overline{R}_{GR} - \overline{R}_{BR} > \Delta_{th})$ **then**
    Select RB n with the highest $\overline{\mathrm{CQI}_n^i}(\mathrm{t})$ from GR zone
    Allocate this RB to the BR zone
else if $(\overline{R}_{BR} - \overline{R}_{GR} > \Delta_{th})$ **then**
    Select RB n with the lowest $\overline{\mathrm{CQI}_n^i}(\mathrm{t})$ from BR zone
    Allocate this RB to the GR zone
else
    Keep the same RB distribution
end if

5.4 Simulation Parameters

System level simulations are done in order to compare the performance of our cooperative technique with that of the frequency reuse-1 model and other state-of-the-art ICIC techniques. The simulated network includes seven adjacent hexagonal LTE/LTE-A cells, with a 5 MHz operating bandwidth. Since the total bandwidth per RB equals 180 kHz, we have 25 RBs available in each cell. Traffic model is full buffer; thus, the available spectrum is permanently used to serve active UEs. With the full buffer model, the maximum ICI is generated since all the available spectrum is simultaneously used in the adjacent cells. Simulation parameters are given in Table 5.1.

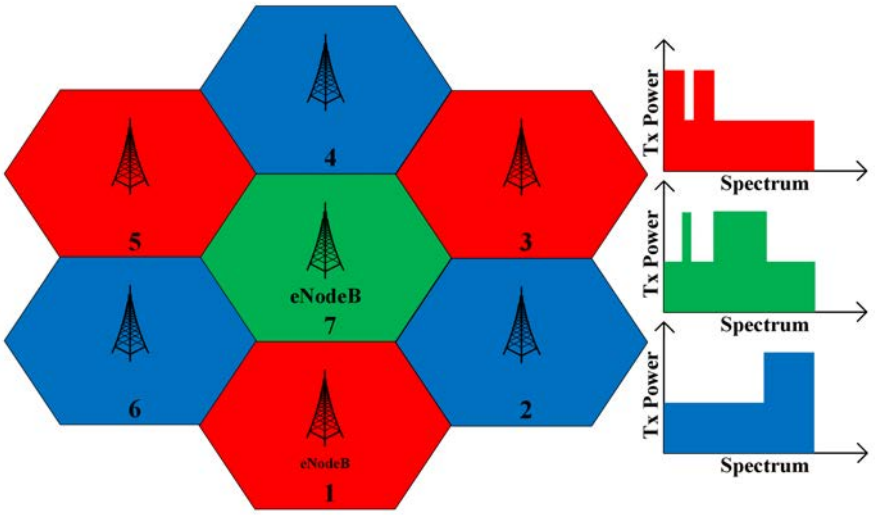

Figure 5.1: LTE/LTE-A network of seven adjacent cells

5.5 Simulation Results

5.5.1 Tolerated Satisfaction Ratio

We simulate an LTE/LTE-A network having seven adjacent hexagonal cells, where each cell is serving 10 UEs. System bandwidth equals 5 MHz; thus, 25 RBs are available in each cell. Traffic model is full buffer: all the available RBs are allocated to the existing UEs in the network. Round Robin scheduler is used to allocate the available RBs for UEs. Simulation time is 350 TTIs (350 ms). Throughput satisfaction threshold for the center cell equals $4R_S$; where R_S is satisfaction threshold for UEs in all the other cells. In other words, throughput demands are not the same through the simulated network: it is required to provide higher throughputs for central cell UEs, since their satisfaction throughput threshold exceeds that of the other UEs.

First, we study the impact of the tolerated satisfaction ratio Δ_S, which is a percentage of the mean satisfaction value, on the central cell satisfaction and mean satisfaction for the entire network. Simulations are repeated 100 times, and satisfaction versus time for central cell UEs and for all UEs versus time are reported in Fig. 5.2 and Fig. 5.3 respectively.

Table 5.1: Simulation Parameters

Parameter	**Value**	**Description**
Cell geometry	Hexagonal	A cell is served by an eNodeB
Inter-eNodeB distance	500 m	Urban area
Operating bandwidth	5 MHz	—
Number of RBs (N)	25	In the 5 MHz bandwidth
Transmission frequency	2 GHz	—
Subcarrier frequency	15 kHz	1 RB = 12 sub-carriers
Total bandwidth per RB	180 kHz	1215 kHz
TTI	1 ms	Transmit Time Interval
Pathloss model	TS 25.814	Same as in HSDPA
Thermal noise density	-174 dBm/Hz	—
Feedback delay	3 ms	3 TTIs
Scheduler	Round Robin	—
Traffic model	Full buffer	—
eNodeB max. power (P_{max})	20 W	43 dBm
Max. RB power (π_{max})	0.8 W	$\frac{P_{max}}{N}$
SINR threshold	3	UE classification
SFR power ratio (α)	0.25	$P_{GR} = \frac{\pi_{max}}{4}$
Intervention period (T)	25 TTIs	$T \geq$ max(1 TTI, feedback delay)
Δ_{th}	512 kbit/s	Satisfaction per zone
Throughput threshold R_S	512 kbit/s	UEs in the center cell
	128 kbit/s	UEs in other cells

For tolerated satisfaction ratios higher than 20%, power allocation over the different RBs is kept the same, since all the cells achieve an acceptable satisfaction compared to mean satisfaction per UE. However, when Δ_S equals 1%, satisfaction for central cell UEs is increased, while mean satisfaction per UE is slightly decreased with time. When the tolerated satisfaction is lower than $0.01\overline{S}$, the central cell decides to increase transmission power allocated to some RBs (that were already used with a lower transmission power), and it orders all its neighbors to reduce the downlink power allocated to these RBs. Satisfaction for central cell UEs is increased in comparison with the remaining cases

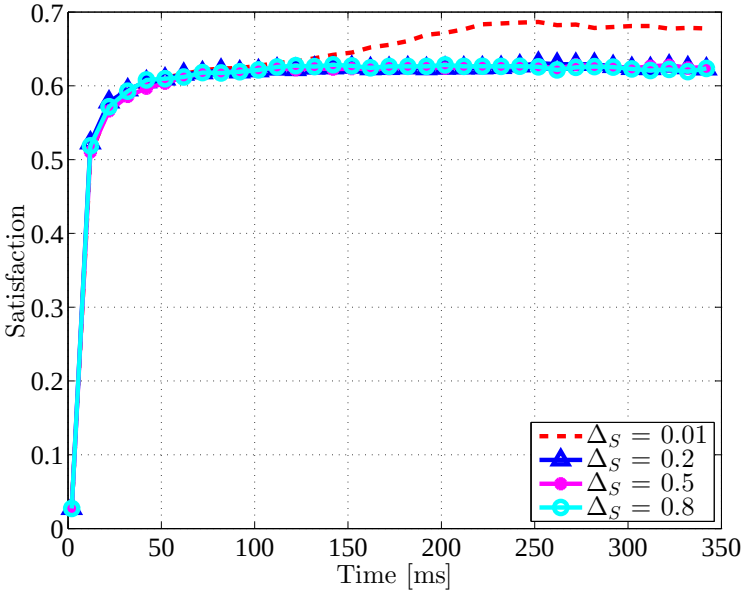

Figure 5.2: Central cell satisfaction versus time

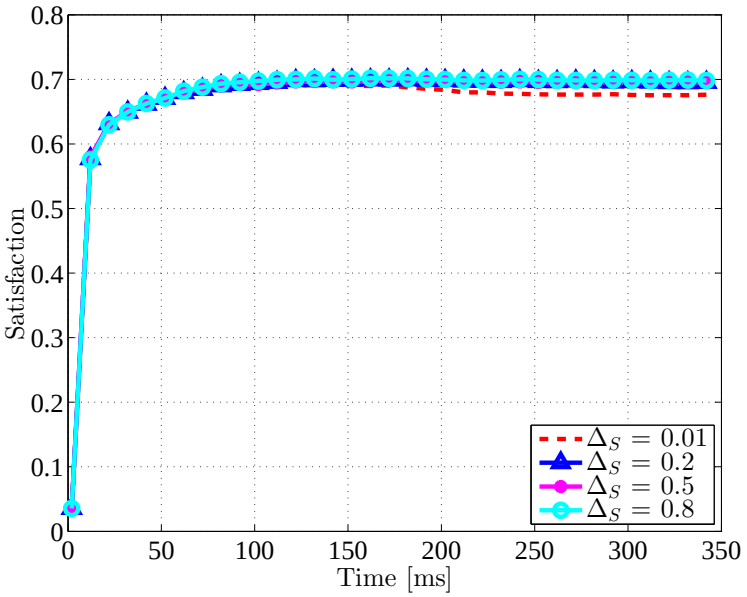

Figure 5.3: Mean satisfaction versus time

where no power adjustments are performed. For the remaining cells, satisfaction is decreased since power reduction will reduce the achievable throughput. Thus, mean satisfaction per UE in the entire network is slightly reduced.

In the following, the tolerated satisfaction ratio Δ_S equals 1%. Hence, when the mean satisfaction per UE exceeds by 1% the satisfaction of a cell, it decides to launch a cooperative ICIC procedure with its neighbors in order to adjust power allocation and improve the satisfaction of its UEs. We compare our proposed cooperative ICIC technique with

the frequency reuse-1 model, FFR, SFR, an adaptive ICIC technique given in [QLS09], and a non-cooperative ICIC technique introduced in [YLI+15], where power allocation for the different RBs is not modified among adjacent eNodeBs. Nevertheless, periodic interventions are made by the scheduler of each eNodeB, locally, in order to find out whether GR or BR users are unsatisfied. RB distribution between cell zones is adjusted according to UEs throughput demands in each zone. More details about the adaptive ICIC technique and the non-cooperative ICIC technique are given in chapter 3.8.

5.5.2 Spectral Efficiency and Energy Efficiency

In this paragraph, we show the spectral efficiency and the energy efficiency for each of the compared techniques. The simulated network of seven adjacent hexagonal cells contains 10 UEs randomly placed in each cell. When using FFR, half of the available spectrum is used according to the frequency reuse-1 model in cell-center zones, while the remaining fraction is used according to the frequency reuse-3 model in cell-edge zones of neighboring cells in a cluster of three adjacent cells. SFR allows using one third of the available spectrum at the maximum downlink power, to be allocated to BR UEs, while the remaining two thirds are used at a lower power (P_{GR}), and are allocated to GR UEs. Simulations are repeated 100 times, and the obtained results are reported in Fig. 5.4.

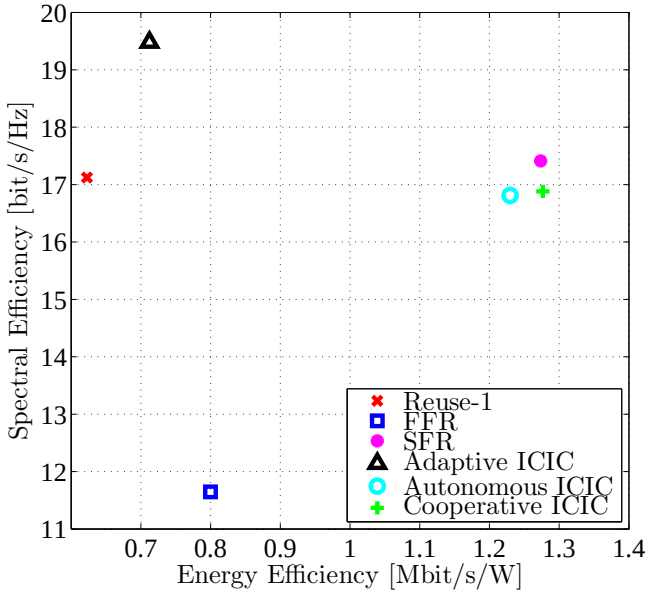

Figure 5.4: Spectral efficiency versus energy efficiency

The frequency reuse-1 model shows the lowest energy efficiency since the maximum downlink transmission power is permanently allocated to the available RBs; however, its spectral efficiency is better than that of FFR since all the available spectrum is used in each cell. FFR improves energy efficiency when compared to the frequency reuse-1 model: no power consumption is made on the unused RBs. However, FFR's spectral efficiency is the lowest among all the compared techniques due to restrictions on RB usage in cell-edge zones. The adaptive ICIC technique increases spectral efficiency in comparison with the frequency reuse-1 model, since it increases the achievable throughput. However, the energy efficiency of this technique is less than that of FFR.

Autonomous ICIC technique shows a better energy efficiency, and a spectral efficiency comparable to that of the frequency reuse-1 model. SFR shows the highest spectral efficiency, due to restrictions made on power allocation for each set of RBs. Our proposed technique brings modifications on power allocation over the different RBs. These power adjustments are done in collaboration with the neighboring cells; however, they do not have a negative impact on energy efficiency. On the contrary, our cooperative ICIC technique shows the best energy efficiency, while its spectral efficiency is comparable to that of reuse-1 and SFR.

5.5.3 Throughput Cumulative Distribution Function

Under the same simulation conditions, we study the impact of each technique on throughput CDF for all UEs existing in the network. Throughput CDF is shown in Fig. 5.5.

Although FFR succeeds in reducing ICI, especially for BR UEs, restrictions on RB usage between the different zones of each cell will reduce the amount of available spectrum dedicated for the existing UEs. Thus, FFR shows the highest percentage of UEs having throughputs lower than 512 kbit/s. Throughput CDF for FFR is the first curve to reach the maximum value. SFR improves the frequency reuse-1 model by reducing the percentage of UEs with throughputs lower than 1 Mbit/s. Our cooperative ICIC technique shows the lowest percentage of UEs having low throughputs, and it reaches its maximum value for the same throughput as for reuse-1. We also notice that the adaptive ICIC technique does not succeed in reducing the percentage of UEs characterized by low throughput values, since its CDF curve shows the highest values for throughputs less than 0.5 Mbit/s. In fact, this technique does not take ICI problems into account, and resource

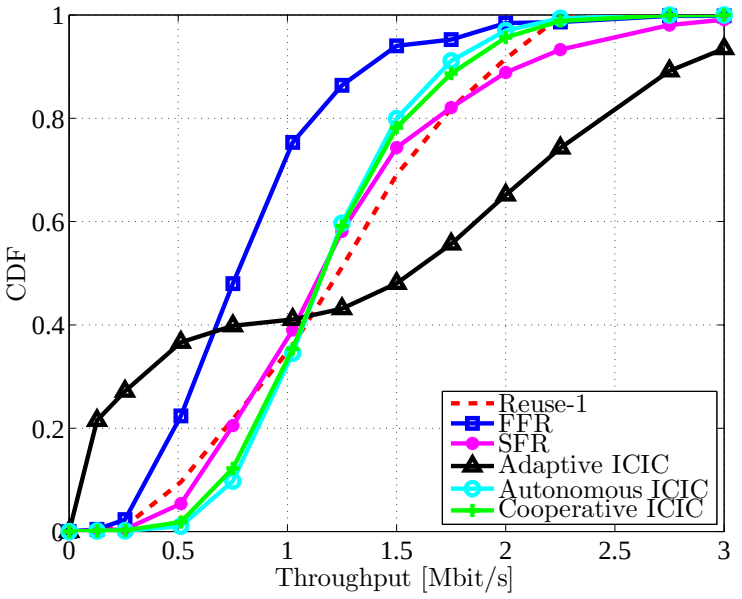

Figure 5.5: Throughput cumulative distribution function

allocation is performed in a manner that improves spectral efficiency. Therefore, BR UEs throughput decreases and more RBs are allocated to GR UEs in order to maximize system throughput.

5.5.4 Satisfaction Cumulative Distribution Function

For the same simulated scenario, we show satisfaction cumulative distribution function for all the compared techniques. Satisfaction function ranges from 0 (minimum satisfaction) to 1 (maximum satisfaction). Satisfaction CDF for the performed simulations are shown in Fig. 5.6.

According to these results, adaptive ICIC always shows the highest percentage of UEs with low satisfaction values. The frequency reuse-1 model, SFR, and autonomous ICIC techniques have approximately the same satisfaction CDF, and our proposed cooperative ICIC technique has the best satisfaction CDF in comparison with the other techniques. For instance, when cooperative ICIC is applied, only 10% of UEs have a satisfaction below 0.9, while 30% of the active UEs have their satisfaction below 0.9 for the adaptive ICIC technique. Therefore, our technique improves UE satisfaction by adjusting power allocation over RBs used simultaneously in adjacent LTE cells.

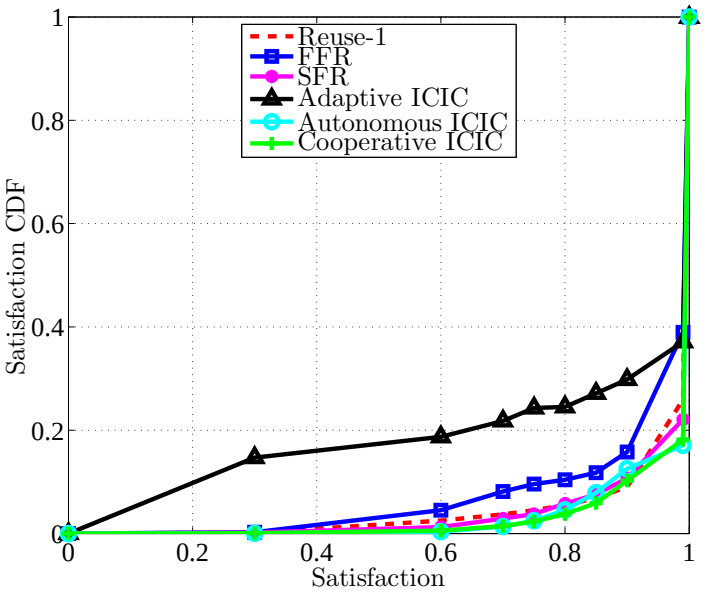

Figure 5.6: Satisfaction cumulative distribution function

5.5.5 Unsatisfied UEs versus Network Load

For an LTE network of seven adjacent LTE cells, with 25 RBs available in each cell, we study the impact of network load (number of UEs per eNodeB) on the percentage of unsatisfied UEs in the network. The percentage of satisfied UEs at 63% denotes the percentage of UEs characterized by a mean throughput higher than the satisfaction throughput threshold R_S. When a UE has its throughput equal to R_S, the satisfaction function equals 0.63. We investigate the percentage of UEs that are unsatisfied at 63% *i.e.*, the number of UEs characterized by a throughput lower than R_S, among all the active UEs in the network. Figure 5.7 shows the percentage of unsatisfied UEs at 63% versus the number of UEs per eNodeB.

For very low network load scenarios, such as two or five UEs per eNodeB, the frequency reuse-1 model and all the other ICIC techniques have approximately the same percentage of unsatisfied UEs. However, when the number of UEs per eNodeB increases, throughput demands become more difficult to satisfy, especially with the increased ICI. FFR has always the highest percentage of unsatisfied UEs, which increases with network load. Unsatisfied UEs with SFR technique are comparable to those with the frequency reuse-1 model. Moreover, their percentage decreases when network load increases. Our proposed cooperative ICIC technique shows the lowest percentage of unsatisfied UEs regardless of the number of UEs per eNodeB. It adjusts power allocation over the available RBs

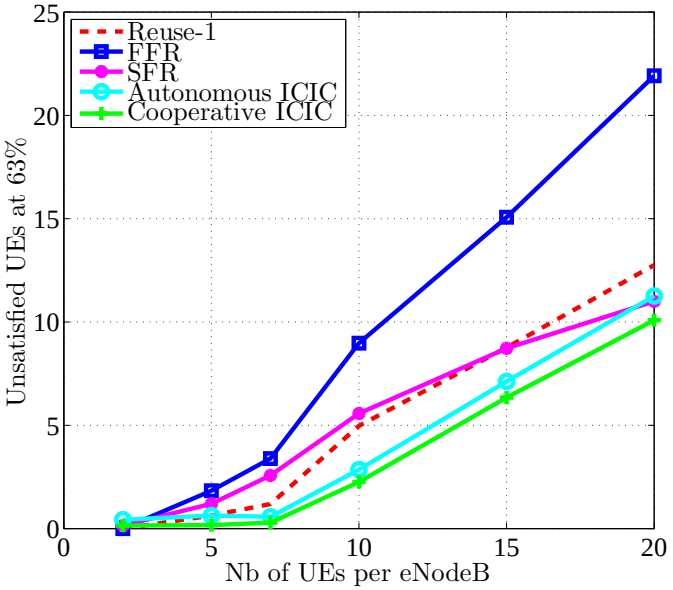

Figure 5.7: Unsatisfied UEs at 63% versus network load

for each cell in a collaborative manner, which reduces the number of UEs with low satisfaction values.

5.5.6 Energy Efficiency versus UE Distribution

We also investigate the impact of UE distribution on the performance of the compared ICIC techniques. We generate scenarios with different UE distributions by controlling the percentage of GR UEs among all the existing UEs in each cell. For every UE distribution scenario, simulations are repeated 50 times, and mean energy efficiency values are shown in Fig. 5.8.

According to these results, the frequency reuse-1 model shows always the lowest energy efficiency among all the compared techniques. In fact, when the maximum downlink transmission power is permanently allocated to all the available RBs, power consumption increases, ICI increases and the achievable throughput is reduced, especially for BR UEs. When using FFR, a fraction of the available spectrum is not used in each cell; therefore, no downlink transmission power is allocated to the unused frequency sub-band. Power consumption is reduced, while also improving SINR for BR UEs. For these reasons, FFR improves energy efficiency when compared to the frequency reuse-1 model. We also notice that the adaptive ICIC technique is a compromise between the frequency reuse-1

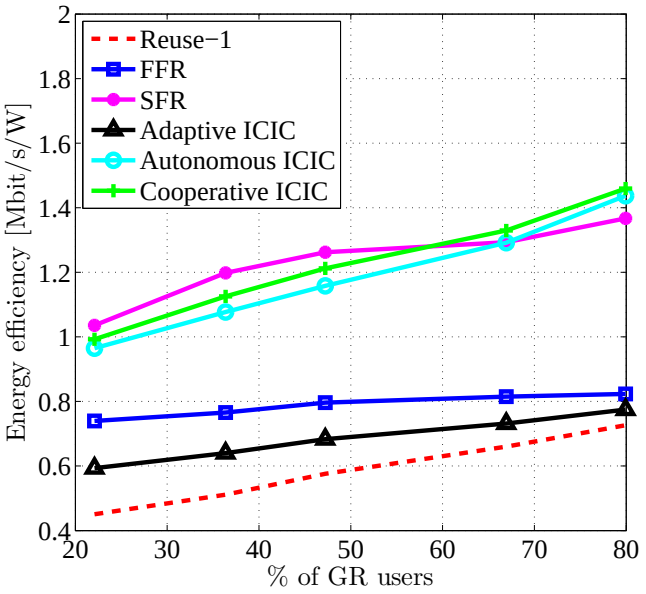

Figure 5.8: Energy efficiency versus UE distribution

model and FFR technique in terms of energy efficiency, since it succeeds in improving system performance in comparison with the frequency reuse-1 model.

Our cooperative ICIC technique shows an energy efficiency comparable to that of SFR. When there is more BR UEs in the network (the percentage of GR UEs is low), ICIC algorithm increases downlink transmission power allocated to selected RBs to increase BR UEs satisfaction. Thus, total power consumption increases, and energy efficiency is slightly lower than that of SFR. However, it shows the highest energy efficiency when the majority of UEs are GR UEs.

5.6 Conclusion

In this chapter, we introduced a cooperative distributed resource and power allocation technique where communications between the adjacent cells are required to adjust resource and power allocation. Our algorithm consists of two phases: in the first phase, signaling messages are exchanged to get the necessary information about UE satisfaction and power allocation in the neighboring cells. Decisions concerning transmission power adjustments are made in a collaborative manner during this phase. In the second phase, the scheduler of each cell locally adjusts restrictions on resource distribution between cell zones according to UE demands per zone. Simulation results show that the spectral

efficiency and energy efficiency of our cooperative technique are comparable to that of SFR technique. It enhances throughput cumulative distribution function in comparison with the frequency reuse-1 model, FFR, and SFR, and shows the lowest percentage of unsatisfied UEs independently of network load. Regardless of UEs distribution between cell zones, our cooperative technique improves energy efficiency when compared to the frequency reuse-1 model, FFR, adaptive ICIC, and non-cooperative ICIC techniques.

In the next chapter, we summarize the main contributions of the thesis, and we introduce additional challenging research topics in future cellular networks.

Chapter 6

Conclusions and Future Work

This chapter summarizes the main contributions of the thesis. In addition, we introduce future research topics, where our current contributions may be efficiently exploited.

6.1 Thesis Summary

In this thesis, we have addressed the resource and power allocation problems in wireless networks such as LTE/LTE-A networks, or dense small cell networks. In fact, the ever increasing demand for mobile broadband communications has led to the deployment of dense cellular networks with aggressive frequency reuse model. Although system capacity increases since the available bandwidth is fully used in each cell, the resulting ICI problems have a negative impact on system performance. The utilization of interference mitigation techniques is a necessity for nowadays and future cellular networks. The objectives of ICIC schemes include improving spectral efficiency, energy efficiency, system capacity, UEs satisfaction, and increasing throughput fairness among the active UEs.

We started this document by providing an exhaustive overview of the existing ICIC techniques. We classified these techniques into multiple categories, according to their working principles. After providing this qualitative analysis, we performed quantitative comparisons of state-of-the-art schemes through a series of system level simulations under uniform and non-uniform UE distributions, and for different network loads and radio conditions. The frequency reuse-3 model shows the lowest spectral efficiency among the compared techniques. However, it improves UE satisfaction for low network loads. SFR scheme shows the highest spectral efficiency, and the highest energy efficiency.

Nevertheless, the static configuration parameters of FFR and SFR should be adjusted to meet UE distribution between cell zones.

After this analysis, we formulated a centralized multi-cell resource and power allocation problem. Contrarily to the existing state-of-the-art approaches that neglect the impact of ICI when solving the resource and power allocation problems locally for each cell, our formulation takes ICI into account. The joint resource and power allocation problem is separable into two independent convex optimization problems. Our objective function consists in maximizing system throughput while guaranteeing throughput fairness among UEs. We use Lagrange duality theory and subgradient projection method to solve the centralized power allocation problem. In the same context, the power allocation problem is solved in a decentralized manner via our proposed game-theoretical method. A multi-player game is defined, where the players are the base stations. Each BS makes its own power allocation decisions independently of the other BSs in the network. The solution to the decentralized power allocation problem is found using subgradient projection method. Our centralized resource and power allocation approach outperforms the decentralized approach and state-of-the-art techniques, but more iterations are required to guarantee the convergence of the centralized problem in comparison with the decentralized power allocation approach.

In addition, we proposed a heuristic power control algorithm based on the received CQI feedbacks. The downlink transmission power allocated to the different frequency resources is adjusted by each cell in a distributed manner. The intuition behind this algorithm is to avoid power wastage, especially for UEs that are close to their serving base stations, and to mitigate ICI for UEs in the neighboring cells. The total downlink transmission power is reduced by 68%, and cell-edge UEs throughput is improved without degrading system performance. We also introduced an autonomous ICIC scheme that aims at satisfying throughput demands in each cell zone. Restrictions on power allocation are not modified in order to avoid increasing interference, while resource allocation between cell zones is adjusted in a distributed manner, according to throughput demands in each zone. It is a dynamic technique that improves system performance, especially under non-uniform UE distributions and throughput demands: throughput fairness and UE satisfaction are improved regardless of UE distribution and network load. Moreover, no additional signaling message is required.

We have also addressed the tradeoff between centralized and decentralized ICIC approaches by introducing a hybrid interference mitigation scheme. For a cluster of adjacent cells, resource and power allocation decisions are made by each cell in collaboration with its neighbors. First, the transmission power is adjusted after receiving the necessary information from the neighboring cells. Second, resource allocation between cell zones is locally modified, according to throughput demands in each zone. The main objectives of this technique are increasing UE satisfaction, improving throughput fairness, and increasing both spectral efficiency and energy efficiency. It is a compromise between the centralized and the decentralized approaches, since it does not require the existence of a central control entity, and it reduces the signaling traffic overhead. Compared to the frequency reuse-1 model, FFR, SFR, and the autonomous ICIC scheme, our proposed hybrid scheme improves UE satisfaction, and increases energy efficiency.

Interference mitigation approaches are classified into centralized, decentralized, and hybrid approaches. The centralized approach requires the existence of a central control entity that collects information about resource usage and power allocation from all the cells. This information is exchanged through signaling messages between the base stations and the control entity. The optimal power allocation requires the deployment of a centralized ICIC approach, as shown in chapter 2.7. Thus, system performance is improved at the expense of a high signaling overhead. Nevertheless, the decentralized approach is more adequate for heuristic resource and power allocation algorithms such as the autonomous ICIC technique proposed in chapter 3.8. This approach allows each base station to perform its own resource and power allocation decisions, independently of the other cells. The optimal solution is not guaranteed due to the lack of cooperation between network base stations. The hybrid interference mitigation approach is proposed as a compromise between the centralized and the decentralized approaches. It makes use of the cooperation between adjacent cells, as presented in chapter 4.10, and it reduces the signaling overhead in comparison with the centralized approach. For instance, UE scheduling is performed by the schedulers of each base station, while resource allocation between the different cells is performed by the central control entity.

6.2 Future Work

The contributions made throughout this thesis offer promising solutions for interference mitigation in present and future cellular networks. However, the exponentially increasing demand for mobile broadband data, the proliferation of mobile devices, and the rapid evolution towards Internet of things are creating additional challenging research issues.

Managing the interference-aware heterogeneous cellular networks is one of these challenges. In fact, heterogeneous networks are an efficient way to deal with the increasing mobile data traffic demands. Several Radio Access Technologies (RATs) may cover the same geographical area in order to increase network capacity, and to improve UE throughput. In this context, the RAT selection problem is an additional issue to be addressed along with the co-tier and the cross-tier interference problems. Co-tier interference occurs among network elements of the same type, *e.g.*, between neighboring femtocells, while cross-tier interference occurs among network elements that belong to different tiers, *e.g.*, between macrocells and femtocells. Our current work may be easily extended to include scenarios where the heterogeneous network solves the RAT selection problem independently of the resource and power allocation strategy. In this case, our proposed ICIC techniques are implemented after the UE association process. Otherwise, the RAT selection and the resource allocation problems should be jointly considered in a single optimization problem, which can be overly costly in computing power. Several objective functions can be defined to improve network performance, such as maximizing system throughput, spectral efficiency, energy efficiency, or throughput fairness, while guaranteeing the minimum required QoS for all the UEs.

In the same context, downlink/uplink imbalance and cell range expansion problems exist in multi-tier wireless networks. These problems motivate the need for enhanced ICIC techniques that manage UE association and downlink/uplink decoupling in addition to resource management. In fact, the downlink coverage of a macrocell is larger than that of a femtocell, since small cells operate at a lower downlink transmission power. However, this power difference does not affect the coverage in the uplink, since the transmitter is the UE. Consequently, the eNodeB providing the best downlink coverage is not necessarily the one that offers the best uplink coverage. An additional problem is that more UEs are connected to the macrocell, which leads to inefficient resource utilization. Thus, it is preferable to handover more UEs towards the small cell eNodeB even when it does not

provide the highest received signal strength. It is interesting to study the advantages of downlink/uplink decoupling in terms of SINR improvement, transmit power reduction, interference mitigation, and throughput improvement.

Another interesting issue for future investigations is studying the compromise between spectral efficiency and energy efficiency maximization. Throughout this thesis, we noticed that spectral efficiency and energy efficiency maximization cannot be achieved simultaneously. For instance, the frequency reuse-3 model and FFR technique improve the energy efficiency, while their spectral efficiency is reduced in comparison with the frequency reuse-1 model. In addition, many state-of-the-art contributions focus on improving system throughput and spectral efficiency without taking into account the energy efficiency degradation. Controlling the tradeoff between spectral efficiency and energy efficiency maximization is achieved by adjusting the radio resource allocation and the power allocation strategies. Since the energy consumption becomes one of the major concerns for mobile network operators, maximizing the spectrum usage should take power considerations into account. This resource efficiency tradeoff could be addressed by modifying the objective function of the optimization problem, in order to improve both spectral efficiency and energy efficiency. The constraints of this optimization problem have to verify that the minimum requirements for all the UEs are satisfied. For a given set of frequency resources, the spectral efficiency is improved when the transmission power is increased. However, the energy efficiency is reduced, since the power consumption increases. Therefore, managing this tradeoff is a crucial need for future green cellular networks.

We are also planning to investigate practical implementation of centralized schemes for managing RAN functionalities in future 5G networks. With the spreading of cloud computing technologies, more interest is given to the logically centralized management of network functionalities in order to improve system performance. Although it achieves a better performance, the implementation of a logically centralized approach may show several drawbacks and limitations related to latency, processing time, and reliability. In 5G networks, the challenge consists in finding the optimal *functionality split* between the access network and the core network. For instance, scheduling and interference management functionalities can be delegated to the cloud, while delay sensitive and radio transmission functionalities should be managed locally in the radio access points *e.g.*, the eNodeBs.

Appendix A

List of Publications

Journal Articles

[J6] M. Yassin, S. Lahoud, K. Khawam, M. Ibrahim, D. Mezher, and B. Cousin, "Centralized versus Decentralized Multi-Cell Resource and Power Allocation for Multiuser OFDMA Networks," submitted for publication in *IEEE Trans. Wireless Commun.*

[J5] M. Yassin, S. Lahoud, M. Ibrahim, K. Khawam, D. Mezher, and B. Cousin, "Cooperative Resource Management and Power Allocation for Multiuser OFDMA Networks," submitted for publication in *Springer Wireless Commun.*, special issue Advanced Technologies and Applications for Future Wireless and Mobile Communication Systems.

[J4] M. Yassin, S. Lahoud, M. Ibrahim, K. Khawam, D. Mezher, and B. Cousin, "An Autonomous Dynamic Inter-Cell Interference Coordination Technique for Multiuser OFDMA Networks," submitted for publication in *Springer Wireless Commun.*, special issue Advanced Technologies and Applications for Future Wireless and Mobile Communication Systems.

[J3] M. Yassin, M. AboulHassan, S. Lahoud, M. Ibrahim, D. Mezher, B. Cousin, and E. Sourour, "Survey of ICIC Techniques in LTE Networks under Various Mobile Environment Parameters," accepted for publication in *Springer Wireless Networks.*

[J2] K. Khawam, S. Lahoud, M. Ibrahim, M. Yassin, S. Martin, M. ElHelou, and F. Moety, "Radio Access Technology Selection in Heterogeneous Networks," accepted for publication in *Elsevier Physical Commun.*, special issue Radio Access Network Architectures and Resource Management for 5G.

[J1] C. Gueguen, M. Ezzaouia, and M. Yassin, "Inter-Cellular Scheduler for 5G Wireless Networks," accepted for publication in *Elsevier Physical Commun.*, special issue Radio Access Network Architectures and Resource Management for 5G.

Conference Papers

[C8] M. Yassin, S. Lahoud, M. Ibrahim, K. Khawam, D. Mezher, and B. Cousin, "Centralized Multi-Cell Resource and Power Allocation for Multiuser OFDMA Networks," submitted for publication in *IFIP Networking Conf.*, Vienna, 2016.

[C7] M. Yassin, Y. Dirani, M. Ibrahim, S. Lahoud, D. Mezher, and B. Cousin, "A Novel Dynamic Inter-Cell Interference Coordination Technique for LTE Networks," in *IEEE* 26^{th} *Annual Int. Symp. Personal, Indoor, and Mobile Radio Communications*, Hong Kong, 2015.

[C6] M. AboulHassan, M. Yassin, S. Lahoud, M. Ibrahim, D. Mezher, B. Cousin, and E. Sourour, "Classification and Comparative Analysis of Inter-Cell Interference Coordination Techniques in LTE Networks," in 7^{th} *IFIP Int. Conf. New Technologies, Mobility and Security*, Paris, 2015.

[C5] M. Yassin, S. Lahoud, M. Ibrahim, K. Khawam, D. Mezher, and B. Cousin, "Non-Cooperative Inter-Cell Interference Coordination Technique for Increasing Throughput Fairness in LTE Networks," in *IEEE* 81^{st} *Vehicular Technology Conf.*, Glasgow, 2015.

[C4] M. Yassin, S. Lahoud, M. Ibrahim, and K. Khawam, "A Downlink Power Control Heuristic Algorithm for LTE Networks," in *The* 21^{st} *Int. Conf. Telecommunications*, Lisbon, 2014.

[C3] M. Yassin, M. Ibrahim, and S. Lahoud, "A Hybrid Approach for RAT Selection in Wireless Heterogeneous Networks," in *The* 3^{rd} *Int. Conf. Communications and Information Technology*, Beirut, 2013.

[C2] M. Yassin and E. Rachid, "A Survey of Positioning Techniques and Location Based Services in Wireless Networks," in *IEEE Int. Conf. Signal Processing, Informatics, Communication and Energy Systems*, Kozhikode, 2015.

[C1] M. Yassin, E. Rachid, and R. Nasrallah, "Performance Comparison of Positioning Techniques in Wi-Fi Networks," in 10^{th} *Int. Conf. Innovations in Information Technology*, Al Ain, 2014.

Bibliography

[3GP06a] 3GPP. Physical Layer Aspects for Evolved Universal Terrestrial Radio Access (UTRA) (Release 7). Technical report, 3GPP TR 25.814 V7.1.0, 2006.

[3GP06b] 3GPP. Radio Frequency (RF) System Scenarios. Technical report, 3GPP TR 36.931 Release 9, 2006.

[3GP06c] 3GPP. Radio Frequency (RF) System Scenarios. Technical report, 3GPP TR 36.922, June 2006.

[3GP08] 3GPP. Requirements for Further Advancements for E-UTRA (LTE-Advanced) (Release 8). Technical specification, 3GPP TS 36.913 V8.0.0, June 2008.

[3GP09] 3GPP. Evolved Universal Terrestrial Radio Access (E-UTRA): Physical Layer Procedures. Technical specification, 3GPP TS 36.213 V8.8.0, 2009.

[3GP10] 3GPP. Evolved Universal Terrestrial Radio Access (E-UTRA): Further Advancements for E-UTRA Physical Layer Aspects (Release 9). Technical report, 3GPP TR 36.814 V9.0.0, March 2010.

[3GP12a] 3GPP. Evolved Universal Terrestrial Radio Access (E-UTRA) and Evolved Universal Terrestrial Radio Access Network (E-UTRAN); Overall Description; Stage 2. Technical specification, 3GPP TS 36.300, June 2012.

[3GP12b] 3GPP. Evolved Universal Terrestrial Radio Access (E-UTRA); Physical Channels and Modulation. Technical specification, 3GPP TS 36.211, September 2012.

[3GP13] 3GPP. Evolved Universal Terrestrial Radio Access (E-UTRA): Physical Layer Procedures. Technical specification, 3GPP TS 36.213 V11.11.0, December 2013.

[AHS14] Ayaz Ahmad, Naveed Ul Hassan, and Nadir Shah. Robust Channel Quality Indicator Reporting for Multi-Carrier and Multi-User Systems. *Computer Networks*, 74, Part A(0):78 – 88, 2014.

[AHSS14] M.A. Aboul Hassan, E.A. Sourour, and S.E. Shaaban. Novel Resource Allocation Algorithm for Improving Reuse One Scheme Performance in LTE Networks. In *21st International Conference on Telecommunications*, pages 166–170, Lisbon, May 2014.

[AkI08] I.I.M. Al-kebsi and M. Ismail. The Impact of Modulation Adaptation and Power Control on PAPR Clipping Technique in OFDM of 4G Systems. In *6th National Conference on Telecommunication Technologies and 2nd Malaysia Conference on Photonics*, pages 295–299, August 2008.

[Ass08] M. Assaad. Optimal Fractional Frequency Reuse (FFR) in Multicellular OFDMA System. In *IEEE 68th Vehicular Technology Conference*, pages 1–5, Calgary, September 2008.

[Ber99] D. P. Bertsekas. *Nonlinear Programming*, volume 2. MA: Athena Scientific, Massachusetts, 2 edition, 1999.

[BPVG06] P. Bisaglia, S. Pupolin, D. Veronesi, and M. Gobbi. Resource Allocation and Power Control in a TDD OFDM-Based System for 4G Cellular Networks. In *IEEE 63rd Vehicular Technology Conference*, volume 4, pages 1595–1599, May 2006.

[BV09] Stephen Boyd and Lieven Vandenberghe. *Convex Optimization*, volume 7. UK: Cambridge University Press, Cambridge, 7 edition, 2009.

[Chi05] M. Chiang. Geometric Programming for Communication Systems. *Foundations and Trends of Communications and Information Theory*, 2(1-2):1 – 156, August 2005.

[Cis13] Cisco Systems, Inc. Cisco Visual Networking Index: Global Mobile Data Traffic Forecast Update, 2012-2017. White Paper, February 2013.

[Cis14] Cisco Systems, Inc. Cisco Visual Networking Index: Global Mobile Data Traffic Forecast Update, 2013-2018. White Paper, February 2014.

[CKKL04] Jung Min Choi, Jin Sam Kwak, Ho Seok Kim, and Jae Hong Lee. Adaptive Subcarrier, Bit, and Power Allocation Algorithm for MIMO-OFDMA System. In *IEEE 59th Vehicular Technology Conference*, volume 3, pages 1801–1805, May 2004.

[CTP+07] Mung Chiang, Chee Wei Tan, D.P. Palomar, D. O'Neill, and D. Julian. Power Control By Geometric Programming. *IEEE Trans. Wireless Commun.*, 6(7):2640–2651, July 2007.

[CTZK09] R.Y. Chang, Zhifeng Tao, Jinyun Zhang, and C.-C.J. Kuo. Multicell OFDMA Downlink Resource Allocation Using a Graphic Framework. *IEEE Trans. Vehicular Technology*, 58(7):3494–3507, September 2009.

[DA10] M. Dirani and Z. Altman. A cooperative Reinforcement Learning approach for Inter-Cell Interference Coordination in OFDMA Cellular Networks. In *Proceedings of the 8th International Symposium on Modeling and Optimization in Mobile, Ad Hoc and Wireless Networks*, pages 170–176, Avignon, May 2010.

[DK88] J. Denes and A.D. Keedwell. Frequency Allocation for a Mobile Radio Telephone System. *IEEE Trans. Commun.*, 36(6):765–767, June 1988.

[Don79] V.H.Mac Donald. Advanced Mobile Phone Service: The Cellular Concept. *The Bell System Technical J.*, 58(1):15–41, January 1979.

[DPMPS97] F. Delli Priscoli, N.P. Magnani, V. Palestini, and F. Sestini. Application of Dynamic Channel Allocation Strategies to the GSM Cellular Network. *IEEE J. on Selected Areas in Commun.*, 15(8):1558–1567, October 1997.

[DPMZ98] A. De Pasquale, N.P. Magnani, and P. Zanini. Optimizing Frequency Planning in the GSM System. In *IEEE 1998 International Conference on Universal Personal Communications*, volume 1, pages 293–297, Florence, October 1998.

[DPS11] E. Dahlman, S. Parkvall, and J. Skold. *4G LTE and LTE-Advanced for Mobile Broadband*. Elsevier, Oxford, 1 edition, 2011.

[DSZ12] A. Daeinabi, K. Sandrasegaran, and X. Zhu. Survey of Intercell Interference Mitigation Techniques in LTE Downlink Networks. In *2012 Australasian Telecommunication Networks and Applications Conference*, pages 1–6, November 2012.

[DVR03] S. Das, H. Viswanathan, and G. Rittenhouse. Dynamic Load Balancing Through Coordinated Scheduling in Packet Data Systems. In *INFOCOM 2003. Twenty-Second Annual Joint Conference of the IEEE Computer and Communications. IEEE Societies*, volume 1, pages 786–796, March 2003.

[EDB07] J. Skold E. Dahlman, S. Parkvall and P. Beming. *3G Evolution: HSPA and LTE for Mobile Broadband*. Elsevier, Oxford, 1 edition, 2007.

[EJK+98] S. Engstrom, T. Johansson, F. Kronestedt, M. Larsson, S. Lidbrink, and H. Olofsson. Multiple Reuse Patterns for Frequency Planning in GSM Networks. In *IEEE 48th Vehicular Technology Conference*, volume 3, pages 2004–2008, Ottawa, May 1998.

[ELK13] M. ElHelou, S. Lahoud, and M. IbrM. Ibrahim. Khawam. A Hybrid Approach for Radio Access Technology Selection in Heterogeneous Wireless Networks. In *European Wireless*, Guildford, 2013.

[FFSY09] G. Fodor, A. Furuskar, P. Skillermark, and Jinghong Yang. On the Impact of Uplink Scheduling on Inter-Cell Interference Variation in MIMO OFDM Systems. In *IEEE Wireless Communications and Networking Conference*, pages 1–6, April 2009.

[FKR+09] Gabor Fodor, Chrysostomos Koutsimanis, Andras Racz, Norbert Reider, Arne Simonsson, and Walter Muller. Intercell interference coordination in ofdma networks and in the 3gpp long term evolution system. *J. Commun.*, 4:445–453, 2009.

[Fuj11] Fujitsu Network Communications Inc. Enhancing LTE Cell-Edge Performance via PDCCH ICIC. White Paper, 2011.

[GGLBL13] D. Gonzalez, M. Garcia-Lozano, S. R. Boque, and D. S. Lee. Optimization of Soft Frequency Reuse for Irregular LTE Macrocellular Networks. *IEEE Trans. Wireless Commun.*, 12(5):2410–2423, May 2013.

[HA09] N.U.L. Hassan and M. Assaad. Optimal Fractional Frequency Reuse (FFR) and Resource Allocation in Multiuser OFDMA System. In *2009 International Conference on Information and Communication Technologies*, pages 88–92, Karachi, August 2009.

[HKHE13] A.S. Hamza, S.S. Khalifa, H.S. Hamza, and K. Elsayed. A Survey on Inter-Cell Interference Coordination Techniques in OFDMA-Based Cellular Networks. *IEEE Commun. Surveys Tutorials*, 15(4):1642–1670, 2013.

[HRTA14] E. Hossain, M. Rasti, H. Tabassum, and A. Abdelnasser. Evolution Toward 5G Multi-Tier Cellular Wireless Networks: An Interference Management Perspective. *IEEE Wireless Commun.*, 21(3):118–127, June 2014.

[HTV14] F. Huang, J. Tomasik, and V. Veque. Improvement of Cell Edge Performance by Coupling RB Allocation with Beamforming. In *IEEE Int. Conf. Communication Systems*, pages 333–338, Macau, 2014.

[Hua05] Huawei. Soft Frequency Reuse Scheme for UTRANLTE (R1-050507). Technical report, 3GPP RAN WG1 no. 41, Athens, Greece, May 2005.

[IWAYB13] Mauricio Iturralde, Anne Wei, Tara Ali-Yahiya, and Andre-Luc Beylot. Resource Allocation for Real Time Services in LTE Networks: Resource Allocation Using Cooperative Game Theory and Virtual Token Mechanism. *Springer Wireless Personal Commun.*, 72(2):1415–1435, 2013.

[IWR10] J.C. Ikuno, M. Wrulich, and M. Rupp. System Level Simulation of LTE Networks. In *IEEE 71st Vehicular Technology Conference*, pages 1–5, Taipei, May 2010.

[JCH84] Rajendra K. Jain, DahMing W. Chiu, and William R. Hawe. A Quantitative Measure of Fairness and Discrimination for Resource Allocation and Shared Computer System. Technical report, Digital Equipment Corporation, September 1984.

[JPJ13] Chen Jiming, Wang Peng, and Zhang Jie. Adaptive Soft Frequency Reuse Scheme for in-Building Dense Femtocell Networks. *China Communications*, 10(1):44–55, January 2013.

[JPJS05] D. Lacroix J. P. Javaudin, J. Laine and O. Seller. On Inter-Cell Interference in OFDMA Wireless Systems. In *Proc. European Signal Processing Conf.*, Antalya, 2005.

[Kel97] Frank Kelly. Charging and Rate Control for Elastic Traffic. *European Trans. Telecommunications*, 8(1):33–37, 1997.

[KHH+12] Mohammad T. Kawser, Nafiz Imtiaz Bin Hamid, Md. Nayeemul Hasan, M. Shah Alam, and M. Musfiqur Rahman. Downlink SNR to CQI Mapping for Different Multiple Antenna Techniques in LTE. *Int. J. Information and Electronics Engineering*, 2(5):756–760, September 2012.

[KHQT13a] C. Kosta, B. Hunt, A.U. Quddus, and R. Tafazolli. On Interference Avoidance Through Inter-Cell Interference Coordination (ICIC) Based on OFDMA Mobile Systems. *IEEE Commun. Surveys Tutorials*, 15(3):973–995, December 2013.

[KHQT13b] Chrysovalantis Kosta, Bernard Hunt, Atta U. Quddus, and Rahim Tafazolli. An Improved Inter-cell Interference Coordination (ICIC) for OFDMA Multi-Cell Systems. In *Proceedings of the 19th European Wireless Conference*, pages 1–5, April 2013.

[KLL03] D. Kivanc, Guoqing Li, and Hui Liu. Computationally Efficient Bandwidth Allocation and Power Control for OFDMA. *IEEE Trans. Wireless Commun.*, 2(6):1150–1158, November 2003.

[KW11] Martin Kasparick and Gerhard Wunder. Autonomous Distributed Power Control Algorithms for Interference Mitigation in Multi-Antenna Cellular Networks. In *11th European Wireless Conference*, pages 1–8, April 2011.

[LCLV14] Ying Loong Lee, Teong Chee Chuah, J. Loo, and A. Vinel. Recent Advances in Radio Resource Management for Heterogeneous LTE/LTE-A Networks. *IEEE Commun. Surveys Tutorials*, 16(4):2142–2180, 2014.

[LCN+12] Y. S. Liang, W. H. Chung, G. K. Ni, I. Y. Chen, H. Zhang, and S. Y. Kuo. Resource Allocation with Interference Avoidance in OFDMA Femtocell Networks. *IEEE Trans. Vehicular Technology*, 61(5):2243–2255, June 2012.

[LJC11] K. Lee, O. Jo, and D. H. Cho. Cooperative Resource Allocation for Guaranteeing Intercell Fairness in Femtocell Networks. *Proc. IEEE Commun. Letters*, 15(2):214–216, February 2011.

[LMB14] R.A. Loodaricheh, S. Mallick, and V.K. Bhargava. Energy-Efficient Resource Allocation for OFDMA Cellular Networks with User Cooperation and QoS Provisioning. *IEEE Trans. Wireless Commun.*, 13(11):6132–6146, Nov. 2014.

[LPCVC14] D. Lopez-Perez, Xiaoli Chu, A.V. Vasilakos, and H. Claussen. Power Minimization Based Resource Allocation for Interference Mitigation in OFDMA Femtocell Networks. *IEEE J. Selected Areas in Commun.*, 32(2):333–344, February 2014.

[LSC+12] Daewon Lee, Hanbyul Seo, B. Clerckx, E. Hardouin, D. Mazzarese, S. Nagata, and K. Sayana. Coordinated Multipoint Transmission and Reception in LTE-Advanced: Deployment Scenarios and Operational Challenges. *IEEE Commun. Magazine*, 50(2):148–155, February 2012.

[LXCL14] Gubong Lim, Cong Xiong, L.J. Cimini, and G.Y. Li. Energy-Efficient Resource Allocation for OFDMA-Based Multi-RAT Networks. *IEEE Trans. Wireless Commun.*, 13(5):2696–2705, May 2014.

[MET13] METIS D1.1. Scenarios, Requirements and KPIs for 5G Mobile and Wireless System. ICT-317669 METIS Deliverable 1.1, Version 1, April 2013.

[MET15] METIS D6.6. Final Report on the METIS 5G System Concept and Technology Roadmap. ICT-317669 METIS Deliverable 6.6, Version 1, April 2015.

[MHL10] Guowang Miao, N. Himayat, and G.Y. Li. Energy-Efficient Link Adaptation in Frequency-Selective Channels. *IEEE Trans. Commun.*, 58(2):545–554, February 2010.

[NBLK14] Wooseok Nam, Dongwoon Bai, Jungwon Lee, and Inyup Kang. Advanced Interference Management for 5G Cellular Networks. *IEEE Commun. Magazine*, 52(5):52–60, May 2014.

[Nec09] MarcC. Necker. Scheduling Constraints and Interference Graph Properties for Graph-based Interference Coordination in Cellular OFDMA Networks. *Springer J. Mobile Networks and Applications*, 14(4):539–550, January 2009.

[NGM15] NGMN Alliance. 5G White Paper. White Paper, February 2015.

[NKL14] D. T. Ngo, S. Khakurel, and T. LeNgoc. Joint Subchannel Assignment and Power Allocation for OFDMA Femtocell Networks. *IEEE Trans. Wireless Commun.*, 13(1):342–355, Jan. 2014.

[Pal05] Daniel Perez Palomar. Convex Primal Decomposition for Multicarrier Linear MIMO Transceivers. *IEEE Trans. Signal Processing*, 53(12):4661–4674, Dec. 2005.

[PB08] M. Pischella and J.-C. Belfiore. Power Control in Distributed Cooperative OFDMA Cellular Networks. *IEEE Trans. Wireless Commun.*, 7(5):1900–1906, May 2008.

[PC06] D.P. Palomar and Mung Chiang. A Tutorial on Decomposition Methods for Network Utility Maximization. *IEEE J. Selected Areas in Commun.*, 24(8):1439–1451, August 2006.

[PCVC14] D. L. Perez, X. Chu, A. V. Vasilakos, and H. Claussen. Power Minimization Based Resource Allocation for Interference Mitigation in OFDMA Femtocell Networks. *IEEE J. Selected Areas in Commun.*, 32(2):333–344, February 2014.

[PSC12] S.S. Prasad, C.K. Shukla, and R.F. Chisab. Performance Analysis of OFDMA in LTE. In *3rd International Conference on Computing Communication Networking Technologies*, pages 1–7, July 2012.

[QLS09] T.Q.S. Quek, Zhongding Lei, and Sumei Sun. Adaptive Interference Coordination in Multi-Cell OFDMA Systems. In *IEEE 20th International Symposium on Personal, Indoor and Mobile Radio Communications*, pages 2380–2384, September 2009.

[QZXB12] Zhiyong Qin, Zhangdui Zhong, Rongtao Xu, and Ge Bai. System Performance of Soft Frequency Reuse in LTE Railway Networks. In *IEEE 11th*

International Conference on Signal Processing, volume 2, pages 1566–1570, Beijing, October 2012.

[Raz13] H. Raza. A Brief Survey of Radio Access Network Backhaul Evolution: Part II. *IEEE Commun. Magazine*, 51(5):170–177, May 2013.

[RBSP09] H.A.M. Ramli, R. Basukala, K. Sandrasegaran, and R. Patachaianand. Performance of Well Known Packet Scheduling Algorithms in the Downlink 3GPP LTE System. In *IEEE 9th Malaysia International Conference on Communications*, pages 815–820, Kuala Lumpur, December 2009.

[Roe11] A. Roessler. Understanding Downlink Power Allocation in LTE [Online]. Available: http://www.wirelessdesignmag.com/blogs/2011/02/understanding-downlink-power-allocation-lte, February 2011.

[Ros65] J. B. Rosen. Existence and Uniqueness of Equilibrium Points for Concave n-Person Games. *Econometrica J.*, 33:520–534, 1965.

[RSV10] B. Rengarajan, A. L. Stolyar, and H. Viswanathan. Self-Organizing Dynamic Fractional Frequency Reuse on the Uplink of OFDMA Systems. In *Proc.* 44^{th} *Annual Conf. Information Sciences and Systems*, Princeton, 2010.

[RY10] M. Rahman and H. Yanikomeroglu. Enhancing Cell-Edge Performance: A Downlink Dynamic Interference Avoidance Scheme with Inter-Cell Coordination. *IEEE Trans. Wireless Commun.*, 9(4):1414–1425, April 2010.

[SA14] S. Sadr and R.S. Adve. Partially-Distributed Resource Allocation in Small-Cell Networks. *IEEE Trans. Wireless Commun.*, 13(12):6851–6862, Dec. 2014.

[SAE05] Z. Shen, J. G. Andrews, and B. L. Evans. Adaptive Resource Allocation in Multiuser OFDM Systems with Proportional Rate Constraints. *IEEE Trans. Wireless Commun.*, 4(6):2726–2737, November 2005.

[SL05] H. Schulze and C. Lueders. *Theory and Applications of OFDM and CDMA Wideband Wireless Communications*, volume 1. UK: Wiley, Chichester, 1 edition, 2005.

[SQ09] R. Schoenen and Fei Qin. Adaptive Power Control for 4G OFDMA Systems on Frequency Selective Fading Channels. In *5th International Conference on Wireless Communications, Networking and Mobile Computing*, pages 1–6, September 2009.

[SSB09] I. Toufik S. Sesia and M. Baker. *LTE - The UMTS Long Term Evolution from Theory to Practice.* Wiley, Chichester, 1 edition, 2009.

[SV09] A.L. Stolyar and H. Viswanathan. Self-Organizing Dynamic Fractional Frequency Reuse for Best-Effort Traffic through Distributed Inter-Cell Coordination. In *IEEE INFOCOM 2009*, pages 1287–1295, April 2009.

[TLZ08] M. Tao, Y. Liang, and F. Zhang. Resource Allocation for Delay Differentiated Traffic in Multiuser OFDM Systems. *IEEE Trans. Wireless Commun.*, 7(6):2190–2201, June 2008.

[Top79] D. M. Topkis. Equilibrium Points in Nonzero-Sum n-Person Submodular Games. *Society for Industrial and Applied Mathematics J. Control and Optimization*, 17(6):773–787, 1979.

[Top98] D. Topkis. *Supermodularity and Complementarity.* Princeton University Press, Princeton, 1998.

[TSAH14] Jie Tang, D.K.C. So, E. Alsusa, and K.A. Hamdi. Resource Efficiency: A New Paradigm on Energy Efficiency and Spectral Efficiency Tradeoff. *IEEE Trans. Wireless Commun.*, 13(8):4656–4669, Aug 2014.

[UH11] Y. Umeda and K. Higuchi. Efficient Adaptive Frequency Partitioning in OFDMA Downlink with Fractional Frequency Reuse. In *International Symposium on Intelligent Signal Processing and Communications Systems*, pages 1–5, December 2011.

[VUT14] VUT. LTE Downlink System Level Simulator, Vienna University of Technology, 2014.

[VZRB15] L. Venturino, A. Zappone, C. Risi, and S. Buzzi. Energy-Efficient Scheduling and Power Allocation in Downlink OFDMA Networks with Base Station Coordination. *IEEE Trans. Wireless Commun.*, 14(1):1–14, January 2015.

[WCLM99] Cheong Yui Wong, R.S. Cheng, K.B. Lataief, and R.D. Murch. Multiuser OFDM with Adaptive Subcarrier, Bit, and Power Allocation. *IEEE J. Selected Areas in Commun.*, 17(10):1747–1758, October 1999.

[WKSV10] G. Wunder, M. Kasparick, A. Stolyar, and H. Viswanathan. Self-Organizing Distributed Inter-Cell Beam Coordination in Cellular Networks with Best Effort Traffic. In *Proceedings of the 8th International Symposium on Modeling and Optimization in Mobile, Ad Hoc and Wireless Networks*, pages 295–302, May 2010.

[WLP+10] Jin Soo Wang, Ji Hye Lee, Jae Cheol Park, Iickho Song, and Yun Hee Kim. Combining of Cyclically Delayed Signals: A Low-Complexity Scheme for PAPR Reduction in OFDM Systems. *IEEE Trans. on Broadcasting*, 56(4):577–583, December 2010.

[WYMC09] Yapeng Wang, Xu Yang, A. Ma, and L. Cuthbert. Intelligent Resource Optimisation Using Semi-Smart Antennas in LTE OFDMA Systems. In *2009 IEEE International Conference on Communications Technology and Applications*, pages 173–179, October 2009.

[WZJW09] Y. Wu, D. Zhang, H. Jiang, and Y. Wu. A Novel Spectrum Management Scheme for Femto Cell Deployment in LTE Macro Cells. In *IEEE 20th Int. Symp. Personal, Indoor, and Mobile Radio Communications*, pages 6–11, Tokyo, September 2009.

[XHC12] Shaoyi Xu, Jing Han, and Tao Chen. Enhanced Inter-Cell Interference Coordination in Heterogeneous Networks for LTE-Advanced. In *IEEE 75th Vehicular Technology Conference (VTC Spring)*, pages 1–5, Yokohama, May 2012.

[XKM13] Xiang Xu, Gledi Kutrolli, and Rudolf Mathar. Autonomous Downlink Power Control for LTE Femtocells Based on Channel Quality Indicator. In *IEEE 24th International Symposium on Personal Indoor and Mobile Radio Communications*, pages 3050–3055, September 2013.

[XLZ+11] Cong Xiong, G.Y. Li, Shunqing Zhang, Yan Chen, and Shugong Xu. Energy and Spectral-Efficiency Tradeoff in Downlink OFDMA Networks. *IEEE Trans. Wireless Commun.*, 10(11):3874–3886, November 2011.

[XLZ+12] Cong Xiong, G.Y. Li, Shunqing Zhang, Yan Chen, and Shugong Xu. Energy-Efficient Resource Allocation in OFDMA Networks. *IEEE Trans. on Commun.*, 60(12):3767–3778, December 2012.

[XTL15] Xiao Xiao, Xiaoming Tao, and Jianhua Lu. Energy-Efficient Resource Allocation in LTE-Based MIMO-OFDMA Systems with User Rate Constraints. *IEEE Trans. Vehicular Technology*, 64(1):185–197, January 2015.

[XYY12] Dengkun Xiao, Xiaoyu Yu, and Dongkai Yang. A Novel Downlink ICIC Method Based on User Position in LTE-Advanced Systems. In *2012 IEEE Vehicular Technology Conference (VTC Fall)*, pages 1–5, September 2012.

[YAL+15] M. Yassin, M. AboulHassan, S. Lahoud, M. Ibrahim, D. Mezher, B. Cousin, and E. Sourour. Survey of ICIC Techniques in LTE Networks under Various Mobile Environment Parameters. *Accepted for publication in Springer Wireless Networks*, 2015.

[Yao95] DavidD. Yao. S-Modular Games, with Queueing Applications. *Queueing Systems*, 21(3-4):449–475, 1995.

[YC11] S. Yoong and J. Cho. Interference Mitigation in Heterogeneous Cellular Networks of Macro and Femto Cells. In *Proc. Int. Conf. ICTC*, pages 177–181, Seoul, September 2011.

[YLI+15] M. Yassin, S. Lahoud, M. Ibrahim, K. Khawam, D. Mezher, and B. Cousin. Non-Cooperative Inter-Cell Interference Coordination Technique for Increasing Through Fairness in LTE Networks. In *IEEE 81st Vehicular Technology Conf*, Glasgow, May 2015.

[YLIK14] M. Yassin, S. Lahoud, M. Ibrahim, and K. Khawam. A Downlink Power Control Heuristic Algorithm for LTE Networks. In *21st International Conference on Telecommunications*, pages 323–327, Lisbon, May 2014.

[YLY+14] Jian Yu, G.Y. Li, Changchuan Yin, Suwen Tang, and Xiaolong Zhu. Multi-Cell Coordinated Scheduling and Power Allocation in Downlink LTE-A Systems. In *IEEE 80th Vehicular Technology Conference*, pages 1–5, Vancouver, September 2014.

[YPW08] K. Yan, N. Prasad, and X. Wang. An Auction Approach to Resource Allocation in Uplink Multi-Cell OFDMA Systems. In *IEEE Global Telecommunications Conf.*, New Orleans, 2008.

[ZCA15] J. Zheng, Y. Cai, and A. Anpalagan. A Stochastic Game-Theoretic Approach for Interference Mitigation in Small Cell Networks. *IEEE Commun. Letters*, 19(2):251–254, February 2015.

[ZCL+14] Jianchao Zheng, Yueming Cai, Yongkang Liu, Yuhua Xu, Bowen Duan, and Xuemin Shen. Optimal Power Allocation and User Scheduling in Multicell Networks: Base Station Cooperation Using a Game-Theoretic Approach. *IEEE Trans. Wireless Commun.*, 13(12):6928–6942, Dec. 2014.

[ZM05] T. Zemen and C.F. Mecklenbrauker. Time-Variant Channel Estimation Using Discrete Prolate Spheroidal Sequences. *IEEE Trans. Signal Processing*, 53(9):3597–3607, Sept 2005.